Studying fouling behavior of crude oil mixtures by mass spectrometry

Dissertation

zur Erlangung des akademischen Grades eines
Doktors der Naturwissenschaften
- Dr. rer. nat. -

vorgelegt von

Aikaterini Kondyli

aus Athen, Griechenland

Fakultät für Chemie

der Universität Duisburg-Essen

2019

DOI: 10.17185/duepublico/72671
URN: urn:nbn:de:hbz:465-20230703-143703-7

Die vorliegende Arbeit wurde im Zeitraum von Mai 2015 bis Mai 2019 im Arbeitskreis von Prof. Dr. Wolfgang Schrader am Max-Planck-Institut für Kohlenforschung in Mülheim an der Ruhr durchgeführt.

Tag der Disputation: 27.07.2020

Gutachter: Prof. Dr. Wolfgang Schrader
PD Dr. Ursula Telgheder

Vorsitzender: Prof. Dr. Eckhard Spohr

Erklärung

Hiermit versichere ich, dass ich die vorliegende Arbeit mit dem Titel

„Studying fouling behavior of crude oil mixtures by mass spectrometry"

selbst verfasst und keine außer den angegebenen Hilfsmitteln und Quellen benutzt habe, und dass die Arbeit in dieser oder ähnlicher Form noch bei keiner anderen Universität eingereicht wurde.

Essen, im Dezember 2019

"If you cannot do great things, do small things in a great way."

Napoleon Hill

ABSTRACT

Crude oil fouling remains one of the biggest and until now unresolved problems in petroleum industry. Deposition of unwanted material during up- or downstream operation results in loss of thermal efficiency on the heat transfer equipment, catalyst poisoning, plugged pipelines or thermal instability. These in turn, can cause a series of operating difficulties, which might finally end with the units shut down. Since the incorporation of heavier crude oils (e.g. extra heavy oil, oil shale) into the market, the problem has become even more severe due to the increased content of heteroatoms (N, O, S), metals (e.g. V, Fe, Ni) and asphaltenes, which are thought to have a negative effect on the fouling phenomenon.

The main challenge regarding the formation of solid deposits is that the reaction mechanisms, let alone the compounds that are responsible for it, are poorly understood. The ability of gaining information on the details is limited, firstly, due to the complex nature of crude oil, which contains more than a million different chemical compounds and, secondly, due to the various reaction pathways (e.g. autoxidation, polymerization and thermal decomposition) involved in fouling.

During the course of this study, a procedure was designed to simulate fouling on a laboratory scale. For this, a reactor was developed that allows the simulation of an industrial reaction in the laboratory. Several parameters such as temperature, oxygen or the presence of water are studied with their effect on the fouling rate. After the successful simulation of fouling using a light crude oil fraction the resulting products were analyzed using ultrahigh resolution mass spectrometry. This method allows a view into the molecular details of such a complex phenomenon by its ability to unambiguously determine the elemental composition of any detected signal.

The behavior of different groups of compounds –based on their heteroatom content- has been studied in detail. According to the results obtained before and after the reactions, it was finally possible to suggest a potential mechanism for crude oil fouling. Using standard reference compounds for a simulated fouling experiment, the mechanism was verified by means of tandem mass spectrometry.

KURZFASSUNG

Fouling zählt zu den größten, bislang ungelösten Problemen der Erdöl verarbeitenden Industrie. Durch das Ausfallen unerwünschter Nebenprodukte während der Förderung oder Raffinierung ergeben sich Effekte wie der Effizienzverlust von Wärmetauschern, das Vergiften von Katalysatoren, Verstopfungen von Pipelines oder allgemein eine verringerte thermische Stabilität. All dies kann zu weiteren Komplikationen, bis zur Stilllegung der gesamten Anlage führen. Seit schwere Öle (z.B. Schwerstöle und Schieferöle) vermehrt eingesetzt werden, treten derartige Probleme immer häufiger auf. Dies ist auf die erhöhten Anteile an Heteroatomen (N, O, S), Metallen (z.B. V, Fe, Ni) und Asphaltenen zurückzuführen, die für negative Auswirkungen bezüglich Fouling verantwortlich gemacht werden.

Hauptproblem hinsichtlich der Bildung von Ablagerungen ist, dass die zu Grunde liegenden Reaktionsmechanismen, ebenso wie die involvierten Substanzen weitgehend unbekannt sind. Die Möglichkeiten, hierüber Erkenntnisse zu erlangen werden zum einen durch die Komplexität des Erdöls erschwert, welches mehrere Millionen chemisch verschiedener Komponenten enthält. Zum anderen kann eine Vielzahl an Reaktionswegen beteiligt sein, wie etwa Autoxidation, Polymerisierung oder thermische Zersetzung.

Im Zuge dieser Arbeit wurde ein Reaktor entwickelt, mit dessen Hilfe Fouling im Labormaßstab simuliert werden kann. Hierin kann der Effekt verschiedener Parameter, wie Temperatur, Atmosphäre oder das Vorhandensein von Wasser, auf die Foulingrate zu untersuchen. Nach der erfolgreichen Simulation von Fouling anhand eines Gaskondensats wurden die erhaltenen Produkte mittels ultrahochauflösender Massenspektrometrie untersucht. Die Methode erlaubt durch die Möglichkeit, zu jedem Signal eine eindeutige Elementarzusammensetzung zu bestimmen, einen Blick auf die molekularen Details dieses komplexen Phänomens.

Das Foulingverhalten verschiedener Stoffgruppen wurde–anhand des Heteroatomgehalts eingehend untersucht. Basierend auf diesen Resultaten konnte ein potentieller Foulingmechanismus gefunden werden. Dieser wurde anhand eines Foulingexperiments mit Referenzsubstanzen mit Hilfe von Tandem Massenspektrometrie verifiziert.

TABLE OF CONTENTS

CHAPTER 1. GENERAL INTRODUCTION

The world's energy consumption has increased dramatically over the last years and is expected to grow by 28% until the end of 2040.[1] Most of the efforts taken to deal with the problem of the depletion of conventional oils are focused on the utilization of alternative sources. Although renewable energy from solar, marine, wind and other sources has lately attracted great attention, these are not yet able to meet the global energy needs.[2] Until there is an adequate energy transition, crude oil remains the dominant energy source. Nowadays, the main question arising is until when conventional oil (light and sweet crude oil) will be able to cover the world's energy needs since the excessive use of it in combination with the fast growth in demand from countries with emerging economies has led to its depletion.[3] In order to ensure a sustainable energy future, the use of heavier crude oils is inevitable.[4, 5]

Incorporation of unconventional oil resources such as extra-heavy oils, oil sands or oil shales in the market is extremely challenging due to numerous technical, economic and environmental limitations.[6] These types of oil require special treatment, since their extremely high viscosity, low solubility and high chemical complexity cause various environmental and industrial problems.[7, 8] In addition, the high amount of heteroatom-containing compounds (N, O, S,), heavy metals and asphaltenes are responsible for adverse effects in petroleum industry.[9, 10] In order to overcome these problems, not only optimizations and advancements in technology within the oil industry are necessary, but also an in-depth understanding of the crude oil chemical composition on a molecular level.[11]

One of the biggest problems in petroleum producing and processing industries is crude oil fouling.[12] Fouling is defined as the deposition of unwanted material on surfaces and is a well-known problem since decades.[13] Although fouling has an effect in almost every unit during upstream (e.g. exploration and production) and downstream (transportation and refinery) operations, the units which experience the highest fouling rates are related to the preheat network of heat exchangers.[14, 15] A simplified schematic of a typical crude oil distillation unit (CDU) with heat exchanger networks can be seen in Figure 1-1.[16-18] Briefly, the crude oil is preheated in a series of heat exchangers to a temperature of 50-180 °C before it enters the desalting unit. Increasing the temperature of crude oil at this stage is very important, since its viscosity will decrease, enhancing the

following mixing and separation processes. Afterwards, the salt content of the feedstock is diluted by adding fresh hot water. Removal of salts (e.g. $CaCl_2$, $MgCl_2$, and NaCl) is a crucial step, since their presence can play an important role in corrosion and in fouling of the downstream processing units. In the desalter, the water-oil mixture is separated into two phases with the help of an electric field. The oil phase flows further to the next heat exchanger network where it is heated up to 280 °C. Further heating of crude oil reduces the energy requirements for the furnace and ensures the maximum heat recovery (up to 70 %) needed for the fractionation. In the furnace, crude oil reaches the desired temperature and then proceeds to the atmospheric distillation unit where it is fractionated into petroleum products (cuts, distillates) according to their boiling temperatures. The residual which remains at the bottom of the column is sent to the vacuum distillation unit where it is further processed.

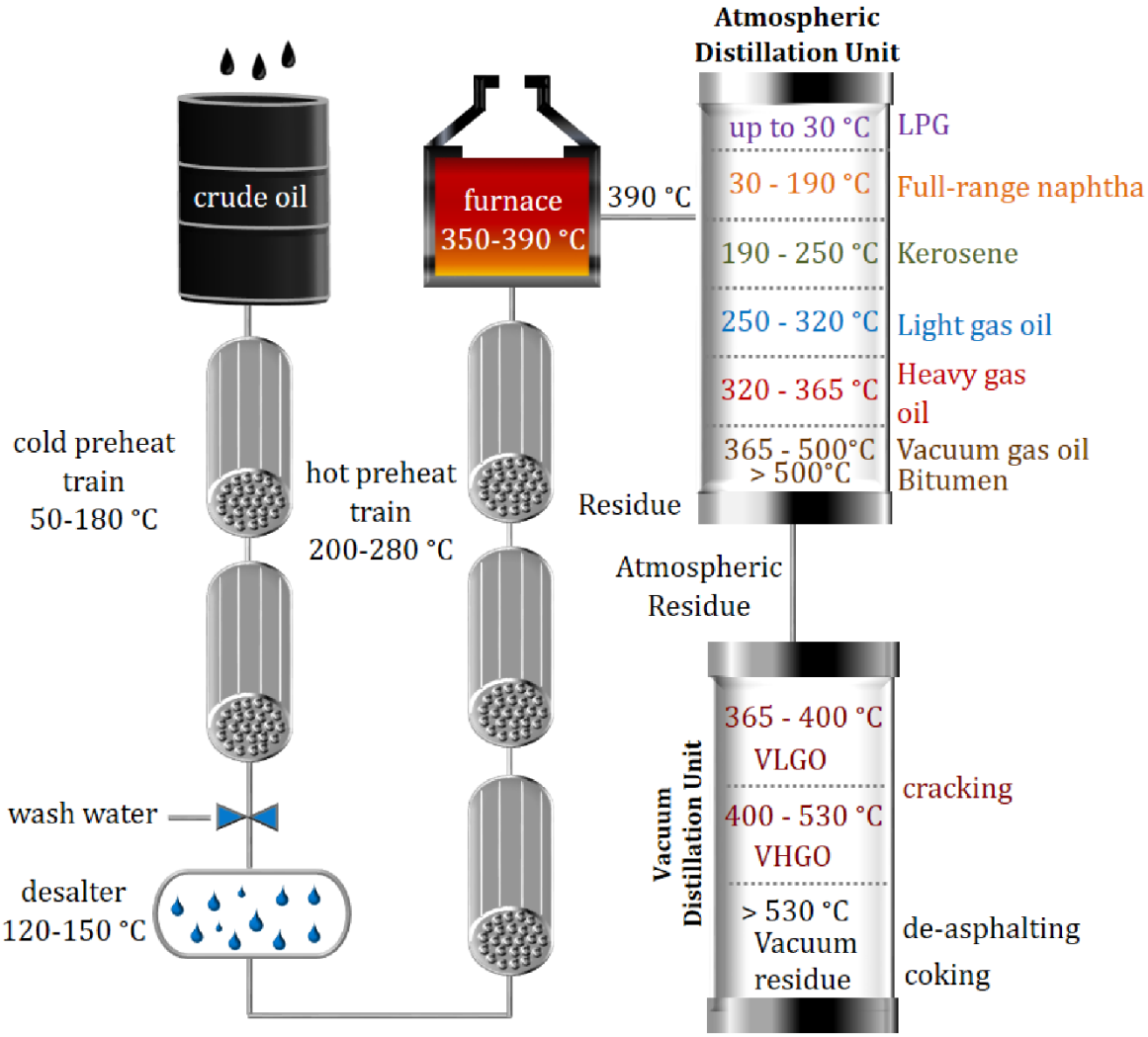

Figure 1-1: A simplified schematic of a crude oil distillation unit (CDU).

Despite numerous attempts over the years to optimize the design and the operating conditions of the heat exchangers, it is not possible until now to prevent, reduce and control the phenomenon of fouling. Fouling is a dynamic process,[19] meaning that its effects increase with time and can be classified either as acute or chronic, depending on the time-scale involved.[20] Acute fouling occurs in a short period of time (e.g. days) and is associated either with the presence of fouling precursors at high concentration or with the processing of thermally unstable feedstocks (oil blending).[21] On the other hand, chronic fouling occurs over a longer period (e.g. months) and in this case, the precursors are either present in low concentration or being formed after a change in operating conditions.[22] Regardless of the time involved, crude oil fouling remains the main unresolved problem in petroleum industry causing various operating difficulties, economic penalties, environmental impacts as well as health and safety hazards.[23-26] Crude oil fouling is arguably a multi-billion dollar problem, though an exact estimation of the fouling costs is extremely difficult, since they differ depending on the size of the industry and on the nature of the feedstock.[27-29] According to a study by Van Nostrand and co-workers , the biggest share of around 50 % of the total fouling costs in a refinery unit is attributed to fouling in the heat exchanger networks.[29] Accumulation of solid material on the heat transfer surface affects the thermal and hydraulic performance of the equipment significantly.[30] The newly formed fouling layer has low thermal conductivity, resulting in loss of thermal efficiency of the heat exchangers by increasing not only the resistance of the heat flow but also the pressure drop.[25] In order to compensate for the reduced thermal efficiency, additional fuel needs to be burnt at the furnace, leading to extremely high energy losses[31] as well as to environmental pollution by adding millions of tons of extra CO_2 to the atmosphere.[32] In Figure 1-2, the formation of solid deposits on the surfaces of the heat exchanger due to fouling can be seen.[33]

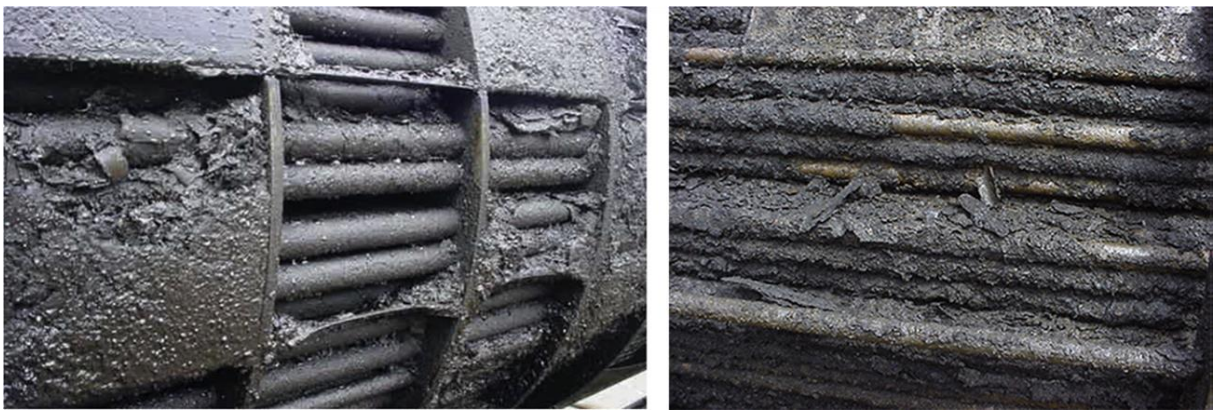

Figure 1-2: Fouling on the shell-side of refinery heat exchangers.

Apart from the above-mentioned problems, the presence of fouling deposits can cause a significant reduction in throughput, plugged pipelines as well as product instability.[34] As reported in the literature, quite often even a drop of 20 % of the thermal efficiency of the heat exchangers can justify decisions regarding cleaning of the affected equipment.[33] The removal of the fouling deposits can be achieved either by mechanical or by chemical cleaning.[26, 35] High pressure water jets and scraping of the surface of the heat exchanger are the most commonly used methods in mechanical cleaning.[34] This process is quite expensive in terms of time (3-14 days), safety and money and requires the dismantlement of the equipment.[33] On the other hand, chemical cleaning involves the use of chemicals in order to dissolve a part or all the constituents of the fouling deposits. This method is performed by flowing the solvent chemical (e.g. kerosene, xylene, toluene, heavy aromatic naphtha) through the exchanger without disassembly of the equipment.[36] Although chemical cleaning is a faster and cheaper method, it raises various environmental problems regarding the disposal of solvents. Despite of the chosen method, restoration of the affected equipment to its previous state is not always possible. In this case, a scheduled unit shutdown is necessary in order to replace the equipment. This process needs to be planned in advance and preferably in periods when the demand of oil is lower. Otherwise, an emergency shutdown will have a huge economic impact due to high production losses.[24]

Apart from the high operating and maintenance costs, the fouling deposits raise a number of environmental concerns regarding their disposal. According to the literature, in case of a small size refinery, where approximately 200,000 bbl per day (each barrel contains around 159 litres) are processed, around 5000 tonnes of solid material can be accumulated within a year.[37] The fouling deposits are very complex in nature and can be a mixture of organic and inorganic material. Defining their nature is very important since useful information regarding the fouling mechanisms and the source of precursors can be revealed.[33] The organic material consists mainly of asphaltenes, polymerization products, as well as thermally degraded material (coke), while in case of the inorganic materials, these can be found in the form of corrosion products (e.g. FeS), and salts (e.g. NaCl, $CaCl_2$, carbonates, chlorides, sulfates).[19, 33] In addition, the deposits can contain sulfur, nitrogen, as well as a large content of polycyclic aromatic hydrocarbons (PAHs) with the latter ones to be considered as toxic not only for the environment but also for humans.[38] Thus, a safe and adequate way of disposal is necessary. Although currently there is limited

information regarding the disposal of the fouling deposits, there are some studies reporting that the biggest share of petroleum coke is mainly used in cement and concrete industries, while a smaller amount is used in brick kilns.[39] Finally, lower grade petroleum coke (containing higher amount of sulfur) is used as a fuel in coal-fired power plants.[40]

1.1. Types of fouling

Although there are many ways to classify crude oil fouling (e.g. according to the type of fluid causing fouling, the type of phase-interphase involved or the type of equipment that undergoes fouling), the most common way is based on the physical, chemical or biological mechanisms that give rise to this phenomenon.[41] Figure 1-3 shows the five main categories of fouling according to Epstein.[42] In crude oil, the different types of fouling can take place individually, but most commonly occur simultaneously.

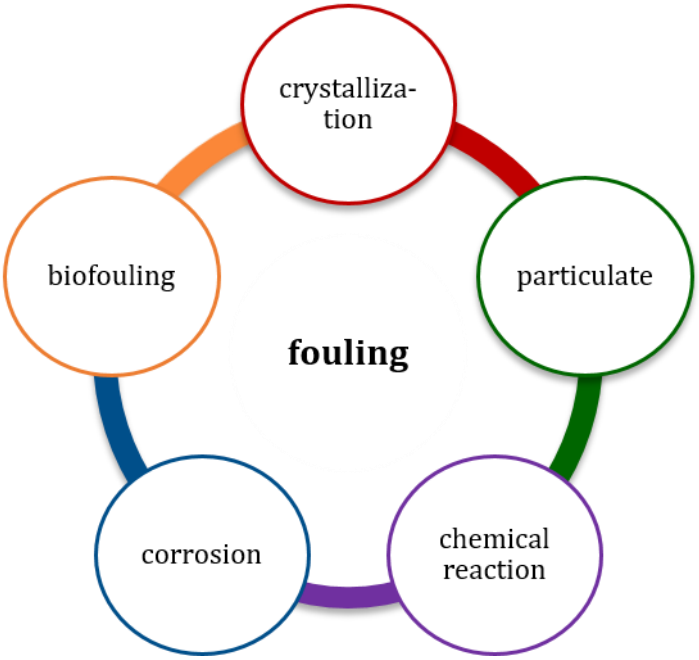

Figure 1-3: Classification of crude oil fouling according to Epstein. [42]

Understanding the mechanisms of fouling is extremely difficult, since the physical and chemical nature of crude oil constituents as well as the interactions among them can have a significant impact. Crude oil is one of the most complex mixtures in the world, containing more than one million different chemical compounds.[43] These compounds can be classified into four major fractions (saturates, aromatics, resins and asphaltenes) differing in terms of chemical composition, molecular weight, solubility and polarity.[44, 45] Under reservoir conditions, crude oil is a stable system, where the constituents remain in

solution and in balance until there is a change in crude oil equilibrium.[34] Thermal alteration, changes of the pressure as well as of the composition of crude oil are among the parameters which not only affect the stability of the system, but also can lead to phase (liquid-solid) separation.[46, 47] This process occurs mainly when the solvent characteristics of the liquid phase are no longer able to maintain the polar and/or the high molecular weight components of crude oil in solution.

Crystallization is a prime example in which such a process can take place and in this case, the asphaltenes and the high-molecular weight paraffins play an important role.[48, 49] In crude oil, the asphaltene fraction remains dispersed and in solution as long as the resin molecules are present in high concentration. However, once a change in the system occurs, either by adding large quantities of alkanes or by removing the resin fraction, asphaltenes tend to form large aggregates and precipitate. Similarly, the paraffin constituents remain in solution as natural components of crude oil until changes in temperature, pressure and composition of crude oil occur. A decrease of the temperature and an increase of the aromaticity of the liquid medium will affect their solubility and the paraffin components will begin to crystallize into solid wax particles (wax crystallization)[34].

In case of *particulate fouling* (also known as sedimentation), particles, mostly originated either from a poor desalting process of have been entered during the distillation process, accumulate and deposit on the heat transfer surface. These are mostly insoluble inorganic particles such as dust, mud and sand particles, inorganic salts (e.g. $CaCl_2$, NaCl and $MgCl_2$), corrosion products or catalyst particles.[50] The precipitation of crystals and particles are responsible for the physical part of fouling.

Chemical reaction fouling is the most dominant mechanism involved in the formation of solid material in preheat trains[34] and simultaneously the most complicated and poorly understood. Despite the various industrial and academic studies over several years to understand the chemical reactions that govern fouling, there are still strong arguments not only on the fouling precursors and the conversion processes involved in deposit production, but also on the location of the reactions as well as on the parameters which influence the fouling rate.[33, 51-53] The investigation of this phenomenon becomes even more difficult since crude oil fouling can proceed through several pathways such as autoxidation, polymerization and thermal decomposition (coking and cracking).[14, 54, 55] According to Watkinson and Wilson, chemical reaction fouling is a multi-step process and

a general overview of this mechanism can be seen in Figure 1-4.[56] Briefly, a soluble precursor A can either enter with the incoming fluid or can be formed as a result of reactions that take place in the crude oil. Later on, it will get transported to the surface of the heat exchanger where it will undergo surface reactions eventually producing the insoluble deposit C on the wall. Another alternative of this process involves firstly the formation of a foulant B from a precursor A either by reactions which occur in the bulk liquid or in the thermal boundary layer. The foulant B will get transferred and adhered to the heat transfer surface and finally might undergo an ageing reaction on the surface, producing the deposit C.

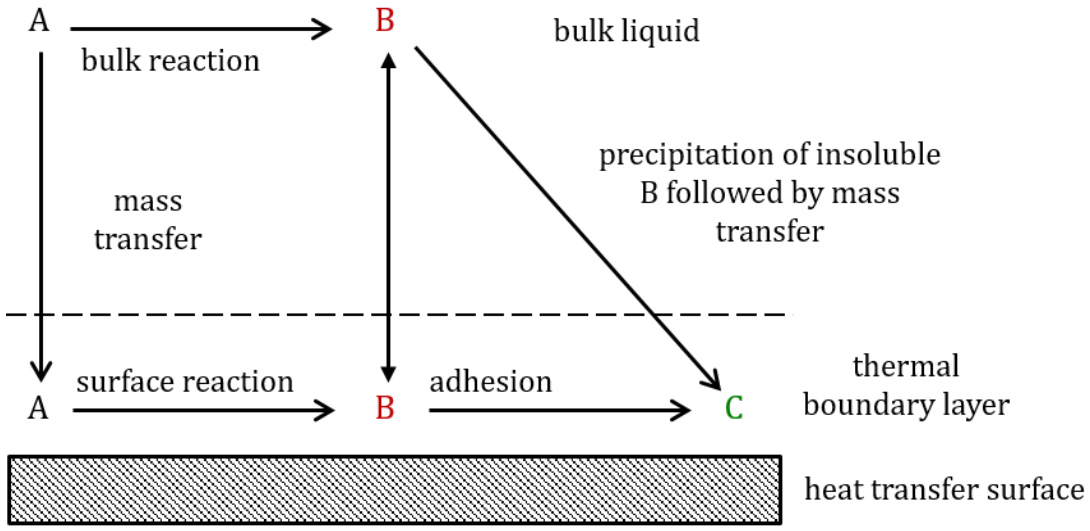

Figure 1-4: Multi-step fouling mechanism according to Watkinson and Wilson.[56]

Corrosion fouling is also known to participate in the formation of deposits. In this case, deposition of solid material occurs as a result of reactions between a reactant and a metal surface. Although the heat exchanger surface material is not reactive, it might act as a catalyst in complex chemical mechanisms.[34] Several factors such as surface roughness, thermal resistance, temperature, or crude oil composition can affect the fouling rate. The presence of H_2S, NH_3 (decomposition products of nitrogen and sulfur containing compounds during refinery), FeS (formed through reaction of H_2S with iron containing surfaces), naphthenic acids, HCl (formed as a result of hydrolysis of calcium and magnesium chlorides), and metals (e.g. V, Cu, and Ni) can cause corrosion problems in the refinery unit.[57]

Finally, *biofouling* can occur either due to microorganisms such as bacteria, algae or fungi, or macroorganisms such as mussels.[31] Once the organisms come into contact with

the heat transfer surface, they will attach and grow, forming an organic film. Biofouling is in general the least expected mechanism taking place in a refinery since its occurrence is mostly associated with the presence of untreated water which can be used as a coolant.[58]

1.2. State of the Art in fouling analysis

Although crude oil fouling has been the subject of many studies over the last decades, the underlying mechanisms that lead to the formation of solid materials are still poorly understood. One main limitation is that most of the current studies are dealing with the symptoms of fouling, meaning that the main focus relies on limiting its impact by productive and engineering means instead of studying the causes, i.e. the fundamental changes within an oil on a molecular level. Therefore, detailed studies of the transformation processes in the liquid and the solid state are necessary. Here, the analytical methods play an important role. Nowadays, most of the analytical methods employed in a refinery unit are limited to the bulk properties of the feedstocks.[59, 60]Defining the bulk properties in terms of boiling point, API gravity, density, acidity or asphaltene content can reveal useful information regarding the nature of the sample as well as their stability and compatibility. However, these features describe only some general characteristics of the raw material, while no information regarding their fouling behavior can be obtained. Only lately, various studies investigate the influence of different crude oil fractions on fouling tendencies, while most of them are focused on the characterization of the heavier fractions (e.g. resins and asphaltenes) since their presence is believed to have a significant impact on fouling rates.[61, 62]

Over the years, various techniques have been used for the characterization of fouling deposits, each providing a specific type of information regarding their elemental composition, morphology or chemical structure. Techniques such as elemental analysis (EA),[63] X-Ray fluorescence (XRF)[64] or inductively coupled plasma optical emission spectrometry (ICP-OES)[65] have been used to determine either the carbon, hydrogen, nitrogen or sulfur content or the presence of metals and other inorganic elements. Information regarding the morphology of the solid material has been obtained with the use of optical microscopy (OM),[66] scanning electron microscopy (SEM)[67] or X-Ray diffraction (XRD).[68] Depending on the chosen method, identification of the nature of coke in fouling deposits, the composition of the deposits or the presence of specific crystalline compounds has been successfully demonstrated. In case of the chemical structure,

information in terms of the aromaticity of the sample, the chemical bonds or the functional groups can be gained with the use of ultraviolet-fluorescence (UV-F),[69] Fourier transform-infrared (FT-IR)[70] or nuclear magnetic resonance (NMR) spectroscopy,[71, 72] respectively.

Regarding the analysis of the soluble fraction of the deposits, only few studies exists in the literature. Among them, Venditti and co-workers demonstrated the combination of several analytical techniques in order to obtain comprehensive information regarding the nature of the deposits.[73] For this purpose, four foulants deposited in a refinery heat exchanger were subjected to solubility tests by using different solvent mixtures. The extracted materials were analyzed by size-exclusion chromatography (SEC) and synchronous UV-F spectroscopy, while the solid materials were examined with the use of thermo-gravimetric analysis (TGA), EA and attenuated total reflection-FTIR (ATR-FTIR). In the analysis of the liquid phase, information regarding the larger aromatic ring systems was obtained, while for the analysis of the solids, information regarding the volatiles, ash content, heteroatom content and structural features of the deposits was acquired. However, the use of these techniques is limited since they mostly cover a small part of fouling. In order to encounter the various problems related to fouling and to establish suitable strategies for preventing it, information on single compounds that are involved in fouling, as a precursor, intermediate or final product is necessary.

1.3. Analytical methods used in this study

1.3.1. Ultra-high resolution mass spectrometry

Over the last decades, the analysis of complex samples such as crude oil has driven the development of analytical techniques even further. The term complexity indicates not only an unmatched number of compounds present within a sample but also a diversity regarding their molecular weight distribution (up to over 1000 Da), polarity (from non-polar to polar with N, O, S heteroatoms) and acidity (acidic, neutral, or basic).[44] Recent reports showed that more than hundred thousand unique elemental compositions were detected in an asphalt volcano sample[74] while, a new record of more than two hundred assignments has been demonstrated at the characterization of vacuum residues.[75] The wide range of compounds present in the sample results in extremely crowded mass spectra and such an example can be seen in Figure 1-5.

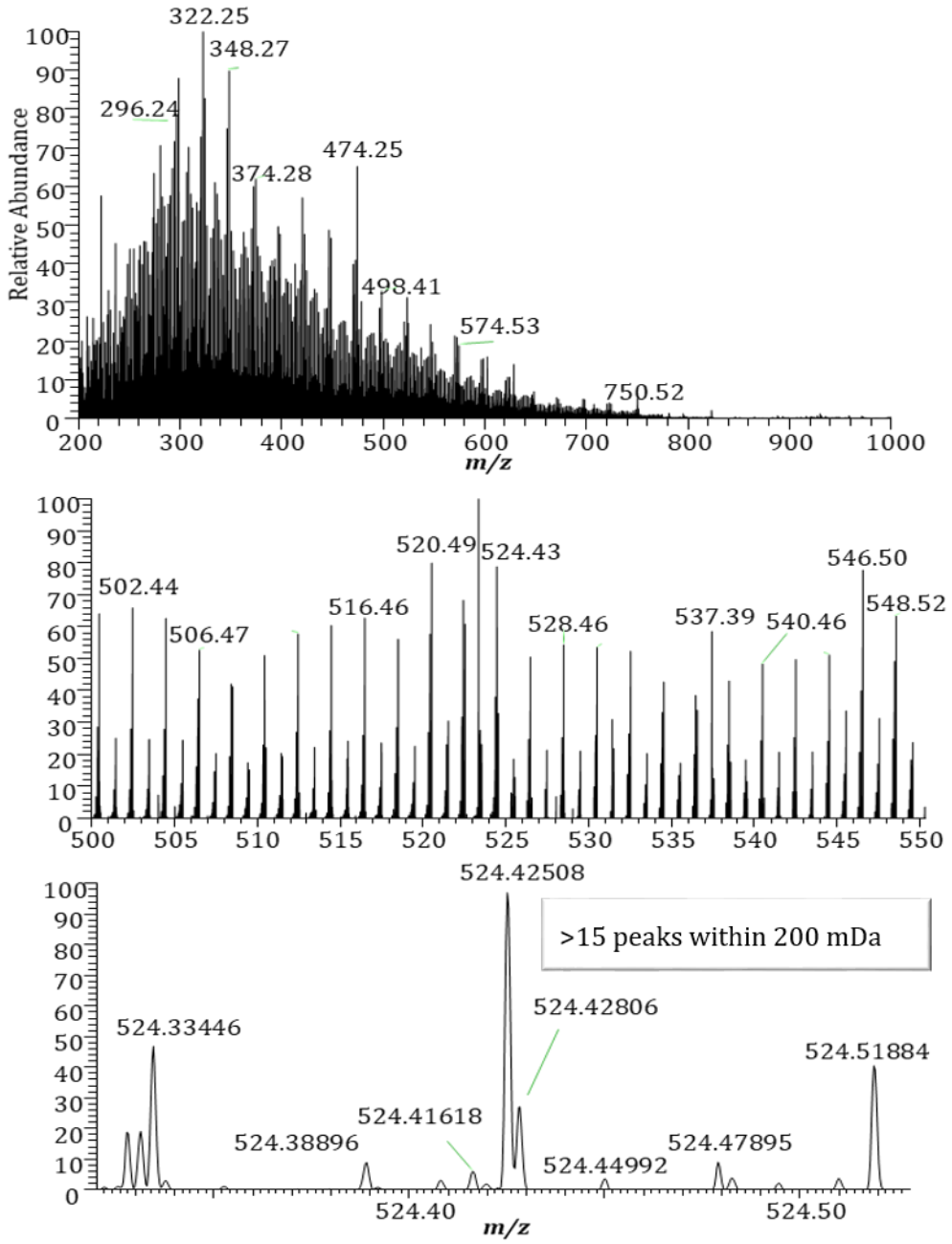

Figure 1-5: Averaged mass spectrum of a crude oil of arabic origin obtained using ESI in positive ion-mode (top) with the mass scale-expanded view at *m/z* 500-550 (middle) with a further zoomed-in mass range between 524.33-524.52 (bottom).

Therefore, for the characterization of these compounds, ultra-high mass resolving power R = $m/\Delta m$ (with Δm being the full peak width at half maximum height (FWHM) as well as high mass accuracy measurements with a large dynamic range over a wide mass range are required. The requirement for high resolving power arises from the need to resolve very narrow mass differences between isobaric functionalities in crude oil. The

most critical mass splits include the differences between CH_4 vs O (0.0364 Da), CH_2 vs N (0.0126 Da) and C_3 vs SH_4 (0.0034 Da) with the latter one to require more than 89,000 resolving power at *m/z* 300.[76, 77] The high mass accuracy is needed in order to determine the chemical composition of a given peak with an error of less than 1 ppm.[78]

Nowadays, several types of mass analyzers such as quadrupoles, time of flight or ion trap are available. However, due to their limitations in providing ultra-high resolution and/or mass accuracy these analyzers are not fully suitable for the analysis of crude oil. Recently, two types of mass spectrometers are predominantly used in the characterization of crude oil that meet the above mentioned requirements; the Fourier transform Orbitrap mass spectrometer (FT Orbitrap MS) and the Fourier transform ion cyclotron resonance mass spectrometer (FT-ICR MS).[77, 79, 80] In both cases, in order to force the ions into their corresponding motion (cyclotron motion or harmonic oscillation) an electromagnetic or electrostatic field is necessary. The motion of the ions induces an image current which is detected as a function of time.[81] The current can be mathematically processed using the Fourier transform algorithm to convert it from a time-domain signal (transient) to a frequency-domain signal. One advantage of the FT-based mass analyzers is that the oscillation frequency is directly related to the *m/z* ratio of the ions meaning that that there is no dependency on the ions kinetic energy. Resolving power in both instruments can be achieved by accumulation of longer time domain transients.[82]

During this study, a research-type Orbitrap Elite (Thermo Fisher Scientific, Bremen, Germany) mass spectrometer was used and its schematic representation can be seen in Figure 1-6. This instrument is a hybrid mass spectrometer, incorporating a dual cell linear ion trap (LTQ, Velos Pro) and a high-field Orbitrap mass analyzer.[83] The LTQ trap consists of a dual pressure technology where the manipulation of the ions takes place. The first cell is operated at a higher pressure of helium gas (5.0×10^{-3} torr) and is used for ion trapping, ion storage, precursor ion isolation and fragmentation purposes. The increase of the pressure in the ion trap results in an increase of the trapping efficiency higher than 90 %. On the other hand, the second cell operates at lower pressure (3.5×10^{-4} torr) and is used for scanning ions out to the electrodes (e.g. mass analysis).[84] The ion trap enables the so called automatic gain control (AGC), a feature to control the filling rate of the subsequent FT analyzer. By setting specific ion target values, space charge effects can be avoided or minimized.[85]

As the ions are axially ejected from the linear trap, they move to a gas-filled curved linear trap (C-trap) where they lose their kinetic energy due to collisions with nitrogen gas. At the entrance and the exit of the orifice, voltages are ramped up in order to squeeze the ions into a smaller packet. Afterwards, a voltage pulse across the C-trap ejects the ions towards the Orbitrap analyzer.

The Orbitrap analyzer consist of a central spindle-shaped electrode and an outer barrel-like electrode (two split halves). A high voltage is applied to the central electrode creating an electrostatic field. The ion trajectories combine rotation motion around the central electrode with harmonic back and forth oscillations along it. The frequency (ω) of the harmonic ion oscillations along the axis is measured non-destructively by acquisition of time-domain image current transients and depends only on the ions' *m/z* and the instrumental constant k.[86]

$$\boldsymbol{\omega} = \sqrt{\frac{\mathbf{z}}{\mathbf{m}} \cdot \mathrm{k}}$$

The instrument used here, incorporates a new design (high field) of the Orbitrap. In this case, the gap between the inner and outer electrode has been decreased, providing a higher field strength for a fixed voltage. Thus, the higher frequencies of ion oscillations result in higher resolving power. The resolving power acquired with this instrument can be over 960,000 at *m/z* 400 with a transient time of 3.04 s.[87]

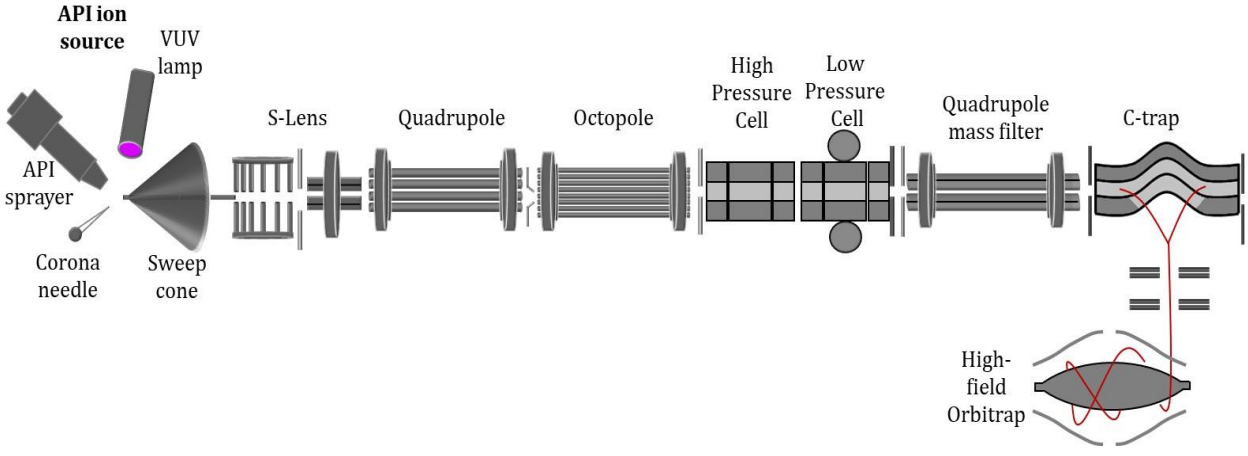

Figure 1-6: Schematic view of an Orbitrap Elite mass spectrometer.

1.3.2. Gas chromatography

One of the main problems in the analysis of crude oil is the presence of various isomeric compounds which contribute to its overall complexity. In order to simplify high complex mixtures, the use of a chromatographic separation is necessary.[88] The oldest and most widely used method in characterization of volatile and semi-volatile compounds in crude oil is gas chromatography (GC).[89, 90] Various aliphatic and polyaromatic hydrocarbons in crude oils as well as heteroatom (N, O, S) containing compounds in crude oil fractions have been successfully analyzed with comprehensive two-dimensional GC (GC×GC).[91, 92] The coupling method of gas chromatography to mass spectrometry (GC-MS) has been successfully used for the characterization of naphthenic acids, thiophenes and sulfides.[93, 94] Until recently, one main limitation in GC-MS analysis was the inability to provide high resolution measurements. Although traditional instrumentation employs several types of mass analyzers (quadrupole, time of flight) these are not able to separate all the individual isobaric components.[95, 96] Their low mass accuracy and their inefficiency to provide high-resolution mass measurements make them not the method of choice for crude oil characterization. Nowadays, the newly developed GC Orbitrap-based mass spectrometer has expanded the analysis of complex mixtures even further. Features such as high resolution, high mass accuracy and sensitivity can be for the first time combined to a powerful chromatographic separation enabling a deeper understanding of the samples on a molecular level.[97] While electron ionization is the most commonly ionization source employed in GC-MS analysis, a newly developed commercial GC-APPI interface exploits the ionization of a broader range of compounds.[88, 98]

1.3.3. Ionization techniques

One important parameter that needs to be considered, especially when dealing with the analysis of a complex mixture such as crude oil, is the choice of an adequate ionization method. Over the years, various analytical techniques have been employed for this purpose, but unfortunately there is no single method which can fully characterize a crude oil.[99] Each ionization technique shows a selectivity towards specific type of compounds and in this case, the nature of the sample plays a significant role. In crude oil analysis, traditional vacuum ionization methods such as EI and CI are mostly used in GC-MS analysis, while atmospheric pressure ionization (API) methods are the most frequently used. During this study, electron ionization (EI), electrospray ionization (ESI),

atmospheric pressure photoionization (APPI), and atmospheric pressure chemical ionization (APCI) were chosen for the investigation of a light crude oil fraction and its fouling reaction.

Electron ionization

Electron ionization (EI) is one of the oldest and most widely used methods in mass spectrometry due to its ability to ionize a wide range of analytes. Saturated and unsaturated aliphatic compounds, aromatic hydrocarbons as well as heterocycles are among the compounds which have been successfully ionized by this method.[100] Electron ionization is a gas-phase process, meaning that the analyte needs to be transferred into the gas phase without thermal decomposition. The neutral analytes in the gas phase enter the ionization chamber which is maintained at low pressure of 10^{-3} –10^{-4} Pa in order to avoid molecule collisions. The vaporized molecules are ionized by an electron beam which is produced from a heated (1600–2000 °C) filament. When an electron with high kinetic energy collides with an analyte molecule, the transferred energy leads to the expulsion of an electron from its highest occupied molecular orbital (HOMO). As a result, an excited radical cation of the analyte molecule ($M^{+\cdot}$*) is formed.[100] Due to the excess of energy imparted on these ions they can undergo a single or multiple fragmentation.

While only 7-12 eV are required for the ionization of most organic compounds, a high energy of 70 eV is commonly used for reproducibility and comparability reasons. Also, from the fragmentation induced at the excess energy structural information can be obtained.[101] Different compounds exhibit a characteristic fragmentation which can be matched to a spectral library. However, the use of this technique in crude oil analysis is quite limited since the interpretation of the spectra is almost impossible.[102] In many cases, the molecular ion is not observed and therefore information on the molecular weight is missing while the presence of different isomers makes the interpretation even more difficult. In the last years, more frequently the use of low-voltage electron ionization (LVEI) is preferred in crude oil analysis.[103] By using lower energy (10-12 eV) EI, little excess energy is transferred to the analyte, resulting in less fragmentation. In this case, a simpler spectrum is obtained enabling to distinguish the fragments and the molecular ions. As has been reported lately, the use of different ionization energies can provide complementary information regarding the analyte.[88]

Electrospray ionization

Electrospray ionization (ESI) is the method of choice for the ionization of polar compounds, and its ionization efficiency depends largely on the basicity or the acidity of the compound. This method typically generates protonated ($[M+H]^+$) or deprotonated ($[M+H]^-$) molecules through Brønsted-Lowry reactions, and/or cationized molecules (e.g. ($[M+Na]^+$) via a Lewis acid-base mechanism.[104, 105] Briefly, a sample solution is introduced into the ion source through a capillary that is held at a potential difference of ± 3-5 kV against the mass spectrometer inlet. In the presence of the high electric field, the emerging liquid from the capillary tip is formed into a fine cone (known as the ''Taylor cone") from which charged droplets are released.[106] This process is assisted by the introduction of a nebulizing gas (usually dry nitrogen) which flows around the capillary to aid solvent evaporation. As the droplets move towards the orifice of the mass spectrometer, desolvated gas-phase ions are formed. For this process, two possible mechanisms are discussed.[107] One is known as the "charged residue model'' in which a complete desolvation of the ions occurs by successive loss of all solvent molecules from the droplets.[108] During solvent evaporation, the charge density at the surface of the droplet increases, until it reaches the Rayleigh limit. Further desolvation then leads to division of charged droplets by Coulomb explosion until individual ions are formed in the gas phase. The other mechanism is known as the "ion evaporation model'' suggesting that droplet charge is reduced by expelling ions from their surface before total droplet fission.[109] Although ESI is excessively used for many decades, its exact mechanism has not been fully explored.

Several studies report that under specific conditions the formation of radical cations is possible. In this case, the ESI source acts as a controlled-current electrolytic (CCE) flow cell where redox reactions take place.[110] Based on this mechanism the detection of polyaromatic hydrocarbons and heterocycles as radical cations from asphaltenes has been shown recently.[111]

Atmospheric pressure chemical ionization

The main principle of atmospheric pressure chemical ionization (APCI) relies on gas-phase ion-molecule reactions occurring at atmospheric pressure. The introduction of the sample solution into the source is performed through a heated sprayer, equipped with a silica capillary and operated at high temperature (300 – 500 °C). The liquid solution is formed into a spray of fine droplets with the assistance of an inert nebulizing gas (usually nitrogen). The droplets undergo evaporation before the ionization takes place. In APCI, a corona discharge needle is placed at the end of the heated region and is held at high potential (2-5 kV) producing an electrical discharge (1-5 μA).[112] This discharge initiates the formation of ions, electrons and excited-state species in a plasma. The ionization pathways of an analyte molecule in APCI can be seen in Scheme 1-1. Briefly, the first step in APCI involves the ionization of nitrogen gas molecules by energetic electrons released from the tip of the corona electrode. The nitrogen ions will then undergo collisions with water vapor molecules, which are present in the ion source, generating water cluster ions. In addition, other reagent ions mostly NO^+ and O_2^+ are also present. These reagent ions are then used for the indirect ionization of gaseous organic compounds either through proton or charge transfer or via hydride abstraction.[113, 114]

$$N_2 + e^- \rightarrow N_2^{\cdot+} + 2e^-$$

$$N_2^{\cdot+} + 2N_2 \rightarrow N_4^{\cdot+} + N_2$$

$$N_4^{\cdot+} + H_2O \rightarrow H_2O^{\cdot+} + 2N_2$$

$$H_2O^{\cdot+} + H_2O \rightarrow H_3O^+ + HO^{\cdot}$$

$$H_3O^+ + H_2O + N_2 \rightarrow [H^+(H_2O)_2] + N_2$$

$$[H^+(H_2O)_{n\text{-}1}] + H_2O + N_2 \rightarrow [H^+(H_2O)_n] + N_2$$

Scheme 1-1: Reaction mechanisms for positive mode APCI.

Atmospheric pressure photoionization

Atmospheric pressure photoionization (APPI) is the last arrival in the family of atmospheric pressure ionization methods and was originally developed as an interface for LC-MS. In crude oil analysis it has become one of the most important ionization methods due to its ability to simultaneously ionize both, nonpolar and polar compounds.[115] In the case of APPI, a noble gas discharge lamp (usually Krypton) is used as a source of photons with a photon emission at 10.0 and 10.6 eV (124 nm and 117 nm). This emitted energy is high enough to ionize most of the organic compounds, but low enough to ionize water, atmospheric gases (e.g. nitrogen) or common solvents such as methanol, acetonitrile or hexane. APPI involves multiple pathways through which an ion can be formed (Scheme 1-2).[116] In case of direct photoionization, a photon (hv) is absorbed by a molecule causing the ejection of an electron. This will eventually lead to the formation of radical cations ($M^{\cdot+}$). This process takes place when the photon energy is higher than the ionization potential of the molecule. The generated radical cations from the direct photoionization can undergo further reactions with a solvent or other analyte molecules. In this case, protonated molecules will be formed as a result of proton transfer reactions from the solvent. Nowadays, a commonly used strategy in order to enhance the signal intensity in APPI, is the addition of a dopant (e.g. toluene, acetone). In dopant assisted APPI, the initial reaction is the formation of a radical dopant ion. This ion, can further react with the molecules of the analyte through charge or proton transfer. Alternatively, the dopant can facilitates the ionization of chemical compounds through the formation of clusters between the analyte, dopant and water molecules, from which a proton transfer forms the resulting protonated molecules.[117, 118]

$$M + hv \rightarrow M^{\cdot+} + e^-$$
$$M^{\cdot+} + S \rightarrow [M + \mathrm{H}]^+ + [S - \mathrm{H}]^{\cdot}$$
$$D + hv \rightarrow D^{\cdot+} + e^-$$
$$D^{\cdot+} + M \rightarrow D + M^{\cdot+}$$
$$D^{\cdot+} + M \rightarrow [M + \mathrm{H}]^+ + [D - \mathrm{H}]^{\cdot}$$
$$D^{\cdot+} + (\mathrm{H_2O})_n \rightarrow [(\mathrm{H_2O})_n + \mathrm{H}]^+ + [D - H]^{\cdot}$$
$$[(\mathrm{H_2O})_n + \mathrm{H}]^+ + M \rightarrow [M + \mathrm{H}]^+ + n\mathrm{H_2O}^{\cdot}$$

Scheme 1-2: Reaction pathways for ionization of an analyte (M) in positive APPI. The letters S and D represent a solvent and a dopant, respectively.

1.4. Tandem mass spectrometry

Tandem mass spectrometry (also known as MS/MS) is a useful technique incorporated in trace analysis in complex mixtures or structural elucidation of unknown compounds.[119] Tandem MS measurements are performed either in space or in time.[120] In tandem-in-space, the processes of ion selection, dissociation and mass analysis are performed in separated regions of the instrument. For example, in case of a triple quadrupole (QqQ), a precursor ion is selected and isolated in the first mass analyzer (Q_1) and transmitted to the collision cell (q_2) in which fragmentation takes place. The generated product ions are transmitted to a second analyzer (Q_3) for mass analysis. Typical tandem in space instruments include quadrupole type, time of flight or double focusing mass spectrometers. In the case of tandem-in-time, the above mentioned processes take place in the same region, but consecutively. This process can be repeated several times and is denoted as MS^n. Tandem in time is achieved with the use of ion traps, Orbitrap and FT-ICR mass analyzers.

During this study, the technique of collision-induced dissociation (CID) was used for the fragmentation of selected ions. Through this technique, information for one of the reaction products formed after the fouling reactions could be obtained. CID is the most common activation method where mass-selected precursor ions are accelerated by applying an RF potential in order to increase their kinetic energy. These highly energetic ions will collide with gas molecules (He, N_2, or Ar) and some of their kinetic energy will be converted into internal energy resulting in bond breakage and fragmentation.[121, 122]

1.5. References

1. *U.S. Energy International Administration (EIA)*; International Energy Outlook: 2018.

2. Azarpour, A.; Suhaimi, S.; Zahedi, G.; Bahadori, A., A Review on the Drawbacks of Renewable Energy as a Promising Energy Source of the Future. *Arabian J. Sci. Eng.* **2013,** *38* (2), 317-328.

3. Cronshaw, I., World Energy Outlook 2014 projections to 2040: natural gas and coal trade, and the role of China. *Aust. J. Agric. Resour. Econ.* **2015,** *59* (4), 571-585.

4. Chengzao, J., Breakthrough and significance of unconventional oil and gas to classical petroleum geology theory. *Petrol. Explor. Develop.* **2017,** *44*, 1-10.

5. Miller, R. G.; Sorrell, S. R., The future of oil supply. *Philos. Trans. A, Math. Phys. Eng. Sci.* **2014,** *372*, 1-27.

6. Zheng, L.; Wei, P.; Zhang, Z.; Nie, S.; Lou, X.; Cui, K.; Fu, Y., Joint exploration and development: A self-salvation road to sustainable development of unconventional oil and gas resources. *Nat. Gas Ind. B* **2017,** *4* (6), 477-490.

7. Hart, A., A review of technologies for transporting heavy crude oil and bitumen via pipelines. *J. Pet. Explor. Prod. Technol.* **2014,** *4* (3), 327-336.

8. Santos, R. G.; Loh, W.; Bannwart, A. C.; Trevisan, O. V., An overview of heavy oil properties and its recovery and transportation methods *Braz. J. Chem. Eng.* **2014,** *31*, 571-590.

9. Watkinson, A. P., Deposition from Crude Oils in Heat Exchangers. *Heat Transfer Eng.* **2007,** *28* (3), 177-184.

10. Watkinson, P.; Asomaning, S., Petroleum Stability and Heteroatom Species Effects in Fouling of Heat Exchangers by Asphaltenes. *Heat Transfer Eng.* **2000,** *21*, 10-16.

11. Panda, S. K.; Andersson, J. T.; Schrader, W., Characterization of Supercomplex Crude Oil Mixtures: What is Really in There? *Angew. Chem.* **2009,** *48* (10), 1788-1791.

12. Deshannavar, U. B.; Rafeen, M. S.; Ramasamy, M.; Subbarao, D., Crude Oil Fouling: A Review. *J. Appl. Sci.* **2010,** *10* (24), 3167-3174.

13. Kovo, A., Mathematical Modelling and Simulation of Fouling of Nigerian Crude Oil Equipment Installations. *Leonardo J. Sci.* **2006,** *5*, 111-124.

14. Crittenden, B.; Kolaczkowski, S. T.; Downey, I. L., Fouling of crude oil preheat exchangers. *Chem. Eng. Res. Des.* **1992,** *70*, 547-557.

15. Smaïli, F.; Vassiliadis, V. S.; Wilson, D. I., Mitigation of Fouling in Refinery Heat Exchanger Networks by Optimal Management of Cleaning. *Energy Fuels* **2001,** *15* (5), 1038-1056.

16. Polley, G.; Morales-Fuentes, A.; Wilson, I., Simultaneous Consideration of Flow and Thermal Effects of Fouling in Crude Oil Preheat Trains. *Heat Transfer Eng.* **2009,** *30*, 815-821.

17. Jones, D. S. J., *Elements of Petroleum Processing*. Wiley & Sons: New York, 1995.

18. Taofeek Popoola, L.; Gutti, B.; Susu, A., A Review of an Expert System Design for Crude Oil Distillation Column Using the Neural Networks Model and Process Optimization and Control Using Genetic Algorithm Framework. *Adv. Chem. Eng. Sci.* **2013,** *03*, 164-170.

19. Bott, T. R., *Fouling of Heat Exchangers.* Elsevier Science: Amsterdam, 1995; p 546.

20. Wilson, D. I., Polley, G. T., Mitigation of Refinery Preheat Train Fouling by Nested Optimization. In *Advances in Refinery Fouling Mitigation Session #46*, AlChE: Huston, 2001; pp 287-294.

21. Wiehe, I. A.; Kennedy, R. J., The Oil Compatibility Model and Crude Oil Incompatibility. *Energy Fuels* **2000,** *14* (1), 56-59.

22. Chhabra, R. P., *CRC Handbook of Thermal Engineering, Second Edition*. CRC Press: 2017.

23. Ogbonnaya, S.; Ajayi, O., Fouling phenomenon and its effect on heat exchanger: A review. *Front. Heat Mass Transfer* **2017,** *9*, 1-12.

24. Pugh, S.; Hewitt, G. F.; Müller-Steinhagen, H., Heat Exchanger Fouling in the Pre-Heat Train od a Crude Oil Distillation Unit - The Development of a "User Guide". In *Proceedings of the 4th International Conference on Heat Exchanger Fouling, Fundamental Approaches & Technical Solutions*, Davos, 2002; pp 201-212.

25. Macchietto, S.; F. Hewitt, G.; Coletti, F.; Crittenden, B.; Dugwell, D.; Galindo, A.; Jackson, G.; Kandiyoti, R.; Kazarian, S.; Luckham, P.; Matar, O.; Millan-Agorio, M.; Müller, E.; Paterson, W.; Pugh, S.; Richardson, S.; Wilson, I., Fouling in Crude Oil Preheat Trains: A Systematic Solution to an Old Problem. *Heat Transfer Eng.* **2011,** *32*, 197-215.

26. Steinhagen, R.; Müller-Steinhagen, H.; Maani, K., Problems and Costs due to Heat Exchanger Fouling in New Zealand Industries. *Heat Transfer Eng.* **1993,** *14* (1), 19-30.

27. Huangfu, E.-P.; B. Panchal, C., Effects of Mitigating Fouling on the Energy Efficiency of Crude-Oil Distillation. *Heat Transfer Eng.* **2000,** *21*, 3-9.

28. Liporace, F.; Gregório de Oliveira, S., Real Time Fouling Diagnosis and Heat Exchanger Performance. *Heat Transfer Eng.* **2007,** *28*, 193-201.

29. Van Nostrand, W. L.; Leach, S. H.; Haluska, J. L., Economic penalties associated with the fouling of refinery heat transfer equipment. In *Fouling of Heat Transfer Equipment*, Somerscales, E. F. C., Knudsen, J. G., Ed. New York, 1981; pp 619-643.

30. Diaz-Bejarano, E.; Coletti, F.; Macchietto, S., Modelling and Prediction of Shell-Side Fouling in Shell-And-Tube Heat Exchangers. *Heat Transfer Eng.* **2018,** *0*, 1-17.

31. Coletti, F.; Macchietto, S., Predicting Refinery Energy Losses Due to Fouling in Heat Exchangers. *Comput.-Aided Chem. Eng.* **2009,** *27*, 219-224.

32. Müller-Steinhagen, H.; Malayeri, M. R.; Watkinson, P., Heat Exchanger Fouling: Environmental Impacts. *Heat Transfer Eng.* **2009,** *30*, 773-776.

33. Coletti, F.; Hewitt, G. F., *Crude Oil Fouling: Deposit Characterization, Measurements, and Modeling*. Gulf Prefessional Publishing: 2015.

34. Speight, G., *Fouling in Refineries*. Gulf Professional Publishing: 2015.

35. Diaz-Bejarano, E.; Coletti, F.; Macchietto, S., A new dynamic model of crude oil fouling deposits and its application to the simulation of fouling-cleaning cycles. *AIChE* **2016,** *62* (1), 90-107.

36. Joshi, H. M.; Brons, G., Chemical Cleaning of Oil Refinery Heat Exchangers - The Need for a Joint Effort. In *Heat Exchanger Fouling and Cleaning: Fundamentals and Applications*, ECI Digital Archives: USA, New Mexico, 2003; pp 219-220.

37. Murphy, G.; Campbell, J., Fouling in refinery heat exchangers: causes, effects, measurement and control. In *Fouling Mechanisms, GRETh Seminar*, Bohnet, M., Ed. Editions Européennes Thermique et Industrie: Grenoble, France, 1992; pp 249-261.

38. Keyte, I. J.; Harrison, R. M.; Lammel, G., Chemical reactivity and long-range transport potential of polycyclic aromatic hydrocarbons – a review. *Chem. Soc. Rev.* **2013,** *42* (24), 9333-9391.

39. González, A.; Navia, R.; Moreno, N., Fly ashes from coal and petroleum coke combustion: Current and innovative potential applications. *Waste Manage. Res.* **2009,** *27*, 976-87.

40. Santos, A.; Silva, R.; Luiza Grillo Renó, M., Analysis of Petroleum Coke Consumption in Some Industrial Sectors. *J. Pet. Sci. Res.* **2015,** *4*, 1-7.

41. Epstein, N. In *Fouling in heat exchangers*, 4th Int. Conf. Fouling of heat transfer equipment, 1981; pp 235-253.

42. Epstein, N., Thinking about Heat Transfer Fouling: A 5 × 5 Matrix. *Heat Transfer Eng.* **1983,** *4* (1), 43-56.

43. Beens, J.; Blomberg, J.; Schoenmakers, P. J., Proper Tuning of Comprehensive Two-Dimensional Gas Chromatography (GC×GC) to Optimize the Separation of Complex Oil Fractions. *J. High Resolut. Chromatogr.* **2000,** *23*, 182-188.

44. Gaspar, A.; Zellermann, E.; Lababidi, S.; Reece, J.; Schrader, W., Characterization of Saturates, Aromatics, Resins, and Asphaltenes Heavy Crude Oil Fractions by Atmospheric Pressure Laser Ionization Fourier Transform Ion Cyclotron Resonance Mass Spectrometry. *Energy Fuels* **2012,** *26* (6), 3481-3487.

45. Fan, T.; Buckley, J. S., Rapid and Accurate SARA Analysis of Medium Gravity Crude Oils. *Energy Fuels* **2002,** *16* (6), 1571-1575.

46. Mansoori, G. A., PHASE BEHAVIOR IN PETROLEUM FLUIDS. In *Encyclopedia of Life Support Systems*, Petroleum Engineering - Downstream section ed.; UNESCO, UN: Paris, France, 2009; p 33.

47. Ahmadi, Y.; Kharrat, R.; Hashemi, A.; Bahrami, P.; Mahdavi, S., The Effect of Temperature and Pressure on the Reversibility of Asphaltene Precipitation. *Pet. Sci. Technol.* **2014,** *32*, 2263-2273.

48. García, M., Crude Oil Wax Crystallization. The Effect of Heavy n-Paraffins and Flocculated Asphaltenes. *Energy Fuels* **2000,** *14*, 1043-1048.

49. Molina V, D.; Ariza León, E.; Chaves-Guerrero, A., Understanding the Effect of Chemical Structure of Asphaltenes on Wax Crystallization of Crude Oils from Colorado Oil Field. *Energy Fuels* **2017,** *31* (9), 8997-9005.

50. Al-Haj Ibrahim, H., Fouling in Heat Exchangers. In *MATLAB – A Fundamental Tool for Scientific Computing and Engineering Applications – Volume 3*, Katsikis, V. N., Ed. Sciyo: 2012; pp 57-96.

51. P Watkinson, A.; Li, Y. H. In *Fouling characteristics of a heavy vacuum gas oil in the presence of dissolved oxygen*, Proceedings of International Conference on Heat Exchanger Fouling and Cleaning VIII, Schladming, Austria, H. Müller-Steinhagen; Malayeri, M. R.; Watkinson, A. P., Eds. Schladming, Austria, 2009.

52. Emani, S.; Ramasamy, M.; Shaari, K. Z. B. K., Effect of Shear Stress on Crude Oil Fouling in a Heat Exchanger Tube Through CFD Simulations. *Procedia Eng.* **2016,** *148*, 1058-1065.

53. Shetty, N.; Marappa Gounder, R.; Pendyala, R., Effect of Bulk Temperature on Formation of Crude Oil Fouling Precursors on Heat Transfer Surfaces. *Appl. Mech. Mater.* **2014,** *625*, 482-485.

54. Wilson, I.; Watkinson, P., A Study of Autoxidation Reaction Fouling in Heat Exchangers. *Can. J. Chem. Eng.* **1996,** *74*, 236-246.

55. Fan, Z.; Rahimi, P.; Alem, T.; Eisenhawer, A.; Arboleda, P., Fouling Characteristics of Hydrocarbon Streams Containing Olefins and Conjugated Olefins. *Energy Fuels* **2011,** *25* (3), 1182-1190.

56. Watkinson, A. P.; Wilson, D. I., Chemical reaction fouling: A review. *Exp. Therm. Fluid Sci.* **1997,** *14* (4), 361-374.

57. Somerscales, E. F. C., Fundamentals of corrosion fouling. *Exp. Therm. Fluid Sci.* **1997,** *14* (4), 335-355.

58. Pugh, S.; F. Hewitt, G.; Müller-Steinhagen, H., Fouling During the Use of "Fresh" Water as Coolant - The Development of a "User Guide". *Heat Transfer Eng.* **2009,** *30*, 851-858.

59. El-Sabagh; El-Naggar, A.; El Nady, M.; Badr, I.; Rashad; Ebiad, M.; Abdullah, E., Bulk Geochemical Characteristics of Crude Oils from Suez Gulf, Egypt. *Int. J. Curr. Res.* **2015,** *7*, 20574-20580.

60. Evdokimov, I. N., The Importance of Asphaltene Content in Petroleum—The Revision of Some Persistent Stereotypes. *Pet. Sci. Technol.* **2010,** *28*, 756-763.

61. Mohan Sinnathamb, C.; Mohamad Nor, N., Relationship Between SARA Fractions and Crude Oil Fouling. *J. Appl. Sci.* **2012,** *12*, 2479-2483.

62. Salimi, F.; Ayatollahi, S.; Vafaie Seftie, M., An Experimental Investigation and Prediction of Asphaltene Deposition during Laminar Flow in the Pipes Using a Heat Transfer Approach %J Iranian Journal of Oil & Gas Science and Technology. *IJOGST* **2017,** *6* (2), 17-32.

63. Fan, Z.; Rahimi, P.; McGee, R.; Wen, Q.; Alem, T., Investigation of Fouling Mechanisms of a Light Crude Oil Using an Alcor Hot Liquid Process Simulator. *Energy Fuels* **2010,** *24* (11), 6110-6118.

64. Bennett, C. A.; Appleyard, S.; Gough, M.; Hohmann, R. P.; Joshi, H. M.; King, D. C.; Lam, T. Y.; Rudy, T. M.; Stomierowski, S. E., Industry-Recommended Procedures for Experimental Crude Oil Preheat Fouling Research. *Heat Transfer Eng.* **2006,** *27* (9), 28-35.

65. Al-Jaroudi, S. S.; Ul-Hamid, A.; Al-Matar, J. A., Prevention of failure in a distillation unit exhibiting extensive scale formation. *Desalination* **2010,** *260* (1), 119-128.

66. Bai, C.; Zhang, J., Thermal, Macroscopic, and Microscopic Characteristics of Wax Deposits in Field Pipelines. *Energy Fuels* **2013,** *27* (2), 752-759.

67. Young, A.; Venditti, S.; Berrueco, C.; Yang, M.; Waters, A.; Davies, H.; Hill, S.; Millan, M.; Crittenden, B., Characterization of Crude Oils and Their Fouling Deposits Using a Batch Stirred Cell System. *Heat Transfer Eng.* **2011,** *32* (3-4), 216-227.

68. Muñoz Pinto, D. A.; Cuervo Camargo, S. M.; Orozco Parra, M.; Laverde, D.; García Vergara, S.; Blanco Pinzon, C., Formation of fouling deposits on a carbon steel surface from Colombian heavy crude oil under preheating conditions. *J. Phys.: Conf. Ser.* **2016,** *687*, 012016.

69. Ryder, A. G., Analysis of Crude Petroleum Oils Using Fluorescence Spectroscopy. In *Reviews in Fluorescence 2005*, Geddes, C. D.; Lakowicz, J. R., Eds. Springer US: Boston, MA, 2005; pp 169-198.

70. Wilt, B. K.; Welch, W. T.; Rankin, J. G., Determination of Asphaltenes in Petroleum Crude Oils by Fourier Transform Infrared Spectroscopy. *Energy Fuels* **1998,** *12* (5), 1008-1012.

71. Duarte, L. M.; Filgueiras, P. R.; Silva, S. R. C.; Dias, J. C. M.; Oliveira, L. M. S. L.; Castro, E. V. R.; de Oliveira, M. A. L., Determination of some physicochemical properties in Brazilian crude oil by 1H NMR spectroscopy associated to chemometric approach. *Fuel* **2016,** *181*, 660-669.

72. Iravani, S., NMR Spectroscopic Analysis in Characterization of Crude Oil and Related Products. In *n book: Analytical Characterization Methods for Crude Oil and Related Products*, John Wiley & Sons: 2017.

73. Venditti, S.; Berrueco, C.; Alvarez, P.; Morgan, T.; Millan-Agorio, M.; Herod, A. A.; Kandiyoti, R., Developing characterisation methods for foulants deposited in refinery heat exchangers. In *Int. Conf. On Heat Exchanger Fouling and Cleaning VIII*, Müller-Steinhagen, H.; Malayeri, M. R.; Watkinson, A. P., Eds. Schladming, Austria, 2009; pp 44-51.

74. Krajewski, L. C.; Rodgers, R. P.; Marshall, A. G., 126 264 Assigned Chemical Formulas from an Atmospheric Pressure Photoionization 9.4 T Fourier Transform Positive Ion Cyclotron Resonance Mass Spectrum. *Anal Chem* **2017,** *89* (21), 11318-11324.

75. Palacio Lozano, D. C.; Gavard, R.; Arenas-Diaz, J. P.; Thomas, M. J.; Stranz, D. D.; Mejía-Ospino, E.; Guzman, A.; Spencer, S. E. F.; Rossell, D.; Barrow, M. P., Pushing the analytical limits: new insights into complex mixtures using mass spectra segments of constant ultrahigh resolving power. *Chemical Science* **2019,** *10* (29), 6966-6978.

76. Byer, J. D.; Siek, K.; Jobst, K., Distinguishing the C3 vs SH4 Mass Split by Comprehensive Two-Dimensional Gas Chromatography-High Resolution Time-of-Flight Mass Spectrometry. *Anal Chem* **2016,** *88* (12), 6101-4.

77. Vetere, A.; Schrader, W., Mass Spectrometric Coverage of Complex Mixtures: Exploring the Carbon Space of Crude Oil. *ChemistrySelect* **2017,** *2* (3), 849-853.

78. Olsen, J. V.; de Godoy, L. M.; Li, G.; Macek, B.; Mortensen, P.; Pesch, R.; Makarov, A.; Lange, O.; Horning, S.; Mann, M., Parts per million mass accuracy on an Orbitrap mass spectrometer via lock mass injection into a C-trap. *Molecular & cellular proteomics : MCP* **2005,** *4* (12), 2010-21.

79. Lim, L.; Yan, F.; Bach, S.; Pihakari, K.; Klein, D., Fourier Transform Mass Spectrometry: The Transformation of Modern Environmental Analyses. *Int J Mol Sci* **2016,** *17* (1), 104.

80. Santos, M. J.; Wisniewski Jr, A.; Eberlin, N. M.; Schrader, W., Comparing Crude Oils with Different API Gravities on a Molecular Level Using Mass Spectrometric Analysis. Part 1: Whole Crude Oil. *Energies* **2018,** *11* (10).

81. Scigelova, M.; Hornshaw, M.; Giannakopulos, A.; Makarov, A., Fourier transform mass spectrometry. *Mol. Cell. Proteomics* **2011,** *10* (7).

82. Kaiser, N. K.; Quinn, J. P.; Blakney, G. T.; Hendrickson, C. L.; Marshall, A. G. J. J. o. T. A. S. f. M. S., A Novel 9.4 Tesla FTICR Mass Spectrometer with Improved Sensitivity, Mass Resolution, and Mass Range. *J. Am. Soc. Mass. Spectrom.* **2011,** *22* (8), 1343-1351.

83. Michalski, A.; Damoc, E.; Lange, O.; Denisov, E.; Nolting, D.; Müller, M.; Viner, R.; Schwartz, J.; Remes, P.; Belford, M.; Dunyach, J.-J.; Cox, J.; Horning, S.; Mann, M.; Makarov, A., Ultra high resolution linear ion trap Orbitrap mass spectrometer (Orbitrap Elite) facilitates top down LC MS/MS and versatile peptide fragmentation modes. *Mol. Cell. Proteomics* **2012,** *11* (3), O111.013698-O111.013698.

84. Olsen, J. V.; Schwartz, J. C.; Griep-Raming, J.; Nielsen, M. L.; Damoc, E.; Denisov, E.; Lange, O.; Remes, P.; Taylor, D.; Splendore, M.; Wouters, E. R.; Senko, M.; Makarov, A.; Mann, M.; Horning, S., A dual pressure linear ion trap Orbitrap instrument with very high sequencing speed. *Mol. Cell. Proteomics* **2009,** *8* (12), 2759-2769.

85. Belov, M. E.; Zhang, R.; Strittmatter, E. F.; Prior, D. C.; Tang, K.; Smith, R. D., Automated Gain Control and Internal Calibration with External Ion Accumulation Capillary Liquid Chromatography-Electrospray Ionization-Fourier Transform Ion Cyclotron Resonance. *Anal. Chem.* **2003,** *75* (16), 4195-4205.

86. Perry, R. H.; Cooks, R. G.; Noll, R. J., Orbitrap mass spectrometry: Instrumentation, ion motion and applications. *Mass Spectrom. Rev.* **2008,** *27* (6), 661-699.

87. Denisov, E.; Damoc, E.; Lange, O.; Makarov, A., Orbitrap Mass Spectrometry with Resolving Powers Above 1,000,000. *Int. J. Mass spectrom.* **2012,** *325–327*, 80–85.

88. Kondyli, A.; Schrader, W., High-resolution GC/MS studies of a light crude oil fraction. *J. Mass Spectrom.* **2018,** *54*.

89. Wang, Z.; Fingas, M., Differentiation of the source of spilled oil and monitoring of the oil weathering process using gas chromatography-mass spectrometry. *J. Chromatogr. A* **1995,** *712* (2), 321-343.

90. van de Meent, D.; Brown, S. C.; Philp, R. P.; Simoneit, B. R. T., Pyrolysis-high resolution gas chromatography and pyrolysis gas chromatography-mass spectrometry of kerogens and kerogen precursors. *Geochim. Cosmochim. Acta* **1980,** *44* (7), 999-1013.

91. Gaines, R. B.; Frysinger, G. S.; Hendrick-Smith, M. S.; Stuart, J. D., Oil Spill Source Identification by Comprehensive Two-Dimensional Gas Chromatography. *Environ. Sci. Technol.* **1999,** *33* (12), 2106-2112.

92. Hua, R.; Wang, J.; Kong, H.; Liu, J.; Lu, X.; Xu, G., Analysis of sulfur-containing compounds in crude oils by comprehensive two-dimensional gas chromatography with sulfur chemiluminescence detection. *J. Sep. Sci.* **2004,** *27* (9), 691-8.

93. Holowenko, F. M.; MacKinnon, M. D.; Fedorak, P. M., Characterization of naphthenic acids in oil sands wastewaters by gas chromatography-mass spectrometry. *Water Res.* **2002,** *36* (11), 2843-2855.

94. Wang, M.; Zhao, S.; Chung, K. H.; Xu, C.; Shi, Q., Approach for Selective Separation of Thiophenic and Sulfidic Sulfur Compounds from Petroleum by Methylation/Demethylation. *Anal. Chem.* **2015,** *87* (2), 1083-1088.

95. Szulejko, J. E.; Solouki, T., Potential Analytical Applications of Interfacing a GC to an FT-ICR MS: Fingerprinting Complex Sample Matrixes. *Anal. Chem.* **2002,** *74* (14), 3434-3442.

96. Mbughuni, M. M.; Jannetto, P. J.; Langman, L. J., Mass Spectrometry Applications for Toxicology. *J. Int. Fed. Clin. Chem. Lab. Med.* **2016,** *27* (4), 272-287.

97. Peterson, A. C.; Hauschild, J.-P.; Quarmby, S. T.; Krumwiede, D.; Lange, O.; Lemke, R. A. S.; Grosse-Coosmann, F.; Horning, S.; Donohue, T. J.; Westphall, M. S.; Coon, J. J.; Griep-Raming, J., Development of a GC/Quadrupole-Orbitrap mass spectrometer, part I: design and characterization. *Anal. Chem.* **2014,** *86* (20), 10036-10043.

98. Kersten, H.; Kroll, K.; Haberer, K.; Brockmann, K. J.; Benter, T.; Peterson, A.; Makarov, A. J. J. o. T. A. S. f. M. S., Design Study of an Atmospheric Pressure Photoionization Interface for GC-MS. *J. Am. Soc. Mass. Spectrom.* **2016,** *27* (4), 607-614.

99. Lababidi, S.; Schrader, W., Online normal-phase high-performance liquid chromatography/Fourier transform ion cyclotron resonance mass spectrometry: effects of different ionization methods on the characterization of highly complex crude oil mixtures. *Rapid communications in mass spectrometry : RCM* **2014,** *28* (12), 1345-52.

100. Gross, J. H., Electron Ionization. In *Mass Spectrometry: A Textbook*, Springer Berlin Heidelberg: Berlin, Heidelberg, 2004; pp 193-222.

101. Kind, T.; Fiehn, O., Advances in structure elucidation of small molecules using mass spectrometry. *Bioanalytical reviews* **2010,** *2* (1-4), 23-60.

102. Yuan, Z.; Shi, J.; Lin, W.; Chen, B.; Wu, F.-X., Features-based deisotoping method for tandem mass spectra. *Adv. Bioinformatics* **2011,** *2011*, 210805-210805.

103. Field, F. H.; Hastings, S. H., Determination of Unsaturated Hydrocarbons by Low Voltage Mass Spectrometry. *Anal. Chem.* **1956,** *28* (8), 1248-1255.

104. Vestal, M. L., Methods of Ion Generation. *Chem. Rev.* **2001,** *101* (2), 361-376.

105. Demarque, D. P.; Crotti, A. E.; Vessecchi, R.; Lopes, J. L.; Lopes, N. P., Fragmentation reactions using electrospray ionization mass spectrometry: an important tool for the structural elucidation and characterization of synthetic and natural products. *Nat Prod Rep* **2016,** *33* (3), 432-55.

106. Wilm, M. S.; Mann, M., Electrospray and Taylor-Cone theory, Dole's beam of macromolecules at last? *Int. J. Mass Spectrom. Ion Processes* **1994,** *136* (2), 167-180.

107. Kebarle, P.; Peschke, M., On the Mechanisms by Which the Charged Droplets Produced by Electrospray Lead to Gas Phase Ions. *Anal. Chim. Acta* **2000,** *406*, 11-35.

108. Dole, M.; L. Mack, L.; L. Hines, R.; Mobley, R. C.; Ferguson, L. D.; Alice, M. B., Molecular Beams of Macroions. *J. Chem. Phys.* **1968,** *49*, 2240-2249.

109. V. Iribarne, J.; Thomson, B., On the Evaporation of Small Ions from Charged Droplets. *J. Chem. Phys.* **1976,** *64*, 2287-2294.

110. Van Berkel, G. J.; Zhou, F., Characterization of an Electrospray Ion Source as a Controlled-Current Electrolytic Cell. *Anal. Chem.* **1995,** *67* (17), 2916-2923.

111. Molnárné Guricza, L.; Schrader, W., Electrospray ionization for determination of non-polar polyaromatic hydrocarbons and polyaromatic heterocycles in heavy crude oil asphaltenes. *J. Mass Spectrom.* **2015,** *50* (3), 549-557.

112. Andrade, F. J.; Shelley, J. T.; Wetzel, W. C.; Webb, M. R.; Gamez, G.; Ray, S. J.; Hieftje, G. M., Atmospheric Pressure Chemical Ionization Source. 1. Ionization of Compounds in the Gas Phase. *Anal. Chem.* **2008,** *80* (8), 2646-2653.

113. Horning, E. C.; Carroll, D. I.; Dzidic, I.; Haegele, K. D.; Horning, M. G.; Stillwell, R. N., Atmospheric Pressure Ionization (API) Mass Spectrometry. Solvent-Mediated Ionization of Samples Introduced in Solution and in a Liquid Chromatograph Effluent Stream. *J. Chromatogr. Sci.* **1974,** *12* (11), 725-729.

114. Carroll, D. I.; Dzidic, I.; Stillwell, R. N.; Haegele, K. D.; Horning, E. C., Atmospheric pressure ionization mass spectrometry. Corona discharge ion source for use in a liquid

chromatograph-mass spectrometer-computer analytical system. *Anal. Chem.* **1975,** *47* (14), 2369-2373.

115. Robb, D. B.; Blades, M. W., Atmospheric pressure photoionization for ionization of both polar and nonpolar compounds in reversed-phase LC/MS. *Anal Chem* **2006,** *78* (23), 8162-4.

116. Raffaelli, A.; Saba, A., Atmospheric pressure photoionization mass spectrometry. *Mass Spectrom. Rev.* **2003,** *22* (5), 318-31.

117. Kauppila, T. J.; Kersten, H.; Benter, T., The Ionization Mechanisms in Direct and Dopant-Assisted Atmospheric Pressure Photoionization and Atmospheric Pressure Laser Ionization. *J. Am. Soc. Mass. Spectrom.* **2014,** *25* (11), 1870-1881.

118. Klee, S.; Albrecht, S.; Derpmann, V.; Kersten, H.; Benter, T., Generation of ion-bound solvent clusters as reactant ions in dopant-assisted APPI and APLI. *Anal. Bioanal. Chem.* **2013,** *405* (22), 6933-6951.

119. Kind, T.; Fiehn, O., Advances in structure elucidation of small molecules using mass spectrometry. *Bioanalytical reviews* **2010,** *2*, 23-60.

120. Glish, G. L.; Vachet, R. W., The basics of mass spectrometry in the twenty-first century. *Nat Rev Drug Discov* **2003,** *2* (2), 140-50.

121. Sleno, L.; Volmer, D. A., Ion activation methods for tandem mass spectrometry. *J. Mass Spectrom.* **2004,** *39* (10), 1091-112.

122. Shukla, A. K.; Futrell, J. H., Tandem mass spectrometry: dissociation of ions by collisional activation. *J. Mass Spectrom.* **2000,** *35* (9), 1069-90.

CHAPTER 2. SCOPE OF THE STUDY

Despite the continuous advances and developments in science and in analytical instrumentation, there are still many reaction mechanisms that are poorly understood. Crude oil fouling is a prime example of a yet unresolved problem in petroleum industry in which various mechanisms take place. The aim of this work was to investigate and gain insight information regarding the oil compounds which are responsible for the formation of solid deposits as well as to understand the reaction mechanisms involved in their formation. A detailed study of the involved processes is almost impossible under industrial conditions. Therefore, fouling reactions were simulated on a laboratory scale with the use of stainless steel autoclaves and a gas condensate which is known for its chemical fouling tendencies.

The procedure required the development and in various stages the improvement of the equipment. Among the features that were to be developed, were means to safely react and recover the samples, as well as methods to control the atmosphere and the water content inside the reactors. In addition, adequate methods for the analysis of the resulting products had to be developed. Besides ultrahigh resolving mass spectrometry by means of direct infusion experiments, different approaches were tested for their suitability. The first two chapters are focused mostly on the analytical instrumentation available in the analysis of complex mixtures, while the remaining chapters are emphasizing on the reaction mechanisms involved in fouling formation.

First, in Chapter 3, the gas condensate is analyzed by the recently introduced Orbitrap based GC-MS system. For the first time, features such as high mass resolving power and a powerful chromatographic separation can be combined, enabling a better understanding of the sample on a molecular level. Here, apart from the commonly used EI source, also the capabilities of a recently introduced GC – atmospheric pressure photoionization (APPI) interface to an Orbitrap based mass analyzer are investigated.

In Chapter 4 the ionization efficiency of different ionization methods (ESI, APPI and APCI) was investigated and especially their simultaneous application as combined sources for the analysis of oil related samples. The combination of more than one method

can be an interesting alternative since through it complementary information regarding the crude oil constituents can be gained.

In Chapter 5 the investigation of the chemical changes that occur within the group of sulfur-containing compounds before and after thermal treatment is discussed. These species are of great interest since they are known for their corrosive and catalyst-poisoning properties. In this study the atmosphere within the reactor was altered as a potential parameter that can have an impact on the fouling behavior. Experiments were carried out using air (oxidative conditions) or argon gas (inert conditions) as atmosphere for the reaction. The effects on the fouling behavior of sulfur containing species is discussed.

In Chapter 6, a different parameter that has a significant impact on the fouling rate is investigated, the presence of water. This chapter illustrates the effect of water within the system based on the detailed analysis of purely hydrocarbon compounds. The formation of new, highly aromatic, high mass compounds is also demonstrated in a fouling experiment using reference compounds.

Chapter 7 shows the successful simulation of fouling under laboratory conditions using nitrogen-containing compounds as an example. The results indicate that the fouling proceeds through multi-step pathways, involving dehydrogenation and radical formation reactions. In order to verify the suggested reaction mechanism, a reaction set-up was developed, allowing the formation of solid deposits from a limited number of reactants. Structural elucidation of the newly formed products was performed by using high resolution MS/MS analysis.

Finally, an overall conclusion of this work is presented in Chapter 8.

CHAPTER 3. HIGH-RESOLUTION GC/MS STUDIES OF A LIGHT CRUDE OIL FRACTION

Redrafted from:

A. Kondyli, W. Schrader. "High-resolution GC/MS studies of a light crude oil fraction." *J. Mass Spectrom.* **2019**, *54*, 47-54.

3.1. Abstract

The continuous development in analytical instrumentation has brought the newly developed Orbitrap-based gas chromatography to mass spectrometry (GC-MS) instrument into the forefront for the analysis of complex mixtures such as crude oil. Traditional instrumentation usually requires a choice to be made between mass resolving power or an efficient chromatographic separation, which ideally enables the distinction of structural isomers which is not possible by mass spectrometry alone. Now, these features can be combined, thus enabling a deeper understanding of the constituents of volatile samples on a molecular level. Although electron ionization is the most popular ionization method employed in GC/MS analysis, the need for softer ionization methods has led to the utilization of atmospheric pressure ionization sources. The last arrival to this family is the atmospheric pressure photoionization (APPI), which was originally developed for liquid chromatography to mass spectrometry (LC-MS). With a newly developed commercial GC-APPI interface, it is possible to extend the characterization of unknown compounds. Here, first results about the capabilities of the GC/MS instrument under high or low energy EI or APPI are reported on a volatile gas condensate. The use of different ionization energies helps matching the low abundant molecular ions to the structurally important fragment ions. A broad range of compounds from polar to medium polar were successfully detected and complementary information regarding the analyte was obtained.

3.2. Introduction

The need to solve complex problems has driven the development of analytical techniques over the last decades even further. One of the most challenging tasks remains is the analysis and characterization of various compounds within environmental, pharmaceutical and other matrices such as food.[1] Among these compounds, environmental pollutants (e.g. pesticides, industrial waste, and degradation products) as well as the so-called contaminants of emerging concern (CECs) have gained attention because of their negative effects on the environment or human health.[2] The main difficulty in characterization and quantification of these compounds is that either they have not been detected before in the environment, or they exist only in trace amounts in complex matrices. In most cases, the analytical approach of these samples requires the use of separation techniques in order to simplify the complexity of the sample.[3, 4] A prime example of a complex mixture is crude oil, which contains more than one million different chemical components.[5] Despite the excessive worldwide use of it as fuel and as feedstock for many chemical products, its detailed chemical composition still remains a mystery for the scientific community.[6] Its constituents differ not only in molecular weight and structure, but also in polarity and heteroatom (N, O, S) content. Although the heteroatom-containing compounds represent only a small portion of crude oil (less than 15% by weight),[7] these are responsible for adverse effects e.g. coke formation, corrosion, catalyst poisoning in petroleum industry. In order to effectively reduce the adverse effects of single compounds, a deeper understanding of the molecular composition of the crude oil is necessary.

Over the years, a number of different analytical techniques such as nuclear magnetic resonance (NMR), infrared (IR) spectroscopy, X-ray crystallography or fluorescence measurements have been used for crude oil characterization. However, these techniques are limited since they provide information only for the bulk material. Ultrahigh-resolution mass spectrometry (UHRMS) is the method of choice in the analysis of complex mixtures. Information regarding the unique elemental composition of the compound, the component classes based on the heteroatom content as well as the level of aromaticity can be easily determined, but unfortunately MS alone does not give any further structural information. One solution to overcome this problem and gain structural information is the use of tandem MS. MS/MS measurements have been used for the study of the structure of aliphatic and aromatic species in heavy crude oils.[8, 9] Although this technique can be quite

useful for structural elucidation, it has two major drawbacks. Firstly, the resulting fragment ions having very low intensity can be accidentally removed as they might be considered as part of the noise peaks and secondly, there are many cases in which it is extremely difficult to interpret the fragment ion spectra especially if the parent ion results from a mixture of structural isomers.[10] As a consequence, the correct interpretation of the spectrum as well as the matching of the fragment ions to the corresponding parent ion is almost impossible.

The main challenge here regarding sample analysis is the presence of various isomeric compounds in crude oil which contribute to the complex nature of it. To address this problem, an effective chromatographic separation is needed before the MS-analysis.[11-16] The oldest and the most widely used hyphenated method is the coupling of gas chromatography to mass spectrometry (GC/MS).[17-21] This technique has been successfully used for the characterization of volatile and semi-volatile compounds in crude oil. Various compounds such as aliphatic, polycyclic aromatic hydrocarbons (PAHs)[22] as well as naphthenic acids have been analyzed by this method.[19, 23, 24] Until now, the major obstacle regarding GC/MS analysis was the choice to be made between high mass resolving power or a chromatographic separation which ideally enables the distinction of structural isomers. Traditional instrumentation available until now employs several types of mass analyzers (e.g. quadrupole, time of flight), but their inefficiency to provide high resolution mass measurements as well as their low mass accuracy, make them not suitable for crude oil characterization.[25-27] The above mentioned problems can now be overcome with the coupling of a gas chromatograph to an ultra-high resolving mass spectrometer. Recently, the combination of GC and APLI has been successfully used for the analysis of polyaromatic hydrocarbons (PAHs) in fossil oil samples.[28] Features such as sensitivity, high mass accuracy and high resolution can now be combined to a powerful chromatographic separation, enabling a deeper understanding of the samples on a molecular level.[29]

This work illustrates the analytical performance of the newly developed GC Orbitrap-based mass spectrometer. Here, apart from the commonly used electron ionization source, the capabilities of a recently introduced GC-atmospheric pressure photoionization (APPI) as interface are investigated.[30] The ability to combine results obtained using different ionization energies and methods provides complementary

information on both molecular and fragment ions, which at the end enhances the capabilities for structural elucidation.

3.3. Experimental

3.3.1. Sample preparation

A gas condensate of Arabic origin was diluted in toluene to a final concentration of 250 ppm and then analyzed without further treatment. Trace elemental analysis of the gas condensate was performed for identification and quantification of the elements. The sample contained 0.28% nitrogen and 0.08% sulfur.

3.3.2. Instrumentation

Measurements during this study were performed on two different instrumental setups. In case of electron ionization, a Q Exactive GC (Thermo Fisher, Bremen, Germany), consisting of a TRACE 1300 series GC coupled to a Q Exactive Orbitrap MS was used. The instrument is equipped with an electron ionization (EI) source with a possible electron energy tuning range between 1.0 to 150 eV. The value of the electron emission current was set to 50 µA. For APPI, the chromatographic separation was performed using a Trace GC Ultra that was joined with a Q Exactive Plus mass spectrometer (both Thermo Fisher, Bremen, Germany) by means of an APPI interface (MasCom Technologies, Bremen, Germany). The interface is equipped with a Krypton VUV lamp (Syagen, Tustin, CA, USA) for photoionization. Nitrogen gas was used in GC-APPI source, with a flow rate of 80.0 arbitrary units (a.u.). Experimental conditions were the same throughout all measurements and are stated below.

3.3.3. Gas chromatography

A ZB-5HT Inferno capillary column (30 m x 0.25 mm i.d. x 0.10 µm film thickness, Phenomenex, CA, USA) was used as stationary phase. The mobile phase was high purity helium (N5.0) at a constant flow of 1.2 $mL \cdot min^{-1}$. The temperature program was set to an initial temperature of 50 °C that was increased to a final temperature of 350 °C at a rate of 10 $°C \cdot min^{-1}$. The final temperature was kept for additional 5 minutes. The transfer line temperature was set to 250 °C. The injector was held at 300 °C and was used in split mode

with a split flow of 10 mL·min^{-1} and a purge flow of 5 mL·$^{-1}$. The injection volume of the sample was 1µL.

3.3.4. Mass spectrometry and data analysis

Mass spectra were acquired in full scan mode (m/z 50-700) at a resolution R = 120,000 (FWHM at m/z 200) at a scan rate of 3.0 Hz in the case of Q Exactive GC; while in the case of Q Exactive Plus, the spectra were recorded at a resolution R = 140,000 at a scan rate of 1.5 Hz. Ionization was performed by EI at an electron energy of 70 eV (high) or 12 eV (low) or by atmospheric pressure photoionization at photon energies of 10.0/10.6 eV, respectively.

Mass calibration was performed using vendor calibration solutions prior to sample analysis in order to meet a mass accuracy better than 1 ppm. The recorded mass spectra were averaged (entire chromatogram and bins of 1 min) by XCalibur 4.0software (Thermo Fischer, Bremen, Germany). Data processing was performed using Composer software (version 1.5.0, Sierra Analytics, Modesto, CA, USA). Assignment of molecular formulae was performed using the following restrictions regarding the number of possible elements: H: 0-300, C: 0-100, N: 0-3, O: 0-3, S: 0-3. The obtained mass lists were sorted into heteroatom classes and double bond equivalence (DBE) distribution and then transferred to Excel (Microsoft Office Professional Plus 2010, Microsoft Excel 2010) for further data evaluation and visualization. DBE refers to the sum of the ring closures and the number of π-bonds within a molecule and can be calculated from the general formula $C_cH_hN_nO_oS_s$ of the analyte using the following equation: $DBE = c - \frac{h}{2} + \frac{n}{2} + 1$.

3.4. Results and discussion

Electron ionization (EI) is the most commonly used ionization method for GC/MS analysis due to its ability to ionize a wide range of compounds. Due to a typically high excess of energy, this method results in excessive fragmentation. Through the fragment ions, structural information can be obtained since the spectrum provides a unique chemical fingerprint of the analytes, which can be matched to a spectral library.[31] Features such as reproducibility and comparability of the mass spectra can be achieved by this method. However, this method is quite limited since molecular ions can only be detected in low intensity if they are present, which can make the interpretation of a spectrum very

difficult, especially when dealing with complex mixtures. To overcome this limitation, the use of softer ionization methods is necessary. Apart from using supersonic molecular beams to enhance the abundance of molecular ions,[20] a commonly used strategy that is applied most frequently in crude oil analysis is the use of low-voltage electron ionization (LVEI).[32-34] Here, only little excess of energy is transferred to the analyte, resulting in reduced fragmentation. The mass spectra in this case are less complex and consist mainly of molecular ions. A different approach is the use of atmospheric pressure ionization (API) methods, as they are known to be soft ionization methods that lead to no or little fragmentation. In this case, of special interest is the APPI as a relatively unselective method that is capable of ionizing a broad range of different compounds by interaction with photons of 10.0/10.6 eV. A newly developed GC-APPI interface allows to combine a gas chromatographic separation with mass spectrometric detection after ionization by APPI on instrumentation originally designed for LC/MS analysis.[30] The design and the individual parts of the above mentioned GC-APPI interface are illustrated in Figure 3-1.

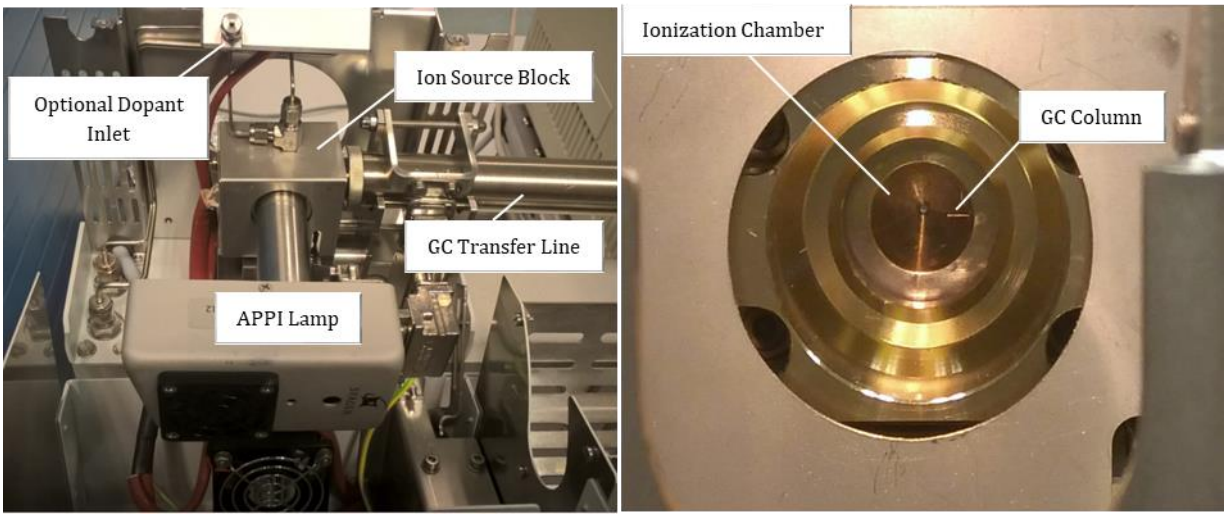

Figure 3-1: Overview of the gas chromatography-atmospheric pressure photoionization (GC-APPI) interface. The main parts of the interface include: The optional dopant inlet; the APPI lamp which is mounted into the entrance of the ion source block; the GC transfer line which is attached to the APPI source; and finally the GC column which is adjusted into the APPI source. The zoomed-in view at the ionization chamber shows the exact position of the GC column which is protruded usually around 0.5 – 1mm in the APPI source (right picture).[30]

The capabilities of the GC-APPI interface are still in prime stage since its utilization has not been fully explored for the analysis of complex mixtures. Here, the GC Orbitrap-

based mass spectrometer is tested under different ionization methods (EI or APPI). Having the choice to shift from high to low ionization energy is of crucial importance since a different part of information regarding the analyte can be revealed. Figure 3-2 shows the resulting total ion chromatograms (TIC) of a gas condensate obtained within 30 minutes by high or low energy EI or APPI of 10/10.6 eV.

From a first look at the TIC, differences between the ionization methods can be observed. In case of EI, both chromatograms show various high intensity peaks eluting from 2.7 to 18.2 minutes. These peaks correspond to *n*-alkanes with a carbon number ranging from C_7 to C_{21}. The ionization of these compounds is favored under EI since the ionization potential of alkanes is around 10 eV. On the other hand, the chromatogram obtained by using APPI looks totally different. With this ionization method, *n*-alkanes were completely missing since their ionization is not favored by this method.

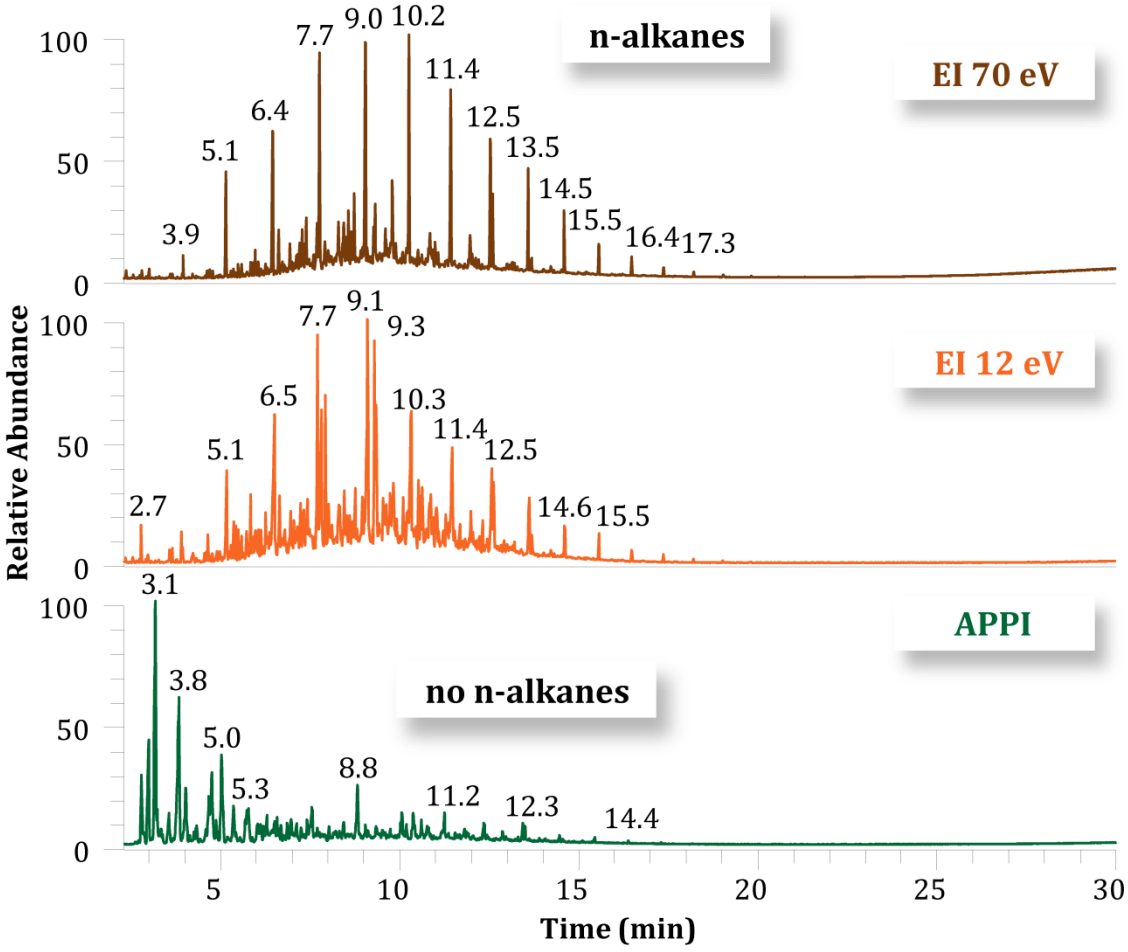

Figure 3-2: Total ion chromatograms (TICs) of a gas condensate with EI of 70 eV (top) or 12 eV (center) or APPI of 10.0/10.6 eV (bottom).

Although the first two chromatograms look similar, a closer look at the averaged mass spectra show many differences between high or low energy EI. As can be seen in Figure 3-3, under EI of 70 eV, most of the signals were detected at *m/z* of 50-150, while by lowering the ionization potential, the highest signal abundance was found at the mass range of 100-250 Da. This tendency is expected since using EI of 70 eV, the molecular ions tend to be unstable and the majority of them breaks into smaller fragments with lower masses. On the other hand, molecules with higher masses are detected by EI of 12 eV, since the degree of fragmentation is limited here, allowing intact molecular ions to pass through the system. Regarding APPI, most of the signals were detected at *m/z* of 150-250. As a soft ionization method, very little excess of energy is deposited at the generated molecular ions.

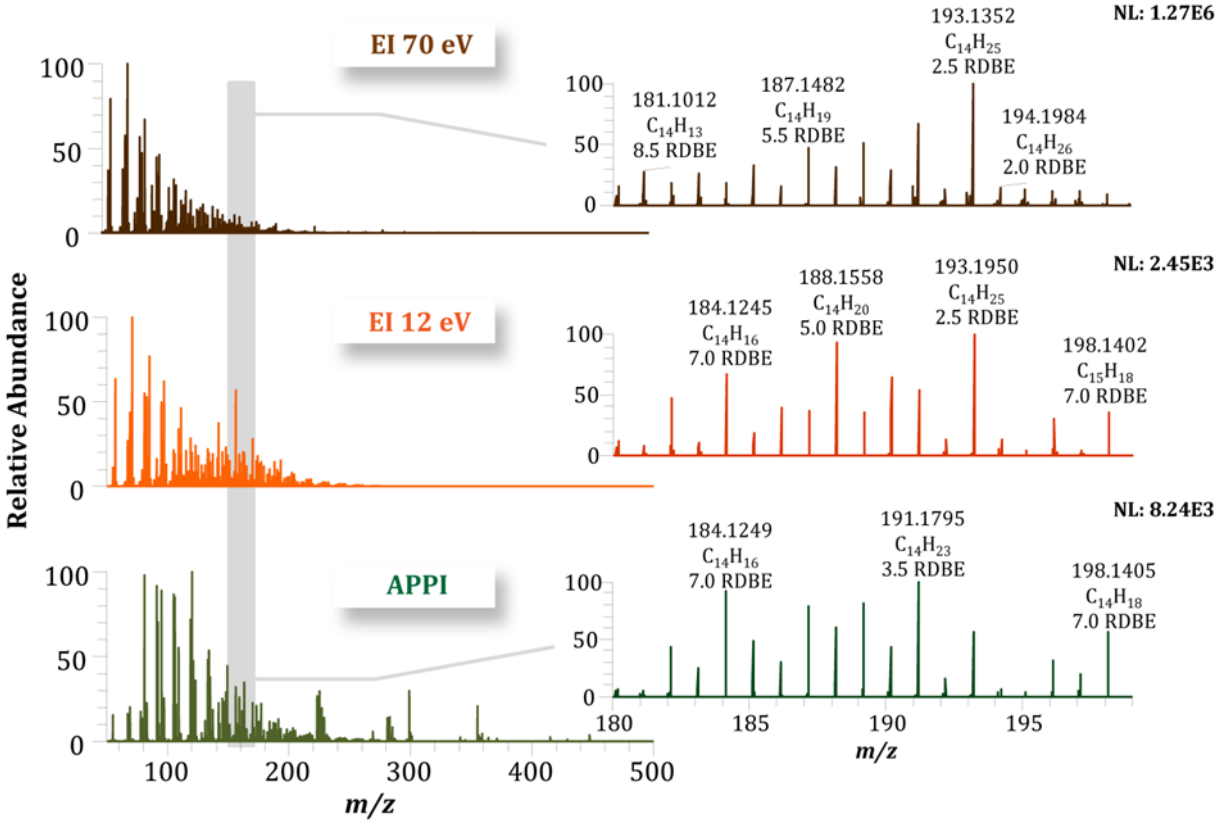

Figure 3-3: Averaged mass spectra of a gas condensate obtained using EI of 70 eV (left, top), EI of 12 eV (left, middle) or APPI (left, bottom) with the mass scale-expanded views at m/z 180-199.

Here, within 7 Da mass units, mostly hydrocarbon species were detected as can be seen from the zoomed-in windows in Figure 3. From a first look, an overall decrease of the signal intensity can be observed by lowering the ionization potential. This decrease of intensity can be attributed to the lower ionization efficiency. In addition, the lower intensity can explain the low abundance of signals of heteroatom-substituted analytes as will be seen later. Under EI conditions, the peaks represent either radical molecular cations or fragment ions. With EI of 70 eV, the highest intensity peaks correspond to fragment ions, mostly with an odd *m/z* value (e.g. $C_{14}H_{15}$ at *m/z* 183.1169) and a DBE value which is not an integer. Signals at an even *m/z* value (e.g. $C_{14}H_{16}$ at *m/z* 184.1247) correspond either to molecular ions or fragment ions after a rearrangement has taken place. In this case, the DBE number of the given molecular formula is an integer. On the other hand, under softer ionization conditions such as EI of 12 eV, the spectrum is simpler as little fragmentation takes place. In this case, the signal of the radical molecular cations is enhanced, allowing the identification and the structural elucidation of the analyte. In case of APPI, the spectrum here remains simple since the photon emission energy is high to ionize the organic compounds, but simultaneously low to create fragmentation. With APPI almost exclusive, formation of molecular radical cations occurs, with little or no fragmentation.

However, since this method involves multiple pathways for ion formation, protonated species are also generated.[35] The addition of a dopant (e.g., toluene) with an IE below the photon energy is a commonly used strategy for the enhancement of the signal intensity in APPI. It facilitates the ionization of different chemical compounds through the formation of clusters between analyte, dopant and water molecules (and potentially other solvent molecules, if present) from which a proton transfer forms the resulting protonated molecules. The details of the ionization mechanism are described in detail here.[36-38] Here, likewise to the previously mentioned results, the signals with an even *m/z* number correspond to molecular radical cations, while the compounds with an odd *m/z* number are likely protonated species. In Figure 3-4, a hydrocarbon compound with the chemical composition of $C_{14}H_{15}$ has been chosen as an example to illustrate this difference.

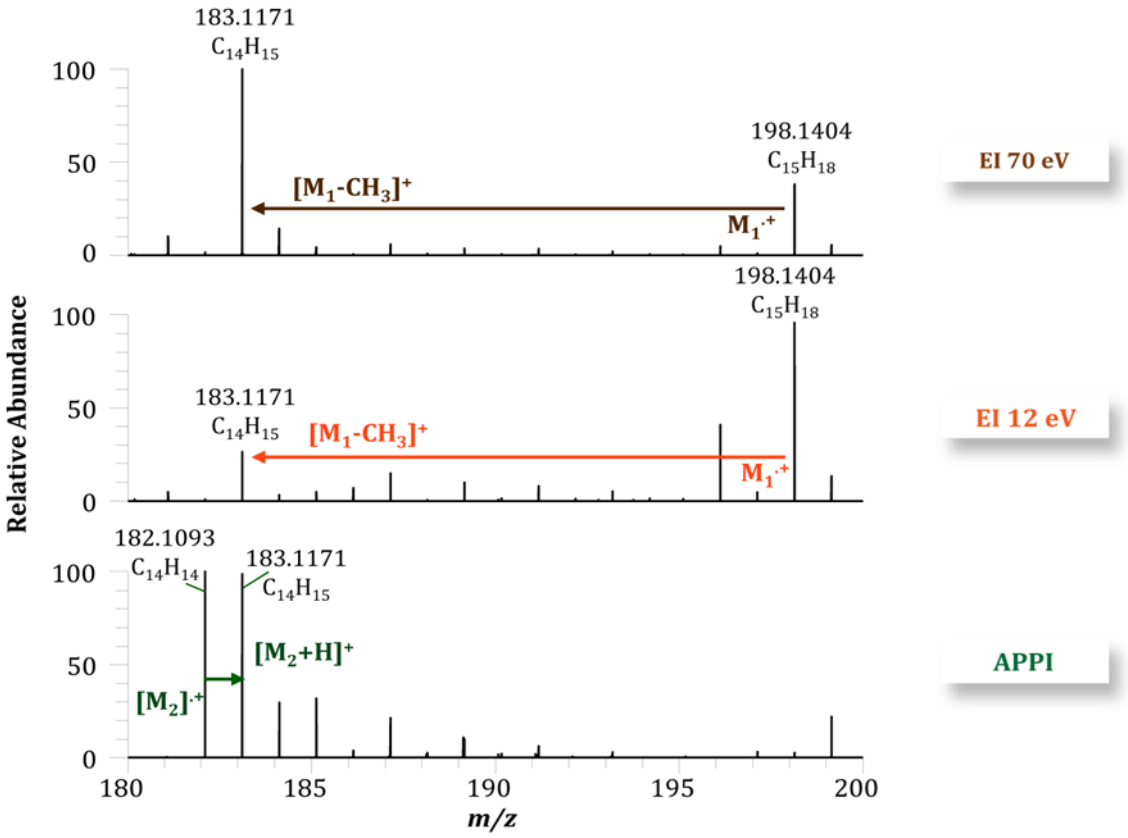

Figure 3-4: Comparison of fragment ion versus protonated ion formation of a single spectrum with high or low energy EI (top and middle spectrum) or APPI of 10.0/10.6 eV (bottom spectrum).

There are many cases in which a compound having the same chemical composition can be formed with different ionization methods. Such an example can be seen in Figure 3-4, where the hydrocarbon compound with the chemical formula of $C_{14}H_{15}$ at *m/z* 183.1171 is compared under high and low energy EI and APPI. Although this hydrocarbon compound is present in all spectra, its formation is a result of different mechanisms. In the case of high or low energy EI, it represents a fragment ion, while in the case of APPI a protonated molecule. In the first case, assuming that the hydrocarbon compound with the chemical formula of $C_{15}H_{18}$ at *m/z* 198.1404 is the molecular radical cation ($M_1^{\cdot+}$) due to its high intensity signal under EI of 12 eV, a difference of 15 Da is observed. This corresponds to the loss of a methyl group resulting in a fragment ion. On the other hand, using APPI the ion $C_{14}H_{15}^+$ has been formed by proton transfer to the initial compound with the chemical formula of $C_{14}H_{14}$.

Dealing with the analysis of complex mixtures is not an easy task, especially since MS alone provides limited information. Various compounds can be detected and sorted according to the amount of heteroatom classes and the type of detected species (protonated or radical ions). However, this representation gives only a general idea about the sample. This is because of the presence of various isomeric compounds which are not taken into consideration, especially if the ion chromatogram is summed. Figure 3-5 shows the distribution of the compound classes and their population abundance obtained from EI of 70 eV, 12 eV and APPI. The species detected under EI correspond only to the molecular radical ions, while under APPI both molecular radical ions and protonated ions (APPI $[M+H]^+$), purple colour) are illustrated here. However, in case of EI, the results might contain fragment ions that result from a rearrangement, as those cannot be easily distinguished from molecular radical ions here.

As can be seen from the Figure 3-5, the most abundant species corresponds to radical hydrocarbons which were detected under high energy electron ionization. Although a different detection approach would be expected since under softer ionization conditions the preservation of the molecular ion is favored; however, lowering the ionization energy results in an overall drop at the signal intensity. This can justify the slightly lower abundance of molecular radicals and protonated hydrocarbons obtained with EI of 12 eV or APPI respectively. On the other hand, oxygen-containing compounds are more abundant using APPI. Under this ionization condition not only nonpolar oxygen containing species such as ethers can be ionized, but also polar species such as phenolics. APPI favors the ionization of compounds which contains π-bonds as well as higher aromatic structure. Regarding the sulfur-containing compounds, with high or low energy EI, only very few species were detected since these compounds are unstable and fragment very easily.

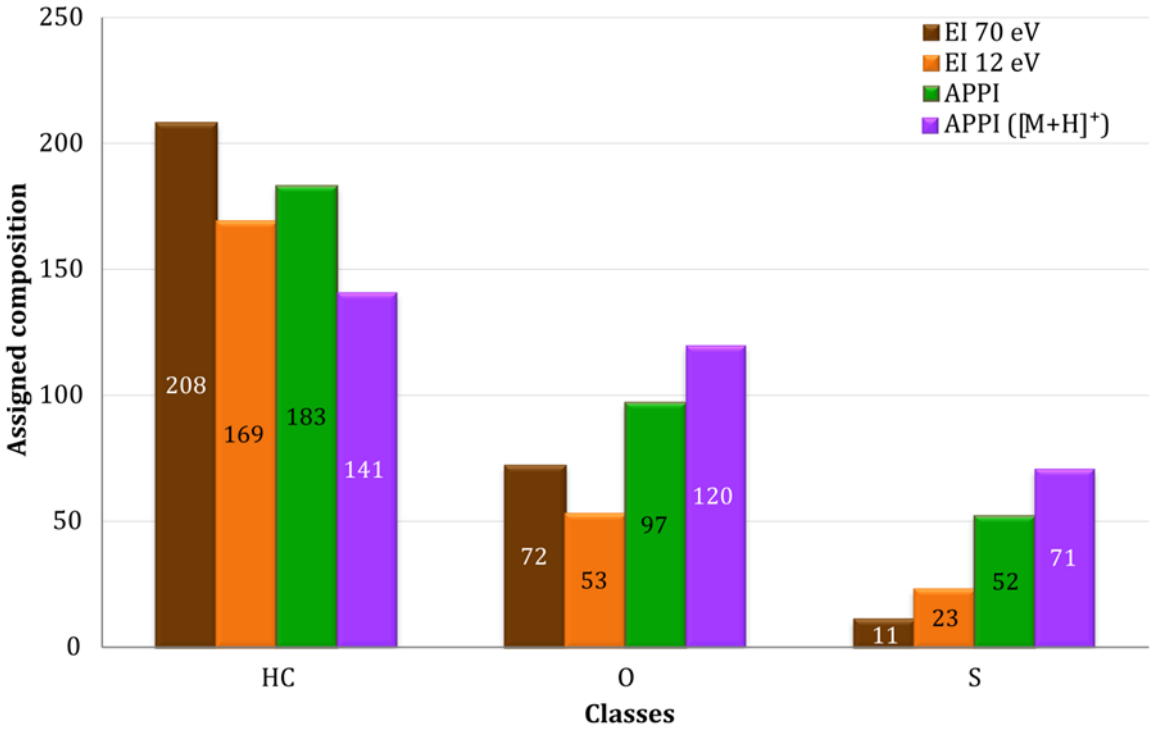

Figure 3-5: Comparison of class distribution based on the number of the main assigned compounds detected with high or low energy EI or APPI. Note that the results refer to the summarized TICs.

However, the above presented results are not representing the real amount of compounds existing in the sample. A calculation of the various isotopic compounds would change drastically the number of assigned chemical compositions. In order to understand the problem facing with the isomers, an example is presented in Figure 3-6. Here, the results were obtained by summarizing 1 minute that was randomly chosen from the total ion chromatogram. Afterwards, the same minute was divided into 0.2 minutes. Bins. With high energy EI in the summarized one scan minute shows a detection of around a hundred hydrocarbon radical compounds, while the rest of the heteroatom containing compounds do not exceed 50 assignments. In addition, detection of sulfur containing species is not observed. On the other hand, dividing the same minute into fractions of time, a remarkable difference in all classes can be observed. In this case, there is an overall increase of compounds in all the classes and especially the abundance of the radical hydrocarbons has been increased six times. Regarding the oxygen containing compounds, an increase is observed with 70 eV after the division of the 1 minute into 0.2 bins compared to low energy EI or to APPI. In addition, here there is the detection of very few sulfur species, which due to their low intensity was not possible to observe before. Using

low energy EI or APPI the trend remains the same. Obviously, a scan to scan data process will result in better representation of the sample constituents. However, this is not possible since first there is no commercially available software that allows studying such complex 3-dimensional data sets and secondly, it is at this stage still an extremely time-consuming procedure.

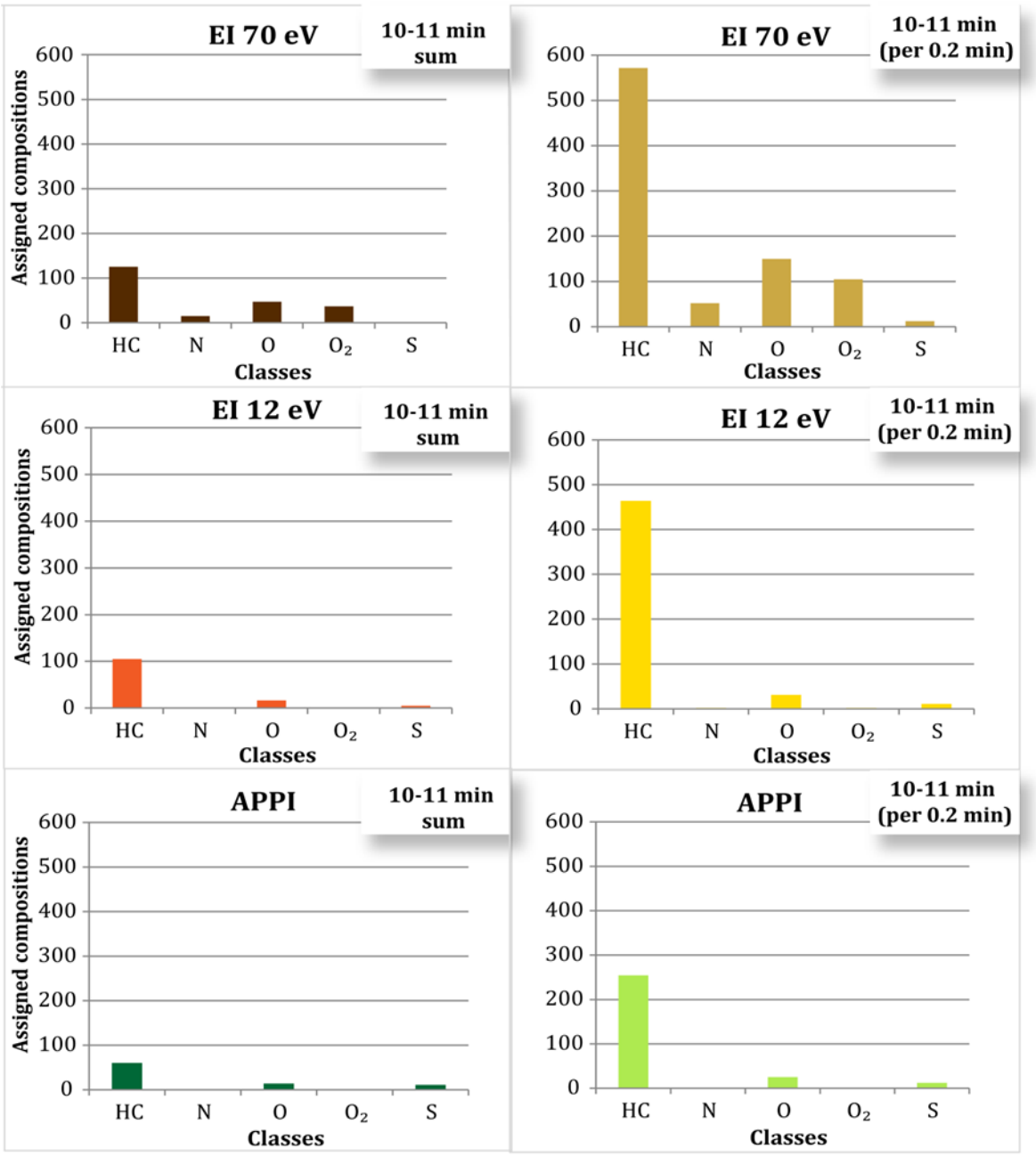

Figure 3-6: Comparison of abundance based distribution of the main assigned compound classes using high or low energy EI or APPI of a summed minute (left) or its division with 0.2 bins time difference (right). Note that the results correspond only to molecular radical cations.

The characterization of complex mixtures such as petroleum samples becomes even more difficult with the presence of various isomeric compounds. The number of isomers increases rapidly with the increase of the number of carbon atoms per molecule. For example, an alkane with 12 carbon atoms ($C_{12}H_{26}$), can form more than 300 different isomers.[39] An illustration of various isomeric compounds, as well as a suggested structure for them with high energy EI (brown colour) or APPI (green colour) can be seen in Figure 3-7. Here, the first compound in the graph shows the hydrocarbon compound of methylnaphthalene ($C_{11}H_{10}$) having two different isomers. The powerful chromatographic separation can be maintained despite the sample complexity. The isomeric compounds of the oxygen containing species are also efficiently separated. Finally, a high increase in the number of thiophenic isomeric compounds is observed with the addition of an alkyl chain. It is quite obvious that the need for a powerful chromatographic separation increases with the increase of the compound complexity.

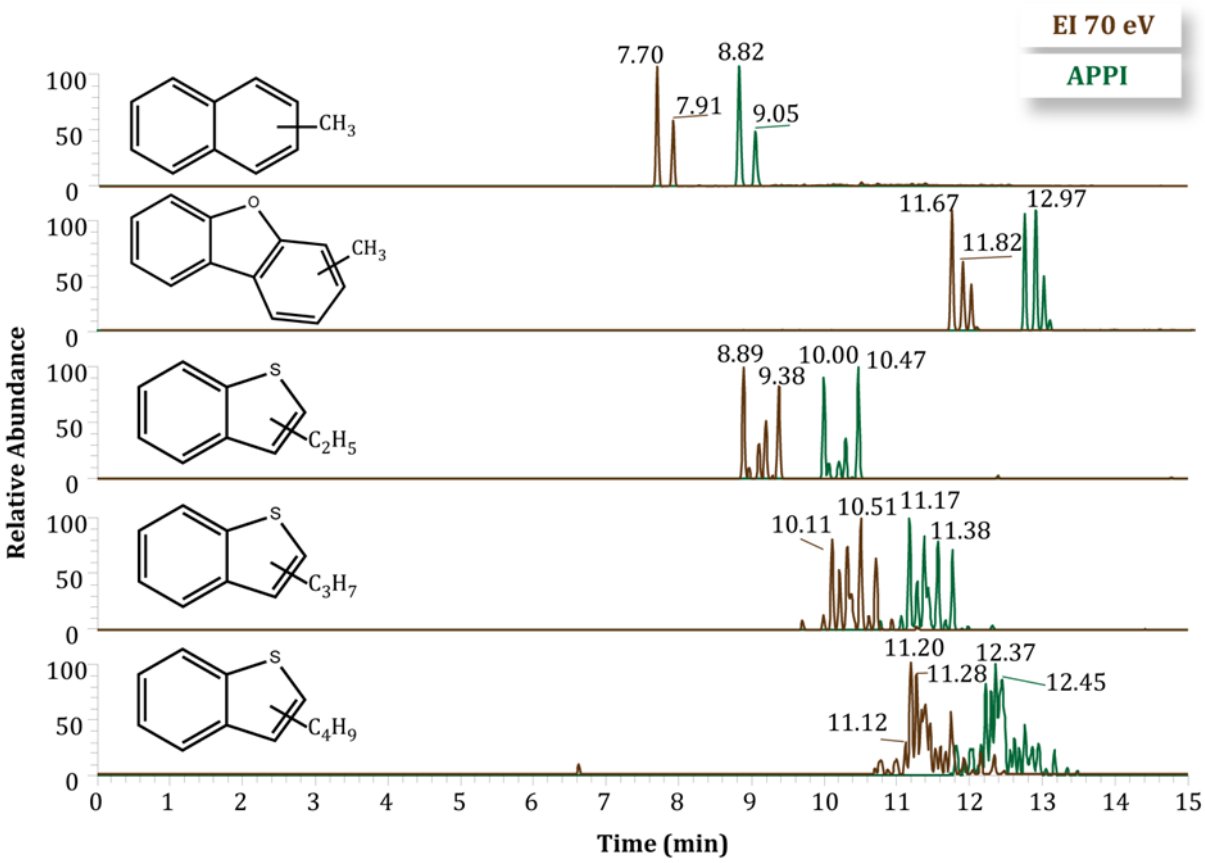

Figure 3-7: Separation of various isomeric compounds with a suggested possible structure for them detected using high energy EI or APPI. The brown colour corresponds to EI, while the green to APPI.

3.5. Conclusion

GC separation with different ionization methods for ultra-high resolution MS was compared for the studies of volatile components of gas condensate. The results show that both methods are suitable for complex mixture analysis. Especially the separation of different isomeric compounds is a helpful tool to characterize complex mixtures such as crude oil. Because of the complexity of the analyte sample, the use of standard electron ionization is difficult because the high fragmentation behaviour makes the complexity even higher, and the characterization even more difficult. Here, the use of lower energy EI with ionization energy at 12 eV is reducing the overall sensitivity, but also reduces the complexity allowing a better distinguishing between fragment and molecular ions. Additionally, the use of atmospheric pressure photoionization can be an interesting alternative. Since APPI can detect a wide number of different compounds from non polar to medium polar, this would be complementary to standard EI analyses. Both allow to measure different types of compound classes (such as hydrocarbons and classes containing oxygen, nitrogen and sulfur species) and mass ranges with very high resolution capabilities. Nevertheless, in order to explore fully the capabilities of these techniques and understand in details the differences between the ionization methods additional experimental work is needed. In future studies, the chromatographic separation with different ionization methods of a set of alkane standards can be tested.

3.6. References

1. Smyth, W. F., *Analytical Chemistry of Complex Matrices*. Vieweg und Teubner Verlag: Wiesbaden, 1996.

2. Daughton, C. G., Non-regulated water contaminants: emerging research. *Environ. Impact Asses.* **2004,** *24* (7-8), 711-732.

3. van der Hoff, G. R.; van Zoonen, P., Trace analysis of pesticides by gas chromatography. *J. Chromatogr. A* **1999,** *843*, 301-322.

4. Hajslova, J.; Zrostlikova, J., Matrix effects in (ultra)trace analysis of pesticide residues in food and biotic matrices. *J. Chromatogr. A* **2003,** *1000* (1-2), 181-197.

5. Beens, J.; Blomberg, J.; Schoenmakers, P. J., Proper Tuning of Comprehensive Two-Dimensional Gas Chromatography (GC×GC) to Optimize the Separation of Complex Oil Fractions. *J. High Resolut. Chromatogr.* **2000,** *23*, 182-188.

6. Panda, S. K.; Andersson, J. T.; Schrader, W., Characterization of Supercomplex Crude Oil Mixtures: What is Really in There? *Angew. Chem.* **2009,** *48* (10), 1788-1791.

7. Speight, J. G., *Handbook of Petroleum Analysis*. Wiley-Interscience New York, NY, 2001.

8. Reddy, C. M.; Quinn, J. G., GC-MS analysis of total petroleum hydrocarbons and polycyclic aromatic hydrocarbons in seawater samples after the North Cape oil spill. *Mar. Pollut. Bull.* **1999,** *38* (2), 126-135.

9. Summons, R. E., Branched alkanes from ancient and modern sediments: Isomer discrimination by GC/MS with multiple reaction monitoring. *Org. Geochem.* **1987,** *11* (4), 281-289.

10. Yuan, Z.; Shi, J.; Lin, W.; Chen, B.; Wu, F.-X., Features-based deisotoping method for tandem mass spectra. *Adv. Bioinformatics* **2011,** *2011*, 210805-210805.

11. Vetere, A.; Profrock, D.; Schrader, W., Quantitative and Qualitative Analysis of Three Classes of Sulfur Compounds in Crude Oil. *Angewandte Chemie-International Edition* **2017,** *56* (36), 10933-10937.

12. Lababidi, S.; Panda, S. K.; Andersson, J. T.; Schrader, W., Direct coupling of normal-phase high-performance liquid chromatography to atmospheric pressure laser ionization fourier transform ion cyclotron resonance mass spectrometry for the characterization of crude oil. *Anal Chem* **2013,** *85* (20), 9478-85.

13. Makarov, A.; Scigelova, M., Coupling liquid chromatography to Orbitrap mass spectrometry. *J Chromatogr A* **2010,** *1217* (25), 3938-45.

14. Pasadakis, N.; Xekoukoulotakis, N., Gas chromatographic analysis of crude oils with thermal extraction sampling. *Pet. Sci. Technol.* **2007,** *25* (9), 1135-1142.

15. Vetere, A.; Schrader, W., 1-and 2-Photon Ionization for Online FAIMS-FTMS Coupling Allows New Insights into the Constitution of Crude Oils. *Anal. Chem.* **2015,** *87* (17), 8874-8879.

16. Guricza, L. M.; Schrader, W., Optimized asphaltene separation by online coupling of size exclusion chromatography and ultrahigh resolution mass spectrometry. *Fuel* **2018,** *215*, 631-637.

17. van de Meent, D.; Brown, S. C.; Philp, R. P.; Simoneit, B. R. T., Pyrolysis-high resolution gas chromatography and pyrolysis gas chromatography-mass spectrometry of kerogens and kerogen precursors. *Geochim. Cosmochim. Acta* **1980,** *44* (7), 999-1013.

18. Cautreels, W.; Vancauwenberghe, K., Determination of Organic-Compounds in Airborne Particulate Matter by Gas Chromatography Mass Spectrometry. *Atmos. Environ.* **1976,** *10* (6), 447-457.

19. Wang, Z. D.; Fingas, M., Differentiation of the Source of Spilled Oil and Monitoring of the Oil Weathering Process Using Gas Chromatography-Mass Spectrometry. *J. Chromatogr. A* **1995,** *712* (2), 321-343.

20. Dagan, S.; Amirav, A., Electron impact mass spectrometry of alkanes in supersonic molecular beams. *J Am Soc Mass Spectrom* **1995,** *6* (2), 120-31.

21. Amirav, A.; Keshet, U.; Danon, A., Soft Cold EI - approaching molecular ion only with electron ionization. *Rapid Commun. Mass Spectrom.* **2015,** *29* (21), 1954-1960.

22. Richter-Brockmann, S.; Achten, C., Analysis and toxicity of 59 PAH in petrogenic and pyrogenic environmental samples including dibenzopyrenes, 7H-benzo c fluorene, 5-methylchrysene and 1-methylpyrene. *Chemosphere* **2018,** *200*, 495-503.

23. Sutton, P. A.; Lewis, C. A.; Rowland, S. J., Isolation of individual hydrocarbons from the unresolved complex hydrocarbon mixture of a biodegraded crude oil using preparative capillary gas chromatography. *Org. Geochem.* **2005,** *36* (6), 963-970.

24. Holowenko, F. M.; MacKinnon, M. D.; Fedorak, P. M., Characterization of naphthenic acids in oil sands wastewaters by gas chromatography-mass spectrometry. *Water Res.* **2002,** *36* (11), 2843-2855.

25. Mbughuni, M. M.; Jannetto, P. J.; Langman, L. J., Mass Spectrometry Applications for Toxicology. *J. Int. Fed. Clin. Chem. Lab. Med.* **2016,** *27*, 272-287.

26. Szulejko, J. E.; Solouki, T., Potential analytical applications of interfacing a GC to an FT-ICR MS: Fingerprinting complex sample matrixes. *Anal. Chem.* **2002,** *74* (14), 3434-3442.

27. Clench, M. R.; Tetler, L. W., Liquid Chromatography: Detectors: Mass Spectrometry. In *Handbook of Methods and Instrumentation in Separation Science*, Ian D. Wilson, C. F. P., Ed. Elsevier Academic Press: London, 2009; Vol. 1, pp 412-418.

28. Benigni, P.; DeBord, J. D.; Thompson, C. J.; Gardinali, P.; Fernandez-Lima, F., Increasing Polyaromatic Hydrocarbon (PAH) Molecular Coverage during Fossil Oil Analysis by Combining Gas Chromatography and Atmospheric-Pressure Laser Ionization Fourier Transform Ion Cyclotron Resonance Mass Spectrometry (FT-ICR MS). *Energy & fuels : an American Chemical Society journal* **2016,** *30* (1), 196-203.

29. Peterson, A. C.; Hauschild, J.-P.; Quarmby, S. T.; Krumwiede, D.; Lange, O.; Lemke, R. A. S.; Grosse-Coosmann, F.; Horning, S.; Donohue, T. J.; Westphall, M. S.; Coon, J. J.; Griep-Raming, J., Development of a GC/Quadrupole-Orbitrap mass spectrometer, part I: design and characterization. *Anal. Chem.* **2014,** *86* (20), 10036-10043.

30. Kersten, H.; Kroll, K.; Haberer, K.; Brockmann, K. J.; Benter, T.; Peterson, A.; Makarov, A. J. J. o. T. A. S. f. M. S., Design Study of an Atmospheric Pressure Photoionization Interface for GC-MS. *J. Am. Soc. Mass. Spectrom.* **2016,** *27* (4), 607-614.

31. Kind, T.; Fiehn, O., Advances in structure elucidation of small molecules using mass spectrometry. *Bioanalytical reviews* **2010,** *2*, 23-60.

32. Taghizadeh, K.; Hardy, R. H.; Davis, B. H.; Meuzelaar, H. L. C., Comparison of Low-Voltage Electron Ionization and Field-Ionization Mass-Spectra of Coal-Derived Liquids from the Wilsonville Pilot-Plant. *Fuel Process. Technol.* **1990,** *26* (3), 181-195.

33. Field, F. H.; Hastings, S. H., Determination of Unsaturated Hydrocarbons by Low Voltage Mass Spectrometry. *Anal. Chem.* **1956,** *28* (8), 1248-1255.

34. External electron ionization 7T Fourier transform ion cyclotron resonance mass spectrometer for resolution and identification of volatile organic mixtures. *Rev. Sci. Instrum.* **2006,** *77* (2), 025102.

35. Raffaelli, A.; Saba, A., Atmospheric pressure photoionization mass spectrometry. *Mass Spectrom. Rev.* **2003,** *22* (5), 318-31.

36. Klee, S.; Albrecht, S.; Derpmann, V.; Kersten, H.; Benter, T., Generation of ion-bound solvent clusters as reactant ions in dopant-assisted APPI and APLI. *Anal. Bioanal. Chem.* **2013,** *405* (22), 6933-6951.

37. Kauppila, T. J.; Kersten, H.; Benter, T., The Ionization Mechanisms in Direct and Dopant-Assisted Atmospheric Pressure Photoionization and Atmospheric Pressure Laser Ionization. *J. Am. Soc. Mass. Spectrom.* **2014,** *25* (11), 1870-1881.

38. Kauppila, T. J.; Syage, J. A.; Benter, T., Recent developments in Atmospheric pressure photoionization-mass spectrometry. *Mass Spectrom. Rev.* **2017,** *36* (3), 423-449.

39. Speight, J. G., *Handbook of industrial hydrocarbon processes*. Gulf Professional Publishing: Oxford, 2009.

CHAPTER 4. EVALUATION OF THE COMBINATION OF DIFFERENT ATMOSPHERIC PRESSURE IONIZATION SOURCES FOR THE ANALYSIS OF EXTREMELY COMPLEX MIXTURES

Redrafted from:

Kondyli, W. Schrader. "Investigation on the analysis of extremely complex mixtures by combining different atmospheric pressure ionization sources", accepted for publishing in *Rapid Commun. Mass Spectrom.* DOI: 10.1002/rcm.8676

4.1. Abstract

Characterization of complex samples remains a challenging task due to the high number of compounds present. Matrix effects, ion discrimination and suppression are limiting factors, which forces the use of different methods for the same sample to gain a broad understanding of complex mixtures. Various ionization techniques such as ESI, APPI and APCI have been used in various problems for complex mixture analysis. Especially demanding is the analysis of energy related hydrocarbon mixtures, such as crude oil. Here, the different ionization sources alone and in combination with each other have been used on a ultrahigh resolution Orbitrap mass spectrometer to study a light crude oil. Despite the great variety of the available ionization sources, there is no single technique which can fully characterize the crude oil. Each ionization technique shows a selectivity towards specific types of compounds. While ESI is the method of choice for the detection of polar compounds, APPI and APCI favors the detection of non-polar and low-to-medium polar compounds respectively. The combination of ESI/APPI favors hydrocarbons and oxygen containing species. Combining different ionization methods can be used as an alternative in order to gain more information about compounds present in a complex mixture although a combination of different ion sources could enhance suppression effects.

4.2. Introduction

The continuously increasing rate of energy consumption has raised an unpresented interest on the utilization of alternative sources.[1] Although, renewable energy from marine, solar, hydro and other sources will undergo a slight increase from 14% to 18% by the end of 2040, these are not able to fill the gaps of global energy demand.[2] Until there is an adequate sustainable energy transition, crude oil will continue to be the primary energy source. However, the excessive use of it in combination with the development of countries with emerging economies, has led to the depletion of conventional oil sources.[3] In order to meet the world's energy needs, the use of unconventional oil resources (extra-heavy oil, oil sands, oil shales or tight oil) is strongly increasing.[4, 5] Incorporation of heavier crude oils in the market has gained great attention since their upgrading is cost intensive.[6, 7] Their high viscosity and chemical complexity cause various environmental and industrial problems during production, transportation and refinery.[8, 9] In addition, the high amount of heteroatom-containing compounds (N, O, S), heavy metals and asphaltenes is responsible for adverse effects (coke formation, fouling, plugged pipelines) in petroleum industry.[10, 11]

In order to overcome these problems, not only advances on technological level are required, but also an in-depth knowledge of the chemical composition on a molecular level.[8] Over the last years, several analytical techniques have been used in crude oil analysis, but high-resolution mass spectrometry is the method of choice.[12] While high mass resolving power enables the distinction between isobaric compositions,[13-16] its high mass accuracy determines the elemental composition of a given peak with an error of less than 1 ppm.[17] Characterization of heavier crude oils is a challenging task since the amount of volatile or semi-volatile compounds are limited. Thus, the use of GC/MS is not a suitable method for the analysis of such complex samples or its heavier fractions.[18, 19]

The above-mentioned problem has been partially solved with the introduction of atmospheric pressure ionization sources.[20, 21] In this family, electrospray (ESI), atmospheric pressure chemical ionization (APCI) and atmospheric pressure photoionization (APPI) are the most widely used ionization techniques in crude oil analysis.[22, 23] Despite the great variety of the available ionization sources, unfortunately there is no single analytical technique which can fully characterize a crude oil.[21] Each ionization technique shows a selectivity depending on the nature of the analyte. For example, ESI favors the ionization of polar compounds,[24, 25] and the efficiency of the

ionization relies on the basicity or the acidity of the compound.[26] Since this method is based on the proton exchange,[27] ions in (de-) protonated form are generated.[28] Basic nitrogen containing or acidic compounds are successfully ionized by this method.[29, 30] On the other hand, APPI is more suitable for the ionization of non polar to medium-polar compounds such as polyaromatic hydrocarbons (PAHs).[31] Nowadays, quiet often in order to enhance the ionization efficiency and increase the signal intensity a dopant (e.g., toluene) is used.[32-34] In case of APCI, contrary to the other API methods, shows the best results of aliphatic hydrocarbons, providing useful information regarding the analyte.[35] The ion formation in both APPI and APCI takes place under different pathways, generating both radical molecular ions and protonated molecules.[36, 37] However, the main problem regarding the ionization methods remains the complexity of the matrix.[38] The amount and the type of the detected compounds is affected by the sensitivity of the instrument, as well as by various discrimination and ion suppression effects during the ionization process.[39-41] In this aspect, it is not yet known how the combination of different atmospheric pressure ionization methods can be used as a tool for complex sample analysis.

Therefore, in this study the ionization methods of ESI, APPI and APCI as well as all their possible combinations were investigated on the characterization of a light crude oil sample. Through the combination of these methods complementary information regarding the crude oil constituents can be gained.

4.3. Experimental

4.3.1. Sample preparation

A light crude oil of south-east Asian origin was used for this study. The sample was diluted and dissolved in a mixture of toluene (HPLC Chromasolv, Sigma Aldrich, Germany) and methanol (LC-MS grade, J. T. Baker, Germany) (1:1 v/v), to a final concentration of 250 ppm and then analyzed without further treatment.

4.3.2. Mass spectrometry

Mass analysis was performed on a research-type Orbitrap Elite mass spectrometer (Thermo Fisher, Bremen, Germany) at a resolution R= 480,000 (FWHM at *m/z* 400).[13] Mass spectra were collected in spectral stitching mode (using 30 Da SIM windows with 5 Da overlap over the selected mass range)[42] in a range of *m/z* 150-1000. For ionization,

electrospray (ESI), atmospheric pressure photoionization (APPI), atmospheric pressure chemical ionization (APCI) as well as the combination of ESI with APPI, ESI with APCI, and APPI with APCI were used in positive ion mode. In case of ESI, the sample was injected at a flow rate of 5 µl min^{-1} and the ionization potential was set to 4 kV in positive mode. Nebulization was assisted using nitrogen as a sheath gas at a flow rate of 5.0 a.u. (arbitrary units). Auxiliary and sweep gas flow rate was set at 1.0 a.u. for both. The temperature of the transfer capillary was adjusted to 275 °C. For the APPI ionization, a Krypton VUV lamp (Syagen, Tustin, CA, USA) with a photon emission at 10.0/10.6 eV (116.5/123.6 nm) was used. The sample was introduced with a flow rate of 8 µl min^{-1} and evaporated in the heated nebulizer at 350 °C. Sheath, auxiliary and sweep gas values were set at 20.0 a.u., 8.0 a.u. and 8.0 a.u. respectively. In case of atmospheric pressure chemical ionization, a corona discharge needle with a current of 5.0 µA was used, while the rest of the parameters were set similarly to the APPI. For the combination of ESI with APPI, the parameters applied similarly to ESI, while in case of APPI with APCI they remained the same as in the case of APCI. For the combination with ESI, the ESI spray was directed into the corona discharge from APCI or the VUV beam of the APPI lamp, respectively. While for APCI operations the instruments controls were used, the ESI potential was provided by an external high voltage supply (PNC 30000-2, Heinzinger electronic GmbH, Rosenheim, Germany). The VUV lamp for APPI was operated independently from instrument control. For the combination of APCI/APPI both the corona discharge and the light beam were active for the spray of a thermal nebulizer. All combinations are summarized in a scheme in Figure 4-1.

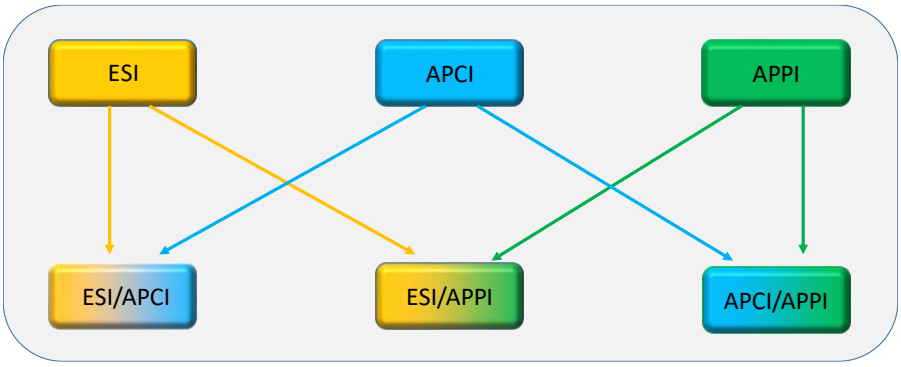

Figure 4-1: Ionization methods and their combinations used for this study

4.3.3. Data analysis

An external mass calibration was performed prior to sample analysis to meet a mass accuracy lower than 1 ppm. The recorded mass spectra were analyzed by XCalibur 2.2 software (Thermo Fischer, Bremen, Germany). The acquired data was imported and calculated to molecular formulae using the Composer software (version 1.5.0, Sierra Analytics, CA USA). The assignment of the molecular formulae was performed with the following constraints: H: 0-1000, C: 0-200, N: 0-3, O: 0-3, S: 0-3. The calculated formulae were sorted into different classes and were distinguished either as protonated molecules (M[H]) or radical ions (M). The obtained mass lists were transferred to Excel (Microsoft Office Professional Plus 2010, Microsoft Excel 2010) for further data evaluation. The calculated molecular formulae were sorted into compound classes based on their denoted Kendrick mass defect (KMD) and their double bond equivalence (DBE) distribution. DBE is an important parameter and can act as an indicator about the aromaticity. The number of DBE results from the sum of the ring closures and the number of π- bonds within a molecule and can be calculated from the general formula $C_cH_hN_nO_oS_s$ of the analyte using the following equation: DBE = $c - \frac{h}{2} + \frac{n}{2} + 1$.

4.4. Results and discussion

4.4.1. Electrospray ionization, atmospheric pressure photoionization and their combination

The effect of individual ionization methods on the selective analysis of compounds within a complex mixture as well as the degree of influence they have when they are combined was investigated on the present light crude oil. The graphical representation of the results was according to the compound class distribution based on the number of assigned compositions. In addition, a proportional Venn diagram was used in order to obtain complementary information on the assigned formulas by each ionization method and their combination. The detected compounds in the protonated form are labelled as [H] while the radical cations are shown without bracket. As can be seen in Figure 4-2, electrospray is the method of choice for the detection of polar compounds. Nitrogen containing species show the highest number of assignments among all the classes. The basic nitrogen classes of N[H]and NO[H] were the most abundant classes followed by

NO_2[H], NO_3[H] and NOS[H]. On the other hand, under APPI conditions the detection of hydrocarbon species in protonated and radical form was favored as has already been reported elsewhere.[43] Here, nonpolar hydrocarbons and aromatic hydrocarbons are efficiently ionized by this method. In addition, with APPI a high population number of oxygen containing compounds such as O[H], O, O_2[H], O_2, O_3[H], O_3 and OS was detected. Sulfur protonated and radical compounds are also present here, since APPI can easily ionize non polar sulfur containing species. Interestingly, the detection of N containing compounds was limited to the detection of only N and N[H] compounds.

Several studies have shown that discrimination and ion suppression effects occur especially during the analysis of complex mixtures.[13, 20, 44] Although in most cases the use of individual ionization methods is preferred since simplification is increasing the data depth, the combination of ion sources can provide new insights. As can be seen from the graph in Figure 4-2, the combination of ESI/APPI cooperates the benefits of both techniques effectively, acting in an intermediate way. Although in this case there is no specific class which is exclusively favored by the combination, however the detection of classes which were not accessible by each method individually as well as the increase of the population in some classes was observed. Here, higher amount of HC[H] and HC compounds were detected compared to ESI alone, as well as a higher number of O_x containing compounds. The ionization of sulfur species in protonated and radical form was also favored compared to the ESI, showing that the combination in this case utilize the properties of APPI. Finally, regarding the nitrogen containing compounds and the NO_x species, a higher amount of them was detected compared to APPI but not to ESI. In this case, the combination makes use of the analytical strength of the ESI mechanism.

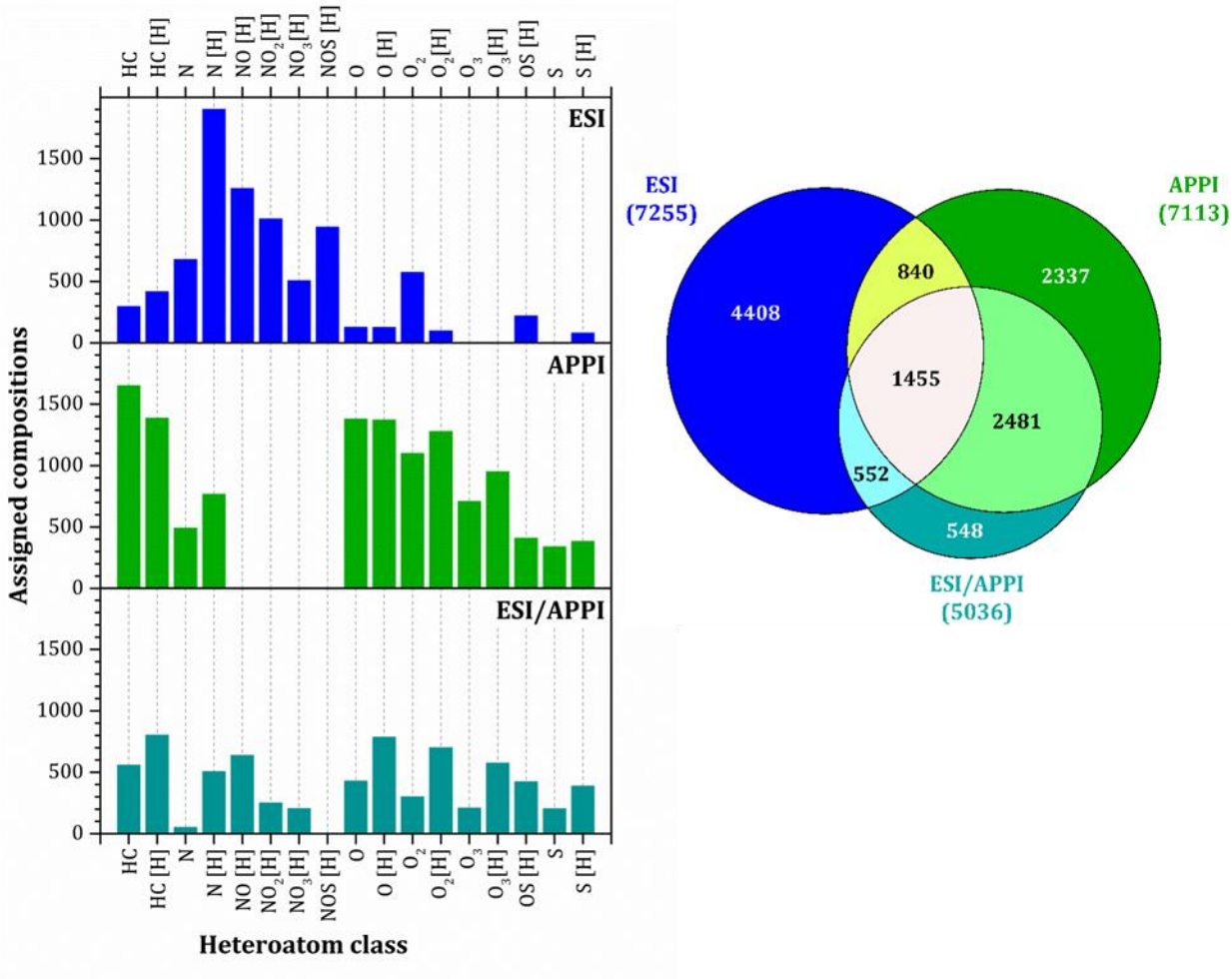

Figure 4-2: Population based distribution of heteroatom classes detected with electrospray (top), atmospheric pressure photoionization (middle) or their combination (bottom) as well as the Venn diagram (right) of the number of assigned composition. For the Venn diagram, both radical and protonated species have been taken into consideration.

In order to have more detailed information on the differences of each ionization method, a Venn diagram representation shows the unique assignments of each method. As can be seen from the graph, from a total of 7255 assignments that were detected with ESI, only 4408 were exclusively ionized by this method. On the other hand, APPI shows a total number of 7113 assigned compositions, however only one third of them (2337) were detected uniquely. These two methods have 840 common compounds, indicating their selectivity towards specific compounds. Now, their combination results in the detection of only 548 individual compounds from a total of 5036. In this case, clearly the combination of ESI/APPI share the biggest part of the detected compounds (2481) with

APPI. With this prime example can be easily seen that each ionization method favors or discriminates specific type of compounds and the use of only one ionization method is not adequate for a complete characterization of a complex mixture.

An example of Kendrick plots (DBE versus carbon number) of three different classes (N[H], O[H] and S[H]) obtained by the above mentioned ionization methods can be seen in Figure 4-3. This representation provides information regarding the aromaticity of the compounds. Basic N[H] species detected with ESI contained 11-75 carbon atoms, with a DBE distribution in the range of 4-50. These likely correspond to pyridines. Molecules that contain a pyridinic ring are selectively detected by ESI due to their high polarity, thus explaining the large number of pyridinic nitrogen species observed in this ionization method.[45] Under APPI conditions, the number of carbon atoms that were detected was slightly lower (11-62) with a DBE value of 4-34. Studies have shown that APPI can ionize efficiently both pyridinic and pyrrolic compounds, while ESI shows a limitation mainly towards the pyridinic type of compounds.[46] With the combination of these two methods, the nitrogen containing compounds detected, contained a carbon number of 14-50 with DBE values of 4-23. In this case, electrospray shows the best sensitivity for the nitrogen class as well as the broadest carbon and DBE distribution. Regarding the oxygen containing compounds the results show a different trend. Here, APPI as well as the combined methods display the highest carbon and DBE distribution with 10-69 carbon atoms and DBE of 1-40, and 14-54 carbon number with 1-26 DBE number respectively. ESI shows the least number of carbon atoms (11-28) as well as DBE distribution (5-22).

Based on some model compounds that have been tested using ESI or APPI, aromatic alcohols (e.g. 1-Pyrenemethanol), aromatic aldehydes (e.g. 1-Pyrenecarbaldehyde), ketons (e.g. Anthraquinone) and furanes (e.g. 2-Acetylfuran) have been successfully ionized by these methods.[46, 47] Finally, the nonpolar S_1 class is not usually ionized by electrospray. However, several studies have shown that sulfur species with DBEs of 2-6, indicating a low aromaticity, can correspond to cyclic-ring sulfides.[48] Higher DBE number indicates that sulfur species were enriched with thiophenic compounds. Under ESI conditions the number of carbon atoms detected was from 10-25 with a DBE distribution of 5-15. On the other hand, APPI or the combined methods show higher amount of carbon atoms and DBE values. Ionization of polycyclic aromatic sulfur heterocycles (PASHs) can be achieved by these methods.

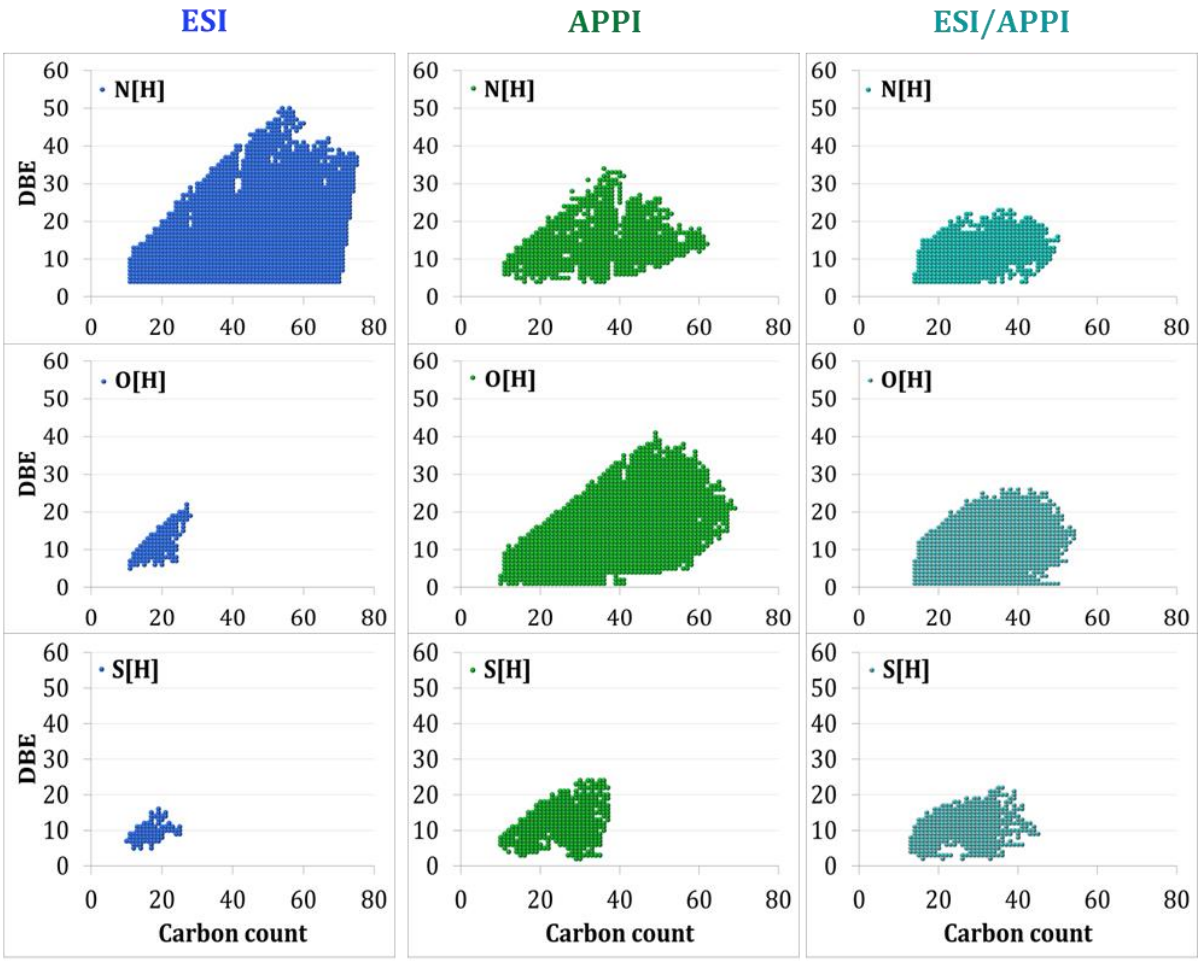

Figure 4-3: Double bond equivalent (DBE) vs. amount of carbon atoms per molecule for the N[H], O[H] and S[H] classed detected with ESI (left), APPI (middle) or their combined ionization method (right).

4.4.2. Atmospheric Pressure photoionization, Atmospheric Pressure Chemical ionization and their combination

The main challenge regarding the analysis of complex mixtures is achieving a broader range of compounds that can be ionized effectively. In 2004, Syage and co-workers introduced a dual ionization source which combined atmospheric pressure photoionization (APPI) with atmospheric pressure chemical ionization (APCI). The main goal behind this combination was to extend the coverage of compounds which could simultaneously be ionized by both techniques.[49] However, the question remains is if the method combination can provide more information regarding the chemical composition of the sample or the use of a single ionization method is preferred. In Figure 4-4, the

results obtained by the single ionization method of APPI, APCI as well as by their combination are displayed.

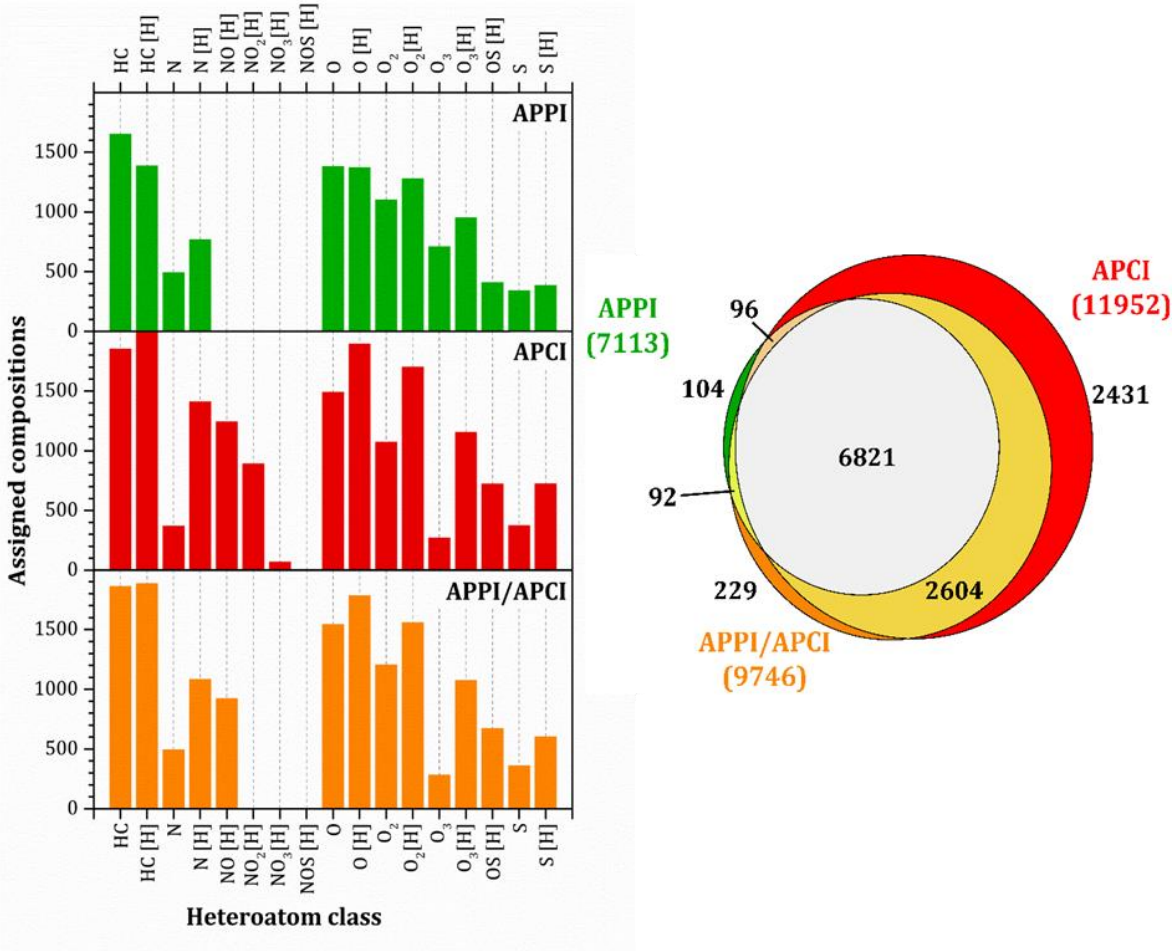

Figure 4-4: Population based distribution of heteroatom classes detected with atmospheric pressure photoionization (top), atmospheric pressure chemical ionization (middle) or their combination (bottom). Venn diagram (right) shows the total number of assigned compositions.

From a first look at the graph, only small differences regarding the population of the heteroatom classes are observed. With APPI, hydrocarbon species as well as oxygen containing compounds in both radical and protonated form showed the highest population abundance. In addition, smaller amounts of OS[H], S and S[H] were detected. Regarding the nitrogen containing compounds, only the N and N[H] classes were ionized by this method. On the other hand, under APCI conditions, the ionization of N and NO_x species was favored. Here, the highest amount of the detected compounds are hydrocarbon and oxygen containing compounds in both protonated and radical form. The combination of these two methods does not present drastic changes on the detection of

classes, since the results show similarities to the results obtained with individual ionization techniques. However, with the Venn diagram it is possible to gain a better understanding of the similarities and differences among them. The diagram in this case has an unusual shape and this is due to the very high overlap among the techniques. The majority of the compounds (6821) were co-assigned showing that the methods share among them more similarities. Interestingly, with APPI only 104 assignments were detected from a total of 7113, while with APCI 2431 from 11952 molecular formula were detected individually. In this case, the combination of these techniques did not favor the ionization of a broader range of compounds since only 229 species were detected alone. The combination of APPI/APCI showed a share of more common compounds with APCI. However, while in MS we only detect *m/z* ratios, it needs to be mentioned that there is no information if the compounds found under these ionization conditions are the same compounds. Unfortunately, MS alone cannot provide any information about the different isomeric compounds while MS/MS is only useful on a limited basis when different fragments are available that reveal structural information.[50, 51]

4.4.3. Electrospray ionization, atmospheric pressure chemical ionization and their combination

Although ESI and APCI alone are powerful ionization methods, there is limited information about the selectivity and the sensitivity when they are combined. In general, the combination of ESI with APCI is not a commonly used technique, since each individual method presents strong matrix effects. Here, these two techniques were combined allowing a deeper insight on their ionization capabilities. It has to be noted, that when the APCI current was varied the distribution changed. At a lower current of 0.5 µA the compounds that also can be seen by ESI are more prominent, while at higher current values that shifts to the compounds more prominent in APCI. Here, we used a value of 5 µA, which gives the broadest distribution. This effect shows that both ionization methods interfer with each other depending on the conditions.

In the mass spectra in Figure 4-5, it can be observed that most of the signals were detected between *m/z* 250-550 under ESI conditions, although various signals are apparent throughout the whole mass range. On the other hand, by using APCI, the highest signal intensity was observed in lower mass range (*m/z* of 150-300). Now, when these

methods are combined and a discharge current of 5.0 μA is applied, the spectrum tends to show similarities to the spectrum of APCI. More detailed information regarding the class distribution as well as the similarities and the differences of these methods can be seen in Figure 4-6.

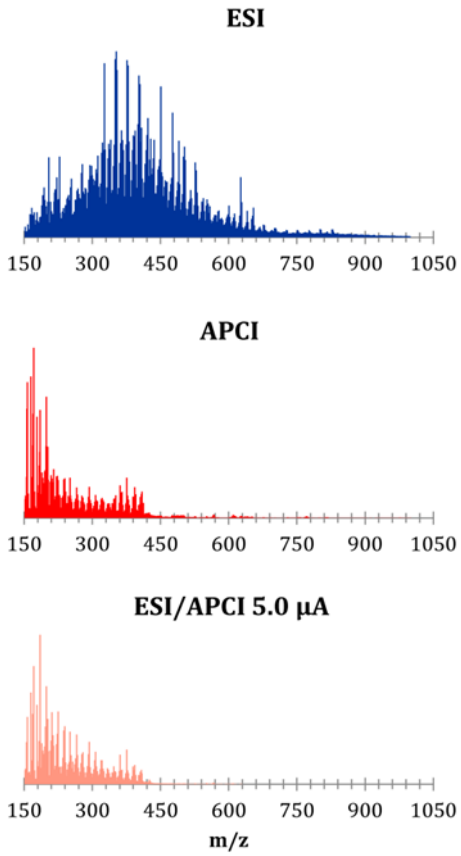

Figure 4-5: Comparison of mass spectra obtained by spectral stitching (SIM) with electrospray ionization, atmospheric pressure chemical ionization, and their combination.

A general decrease on the population of the detected compounds in all classes can be seen in Figure 4-6. Under this ionization method, nitrogen containing species had the highest population abundance. The combination showed an efficiency in ionization towards oxygen containing compounds as well as sulfur species compared to the ESI method. Recent studies performed on a mixture of selected polar compounds using different ionization methods showed that the aromatic nitrogen compound of pyridine could be efficiently ionized by both ESI and APCI, while indole and carbazole could be exclusively ionized by APCI.[52] Regarding the sulfur compounds, benzothiophenes and its

derivatives were detected only under APCI conditions which fits earlier results that they are difficult to ionize by ESI alone.[53] Finally, the ketone model of fluorenone was tested and data showed that it could be efficiently ionized by both methods, contrary to the compound contained a hydroxyl functional group (e.g., naphthalenol) which was detected only under APCI.[52]

The Venn diagram reveals that the combination of these techniques did not favor the ionization of new compounds since only 224 species were detected individually. Surprisingly, the highest amount of the detected compounds are commonly shared with APCI, while only 729 species were in common with ESI. A number of 3262 assigned compositions were detected in common with both ESI and APCI as well as with the combination of ESI/APCI, while the biggest number of individual compounds detected was only under APCI. A possible explanation for this can be due to the fact that ESI is known for ion suppression, showing higher matrix effects compared to APCI. The studies of combining different API methods indicate that when analyzing complex mixtures the discrimination and suppression effects that are already known from such samples are more prevalent. [41] Especially the combination of ESI and APCI indicates, that depending on the conditions, each ionization mechanism can be more or less prominent than the other. The fairly low number of assignments found here could show that the combination creates no new ionization mechanism and the compounds are ionized by most suitable method.

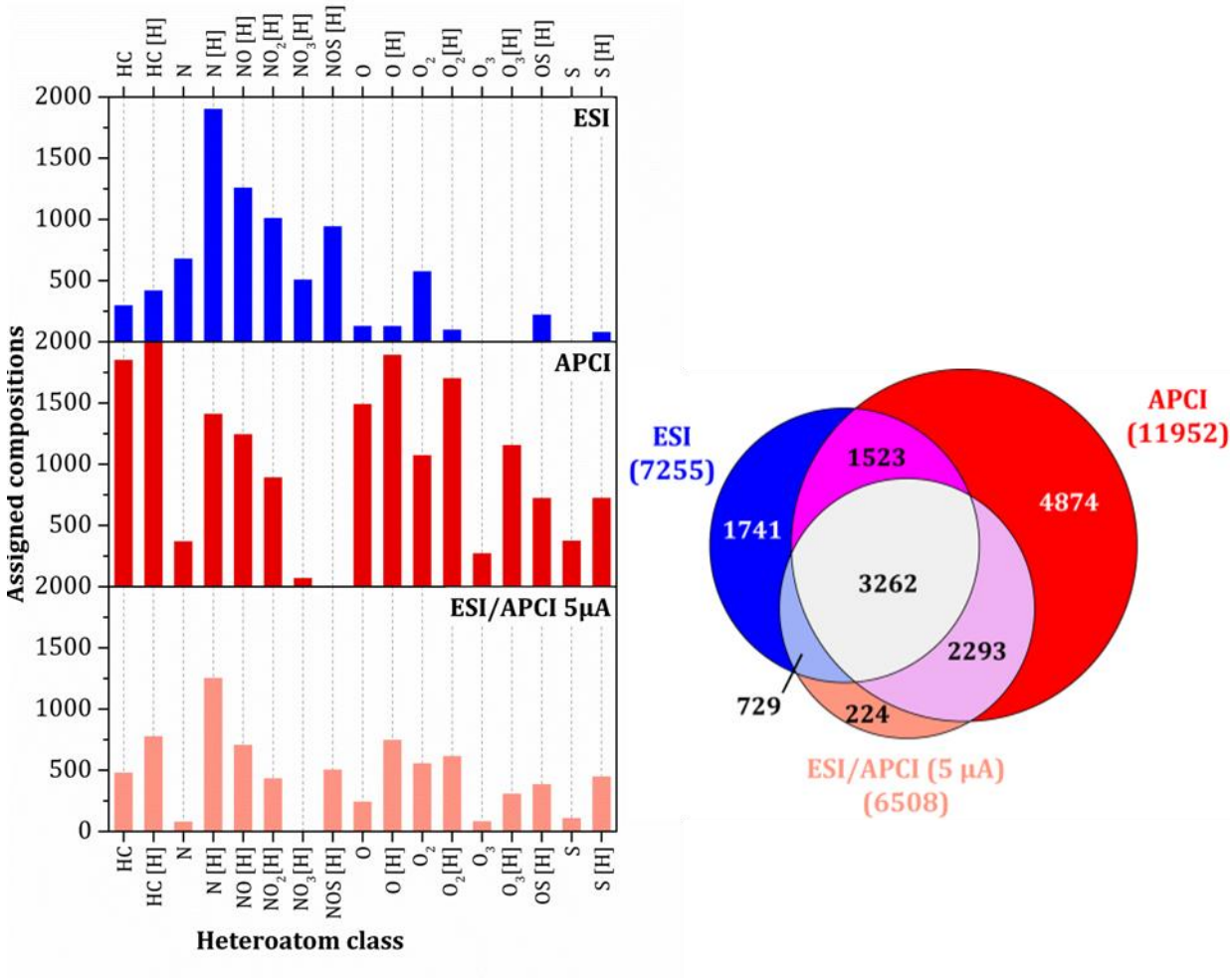

Figure 4-6: Population based distribution of heteroatom classes detected with electrospray (top), atmospheric pressure chemical ionization (middle) or their combination (bottom). Venn diagram (right) shows the total number of assigned compositions.

Still, the results also show, that the combination of two ionization methods can add new information in comparison to using a single method alone. Here, a change in the ionization mechanism can be a reason. However, a complex mixture is not the best sample to investigate ionization mechanisms. For that purpose detailed studies are needed to show how the ionization mechanisms change.

4.5. Conclusion

The efficiency of three different ionization methods as well as their combination was investigated for the analysis of a complex crude oil mixture. Electrospray is the method of choice for the ionization of basic nitrogen compounds while APPI favors the ionization of hydrocarbons as well as oxygen containing compounds. Although the combination of different ionization methods is prone to higher suppression effects, in some cases they can provide complementary information about complex mixture constituents where often the different polarity can play a role. When using the combination of ESI/APPI, higher number of hydrocarbons and O_x species were detected compared to the ESI alone. The combination of APPI with APCI showed overall no significant changes since most of the detected compounds were commonly found among these methods. Finally, the combined ESI/APCI method did not allow the detection of many individual compounds. Different current values of the corona needle in case of APCI would be an interesting approach for future studies in order to investigate how it can influence the ionization of various compounds.

4.6. References

1. Ellabban, O.; Abu-Rub, H.; Blaabjerg, F., Renewable energy resources: Current status, future prospects and their enabling technology. *Renewable Sustainable Energy Rev.* **2014,** *39*, 748-764.

2. Azarpour, A.; Suhaimi, S.; Zahedi, G.; Bahadori, A., A Review on the Drawbacks of Renewable Energy as a Promising Energy Source of the Future. *Arabian J. Sci. Eng.* **2013,** *38* (2), 317-328.

3. Ian, C., World Energy Outlook 2014 projections to 2040: natural gas and coal trade, and the role of China. *Australian Journal of Agricultural and Resource Economics* **2015,** *59* (4), 571-585.

4. Chengzao, J., Breakthrough and significance of unconventional oil and gas to classical petroleum geology theory. *Petrol. Explor. Develop.* **2017,** *44*, 1-10.

5. Miller, R. G.; Sorrell, S. R., The future of oil supply. *Philosophical transactions. Series A, Mathematical, physical, and engineering sciences* **2014,** *372* (2006), 20130179.

6. Saniere, A.; Hénaut, I.; Argillier, J. F., Pipeline Transportation of Heavy Oils, a Strategic, Economic and Technological Challenge. *Oil & Gas Science and Technology - Rev. IFP* **2004,** *59* (5), 455-466.

7. Zheng, L.; Wei, P.; Zhang, Z.; Nie, S.; Lou, X.; Cui, K.; Fu, Y., Joint exploration and development: A self-salvation road to sustainable development of unconventional oil and gas resources. *Nat. Gas Ind. B* **2017,** *4* (6), 477-490.

8. Hart, A., A review of technologies for transporting heavy crude oil and bitumen via pipelines. *J. Pet. Explor. Prod. Technol.* **2014,** *4* (3), 327-336.

9. Santos, R. G.; Loh, W.; Bannwart, A. C.; Trevisan, O. V., An overview of heavy oil properties and its recovery and transportation methods *Braz. J. Chem. Eng.* **2014,** *31*, 571-590.

10. Watkinson, A. P., Deposition from Crude Oils in Heat Exchangers. *Heat Transfer Eng.* **2007,** *28* (3), 177-184.

11. Prado, G. H. C.; Rao, Y.; de Klerk, A., Nitrogen Removal from Oil: A Review. *Energy Fuels* **2017,** *31* (1), 14-36.

12. Cho, Y.; Ahmed, A.; Islam, A.; Kim, S., Developments in FT-ICR MS instrumentation, ionization techniques, and data interpretation methods for petroleomics *Mass Spectrom. Rev.* **2015,** *34* (2), 248-263.

13. Vetere, A.; Schrader, W., Mass Spectrometric Coverage of Complex Mixtures: Exploring the Carbon Space of Crude Oil. *ChemistrySelect* **2017,** *2* (3), 849-853.

14. Roussis, S. G.; Proulx, R., The Characterization of Basic Petroleum Extracts by High-Resolution Mass Spectrometry and Simultaneous Orthogonal Acceleration Time-of-Flight–Magnet Scanning Tandem Mass Spectrometry. *Energy Fuels* **2004,** *18* (3), 685-697.

15. Palacio Lozano, D. C.; Gavard, R.; Arenas-Diaz, J. P.; Thomas, M. J.; Stranz, D. D.; Mejía-Ospino, E.; Guzman, A.; Spencer, S. E. F.; Rossell, D.; Barrow, M. P., Pushing the analytical limits: new insights into complex mixtures using mass spectra segments of constant ultrahigh resolving power. *Chemical Science* **2019,** *10* (29), 6966-6978.

16. Panda, S. K.; Andersson, J. T.; Schrader, W., Mass-spectrometric analysis of complex volatile and nonvolatile crude oil components: a challenge. *Anal. Bioanal. Chem.* **2007,** *389* (5), 1329-39.

17. Olsen, J. V.; de Godoy, L. M.; Li, G.; Macek, B.; Mortensen, P.; Pesch, R.; Makarov, A.; Lange, O.; Horning, S.; Mann, M., Parts per million mass accuracy on an Orbitrap mass spectrometer via lock mass injection into a C-trap. *Molecular & cellular proteomics : MCP* **2005,** *4* (12), 2010-21.

18. McKenna, A. M.; Nelson, R. K.; Reddy, C. M.; Savory, J. J.; Kaiser, N. K.; Fitzsimmons, J. E.; Marshall, A. G.; Rodgers, R. P., Expansion of the analytical window for oil spill characterization by ultrahigh resolution mass spectrometry: beyond gas chromatography. *Environ Sci Technol* **2013,** *47* (13), 7530-9.

19. Kondyli, A.; Schrader, W., High-resolution GC/MS studies of a light crude oil fraction. *J. Mass Spectrom.* **2019,** *54* (1), 47-54.

20. Panda, S. K.; Andersson, J. T.; Schrader, W., Characterization of Supercomplex Crude Oil Mixtures: What Is Really in There? *Angew. Chem.* **2009,** *121* (10), 1820-1823.

21. Lababidi, S.; Schrader, W., Online normal-phase high-performance liquid chromatography/Fourier transform ion cyclotron resonance mass spectrometry: effects of different ionization methods on the characterization of highly complex crude oil mixtures. *Rapid communications in mass spectrometry : RCM* **2014,** *28* (12), 1345-52.

22. Zhan, D.; Fenn, J. B., Electrospray mass spectrometry of fossil fuels11Dedicated to Professor Jim Morrison on the occasion of his 75th birthday. *International Journal of Mass Spectrometry* **2000,** *194* (2), 197-208.

23. Zhang, L.; Zhang, Y.; Zhao, S.; Xu, C.; Chung, K. H.; Shi, Q., Characterization of heavy petroleum fraction by positive-ion electrospray ionization FT-ICR mass spectrometry and collision induced dissociation: Bond dissociation behavior and aromatic ring architecture of basic nitrogen compounds. *Sci. China: Chem.* **2013,** *56* (7), 874-882.

24. Fenn, J. B.; Mann, M.; Meng, C. K.; Wong, S. F.; Whitehouse, C. M., Electrospray ionization for mass spectrometry of large biomolecules. *Science* **1989,** *246* (4926), 64-71.

25. Rostad, C. E., Screening of Polar Components of Petroleum Products by Electrospray Ionization Mass Spectrometry. *Energy Fuels* **2005,** *19* (3), 992-997.

26. Purcell, J. M.; Rodgers, R. P.; Hendrickson, C. L.; Marshall, A. G., Speciation of Nitrogen Containing Aromatics by Atmospheric Pressure Photoionization or Electrospray Ionization Fourier Transform Ion Cyclotron Resonance Mass Spectrometry. *J. Am. Soc. Mass. Spectrom.* **2007,** *18* (7), 1265-1273.

27. Wilm, M., Principles of Electrospray Ionization. *Molecular & Cellular Proteomics : MCP* **2011,** *10* (7), M111.009407.

28. Zhou, S.; Cook, K. D., Protonation in electrospray mass spectrometry: wrong-way-round or right-way-round? *J. Am. Soc. Mass. Spectrom.* **2000,** *11* (11), 961-966.

29. Shi, Q.; Zhao, S.; Xu, Z.; Chung, K. H.; Zhang, Y.; Xu, C., Distribution of Acids and Neutral Nitrogen Compounds in a Chinese Crude Oil and Its Fractions: Characterized by Negative-Ion Electrospray Ionization Fourier Transform Ion Cyclotron Resonance Mass Spectrometry. *Energy Fuels* **2010,** *24* (7), 4005-4011.

30. Xiaobo, C.; Yibin, L.; Jin, W.; Honghong, S.; Chaohe, Y.; Chunyi, L., Characterization of nitrogen compounds in coker gas oil by electrospray ionization Fourier transform ion cyclotron resonance mass spectrometry and Fourier transform infrared spectroscopy. *Appl Petrochem Res* **2014,** *4* (4), 417-422.

31. Purcell, J. M.; Hendrickson, C. L.; Rodgers, R. P.; Marshall, A. G., Atmospheric Pressure Photoionization Fourier Transform Ion Cyclotron Resonance Mass Spectrometry for Complex Mixture Analysis. *Anal. Chem.* **2006,** *78* (16), 5906-5912.

32. Robb, D. B.; Blades, M. W., Effects of Solvent Flow, Dopant Flow, and Lamp Current on Dopant-Assisted Atmospheric Pressure Photoionization (DA-APPI) for LC-MS. Ionizationvia Proton Transfer. *J. Am. Soc. Mass. Spectrom.* **2005,** *16* (8), 1275-1290.

33. Kauppila, T. J.; Kersten, H.; Benter, T., The ionization mechanisms in direct and dopant-assisted atmospheric pressure photoionization and atmospheric pressure laser ionization. *J. Am. Soc. Mass Spectrom.* **2014,** *25* (11), 1870-81.

34. Kauppila, T. J.; Syage, J. A.; Benter, T., Recent developments in atmospheric pressure photoionization-mass spectrometry. *Mass Spectrom. Rev.* **2017,** *36* (3), 423-449.

35. Tose, L. V.; Cardoso, F. M. R.; Fleming, F. P.; Vicente, M. A.; Silva, S. R. C.; Aquije, G. M. F. V.; Vaz, B. G.; Romão, W., Analyzes of hydrocarbons by atmosphere pressure chemical ionization FT-ICR mass spectrometry using isooctane as ionizing reagent. *Fuel* **2015,** *153*, 346-354.

36. Raffaelli, A.; Saba, A., Atmospheric pressure photoionization mass spectrometry. *Mass Spectrom. Rev.* **2003,** *22* (5), 318-31.

37. Kolakowski, B. M.; Grossert, J. S.; Ramaley, L., Studies on the positive-ion mass spectra from atmospheric pressure chemical ionization of gases and solvents used in liquid chromatography and direct liquid injection. *J. Am. Soc. Mass. Spectrom.* **2004,** *15* (3), 311-324.

38. Gaspar, A.; Zellermann, E.; Lababidi, S.; Reece, J.; Schrader, W., Impact of Different Ionization Methods on the Molecular Assignments of Asphaltenes by FT-ICR Mass Spectrometry. *Anal. Chem.* **2012,** *84* (12), 5257-5267.

39. Annesley, T. M., Ion suppression in mass spectrometry. *Clin Chem* **2003,** *49* (7), 1041-4.

40. Axelsson, J.; Scrivener, E.; Haddleton, D. M.; Derrick, P. J., Mass Discrimination Effects in an Ion Detector and Other Causes for Shifts in Polymer Mass Distributions Measured by Matrix-Assisted Laser Desorption/Ionization Time-of-Flight Mass Spectrometry. *Macromolecules* **1996,** *29* (27), 8875-8882.

41. Schmitt-Kopplin, P.; Englmann, M.; Rossello-Mora, R.; Schiewek, R.; Brockmann, K. J.; Benter, T.; Schmitz, O. J., Combining chip-ESI with APLI (cESILI) as a multimode source for analysis of complex mixtures with ultrahigh-resolution mass spectrometry. *Anal. Bioanal. Chem.* **2008,** *391* (8), 2803-9.

42. Gaspar, A.; Schrader, W., Expanding the data depth for the analysis of complex crude oil samples by Fourier transform ion cyclotron resonance mass spectrometry using the spectral stitching method. *Rapid Commun. Mass Spectrom.* **2012,** *26* (9), 1047-52.

43. Rogel, E.; Witt, M., Atmospheric Pressure Photoionization Coupled to Fourier Transform Ion Cyclotron Resonance Mass Spectrometry To Characterize Asphaltene Deposit Solubility Fractions: Comparison to Bulk Properties. *Energy Fuels* **2016,** *30* (2), 915-923.

44. Cho, Y. J.; Na, J. G.; Nho, N. S.; Kim, S.; Kim, S., Application of Saturates, Aromatics, Resins, and Asphaltenes Crude Oil Fractionation for Detailed Chemical Characterization of Heavy Crude Oils by Fourier Transform Ion Cyclotron Resonance Mass Spectrometry Equipped with Atmospheric Pressure Photoionization. *Energy Fuels* **2012,** *26* (5), 2558-2565.

45. Al-Hajji, A. A.; Muller, H.; Koseoglu, O. R., Characterization of Nitrogen and Sulfur Compounds in Hydrocracking Feedstocks by Fourier Transform Ion Cyclotron Mass Spectrometry. *Oil & Gas Science and Technology - Rev. IFP* **2008,** *63* (1), 115-128.

46. Huba, A. K.; Huba, K.; Gardinali, P. R., Understanding the atmospheric pressure ionization of petroleum components: The effects of size, structure, and presence of heteroatoms. *Sci. Total Environ.* **2016,** *568*, 1018-1025.

47. Staš, M.; Chudoba, J.; Auersvald, M.; Kubička, D.; Conrad, S.; Schulzke, T.; Pospíšil, M., Application of orbitrap mass spectrometry for analysis of model bio-oil compounds and fast pyrolysis bio-oils from different biomass sources. *J. Anal. Appl. Pyrolysis* **2017,** *124*, 230-238.

48. Liu, P.; Xu, C.; Shi, Q.; Pan, N.; Zhang, Y.; Zhao, S.; Chung, K. H., Characterization of Sulfide Compounds in Petroleum: Selective Oxidation Followed by Positive-Ion Electrospray Fourier Transform Ion Cyclotron Resonance Mass Spectrometry. *Anal. Chem.* **2010,** *82* (15), 6601-6606.

49. Syage, J. A.; Hanold, K. A.; Lynn, T. C.; Horner, J. A.; Thakur, R. A., Atmospheric pressure photoionization: II. Dual source ionization. *J. Chromatogr. A* **2004,** *1050* (2), 137-149.

50. Jeanne Dit Fouque, D.; Maroto, A.; Memboeuf, A., Purification and Quantification of an Isomeric Compound in a Mixture by Collisional Excitation in Multistage Mass Spectrometry Experiments. *Anal. Chem.* **2016,** *88* (22), 10821-10825.

51. Vetere, A.; Alachraf, M. W.; Panda, S. K.; Andersson, J. T.; Schrader, W., Studying the fragmentation mechanism of selected components present in crude oil by collision-induced dissociation mass spectrometry. *Rapid Commun. Mass Spectrom.* **2018,** *32* (24), 2141-2151.

52. Pudenzi, M. A.; Eberlin, M. N., Assessing Relative Electrospray Ionization, Atmospheric Pressure Photoionization, Atmospheric Pressure Chemical Ionization, and Atmospheric Pressure Photo- and Chemical Ionization Efficiencies in Mass Spectrometry Petroleomic Analysis via Pools and Pairs of Selected Polar Compound Standards. *Energy Fuels* **2016,** *30* (9), 7125-7133.

53. Muller, H.; Andersson, J. T.; Schrader, W., Characterization of high-molecular-weight sulfur-containing aromatics in vacuum residues using Fourier transform ion cyclotron resonance mass spectrometry. *Anal. Chem.* **2005,** *77* (8), 2536-2543.

CHAPTER 5. STUDYING CRUDE OIL FOULING WITH FOCUS ON SULFUR CONTAINING COMPOUNDS USING HIGH RESOLUTION MASS SPECTROMETRY

Redrafted from:

A. Kondyli, W. Schrader. "Studying crude oil fouling with focus on sulfur containing compounds using high-resolution mass spectrometry", will be submitted to *Fuel*.

5.1. Abstract

With the depletion of conventional resources heavier and more sulfur-rich crude oils come into the focus of interest. However, the utilization of such feedstocks is extremely undesirable since their high sulfur content causes corrosion fouling, catalyst poisoning and emissions of toxic pollutants into the atmosphere. As known catalyst poisoners sulfur containing compounds are also suspected to play an important role in crude oil fouling, i.e. the formation of undesired solid deposits. In order to overcome these problems, insight knowledge on the chemical composition of the sulfur containing compounds on a molecular level and their behavior is necessary. Here, fouling reactions of a light crude oil fraction were simulated in the laboratory under atmospheric and inert conditions, with special focus on sulfur containing compounds. The results indicate that sulfur containing compounds decompose at elevated temperatures, partly by a radical induced mechanism. Furthermore, the resulting intermediates show a limited stability in the presence of oxygen.

5.2. Introduction

The ever-increasing energy demand has led to the depletion of conventional light and sweet (low-sulfur) crude oil reservoirs. In order to meet the world's energy needs, heavier and more sour (high-sulfur) feedstocks need to be incorporated into the market.[1, 2] However, utilization of these types of oil is highly unfavorable since they require special treatment and technological improvements in order to be upgraded into economically valuable products.[3] Their high content of heteroatoms (N, O, S) and metals (e.g. V, Ni, Fe) have adverse effects during production, refining, storage and transportation.[4, 5]

One of the biggest and till now unresolved problem in petroleum industry is crude oil fouling. The formation of organic solid deposits is a highly complex phenomenon involving not only different processes (crystallization of inorganics, corrosion) but also different chemical reactions (polymerization, oxidation, thermal decomposition).[6] In order to encounter these problems characterization of crude oil with emphasis on heteroatom containing compounds (N, O, S) is necessary. Among them, sulfur species have attracted great attention due to their corrosive character. Sulfur is usually the most abundant hetero-element in crude oil and its content can reach up to 14 wt.-%.[7] Sulfur-containing compounds can be found in all boiling fractions, but usually their amount increases with the increase of the boiling point of the fraction.[8] Sulfur species are among the most undesirable constituents in crude oil since they decrease the quality of the products, especially the fuels that derive from it. In addition, they can cause catalyst poisoning, corrosion of the processing equipment as well as various problems related to product odour and storage stability.[9-12] Sulfur has an effect in crude oil fouling, with thiols, sulfides and some condensed thiophenes to be considered as the most problematic.[13] Free sulfur, disulfides, and thiophenol have been found to promote sludge formation,[14] while the presence of hydrogen sulfide is extremely corrosive at high temperatures.[15, 16] A major problem in the refinery heat exchangers is the formation of corrosion fouling due to chemical reactions triggered by sulfur compounds in crude oil on metallic surfaces. According to Watkinson, deposition of solid material can be attributed to the presence of iron sulfides in case of a medium-sulfur crude oil.[5]

Nowadays, in order to overcome the above mentioned problems, several efforts have been made to reduce fouling formation either by improving the operating conditions or the design of the heat exchanges.[17] However, the ability to solve this problem is limited firstly, due to the complex nature of crude oil which contains more than a million different

chemical compositions, secondly, due to the still unknown reaction mechanisms that lead to the deposit formation and finally, due to the almost impossible simulation of an industrial fouling reaction under laboratory conditions. In order to optimize various industrial processes during oil processing as well as to prevent unfavourable sulfur reactions, a better understanding of the sulfur compounds is necessary.[18, 19] In the petroleum industry, elemental analysis is usually performed to determine the sulfur content. However, this method is quite limited since it provides information only for the bulk properties of the sample, while no information on a molecular level can be obtained.

Over the years, various analytical techniques have been used to characterize sulfur species in crude oil. Among them, gas chromatography/mass spectrometry (GC/MS) has been used to determine elemental sulfur in naphtha and gasoline,[20] gel permeation chromatography (GPC) and ultra-high resolution mass spectrometry have been successfully applied in the characterization of aromatic hydrocarbons and sulfur heterocycles in a heavy crude oil,[21] while recently the analysis of three classes of sulfur compounds has been shown by using LC-separation and an online detection and quantification by ICP-MS.[22] High-resolution mass spectrometry (HRMS) is the method of choice for the investigation of complex mixtures due to its ability to provide high resolving power and highly accurate mass measurements.[23, 24] Electrospray ionization (ESI) is not commonly selected for the ionization of polycyclic aromatic sulfur hydrocarbons (PASHs) since these species are typically not basic enough to be easily protonated. Thus, atmospheric pressure photoionization (APPI) is preferably used for their ionization. However, reports in the literature show that by using chemical methods such as alkylation a selectivity towards sulfur containing species can be achieved, producing pre-formed ions and thus making their characterization by ESI possible.[25] In addition, Wang and co-workers have successfully demonstrated the selective analysis of sulfur containing compounds in a heavy crude oil by deuterium labeling reactions and their detection with ultra-high resolution mass spectrometry by positive electrospray.[26]

In this study, a light fraction of crude oil has been selected in order to investigate the fouling behavior of sulfur containing compounds at different temperatures as well as to test the influence of oxygen on fouling. The results shown here indicate that sulfur-containing compounds undergo chemical changes after thermal treatment, forming different types of sulfur species which are detectable with the use of electrospray. The results obtained with ESI are compared to the results obtained with APPI in order to obtain comprehensive information regarding the polar and nonpolar sulfur species.

5.3. Experimental

5.3.1. Simulation of crude oil fouling on laboratory scale

For the fouling simulation, a laboratory-built reactor made of stainless steel was used. The experimental setup can be seen in Figure 5-1. A quartz crucible was filled with 0.3 mL of sample and then placed inside the autoclave. A quartz cover was placed on the top of the crucible in order to avoid sample losses. Then, the autoclave was sealed with a stainless steel ring and was set inside a heating mould. The sample was heated for 3 days to temperatures of 150 °C, 250 °C, 350 °C or 450 °C. In order to test the influence of the oxygen on the fouling rate, a second batch of experiments was performed under inert conditions (IC). In this case, the reactors were filled and sealed inside an argon-filled glove bag to create an inert reaction atmosphere. The reaction time and temperature conditions remained the same as before.

Figure 5-1: Equipment used in fouling simulation under laboratory conditions.

5.3.2. Solid deposit analysis

The solid material was analyzed microscopically by transmission electron microscopy (TEM) and energy-dispersive X-ray spectroscopy (EDX). High-resolution imaging and chemical analysis were performed using a 200 kV electron microscope with cold field emitter and CCD-camera (Hitachi HF-2000).

5.3.3. Mass Spectrometry and data analysis

For mass spectrometric analysis a research-type Orbitrap Elite (Thermo Fisher, Bremen, Germany) was used.[24] Mass spectra were acquired using spectral stitching (30

Da windows with 5 Da overlap) in a range of *m/z* 200-1000 and with a resolving power of *R* = 480,000 (FWHM at *m/z* 400). All samples were dissolved and diluted in a solvent mixture of toluene (HPLC grade, Sigma-Aldrich, Germany) and methanol (LC-MS grade, J. T. Baker, Germany) in a ratio of 1:4 (*v*/*v*), to a final concentration of 250 ppm and then analyzed without further treatment. Electrospray (ESI) in positive ion mode was used as ionization method. The ionization was performed using a stainless-steel needle at a capillary voltage of 4 kV. Nebulization was assisted by a sheath gas flow of 4.0 a.u. (arbitrary units) while the auxiliary and the sweep gas flow were set to 1.0 a.u. The transfer capillary temperature was set to 275 °C. For APPI ionization, a Krypton VUV lamp (Syagen, Tustin, CA, USA) with a photon emission at 10.0/10.6 eV was used. The sample was introduced with a flow rate of 8 µl min^{-1} and evaporated in the heated nebulizer at 350 °C. Nitrogen was used as sheath, auxiliary and sweep gas and the flow rate was set at 20.0 a.u., 8.0 a.u. and 8.0 a.u. respectively. External mass calibration was performed prior to sample analysis in order to meet a mass accuracy better than 1 ppm. The recorded mass spectra were recombined by Xcalibur 4.0 software (Thermo Fisher, Bremen, Germany) and further processed using the Composer software (version 1.5.0, Sierra Analytics, Modesto, CA, USA). Calculations and assignments of molecular formulae were performed using the following restrictions regarding the number of possible elements and the number of double bond equivalents (DBE): H: 0-1000, C: 0-200, N: 0-3, O: 0-3, S: 0-2 and DBE: 0-100. The calculated molecular formulae were sorted into heteroatom classes based on their denoted Kendrick mass defects and their double bond equivalent distribution. The obtained mass lists were transferred to Excel (Microsoft Office Professional Plus 2010, Microsoft Corporation, Redmond, WA, USA) for further data evaluation. Double bond equivalent refers to the sum of ring closures and π-bonds present within a molecule and is calculated from the molecular formula ($C_cH_hN_nO_oS_s$) of the assigned individual peaks using the equation: $\mathrm{DBE} = c - \frac{h}{2} + \frac{n}{2} + 1$.

5.4. Results and discussion

One of the biggest problems to overcome in order to investigate the fouling behavior of sulfur containing compounds was to simulate a costly industrial process under laboratory conditions. Here, for the first time, the successful simulation of fouling was achieved with the use of the reactors. Formation of solid material was observed only at the highest temperature of 450 °C after 3 days of reaction in both cases under inert or

oxygenated conditions. The resulting insoluble solid deposit was analyzed microscopically and as can be seen from Figure 5-2 is amorphous carbon material consisting of more than 95 % carbon content.

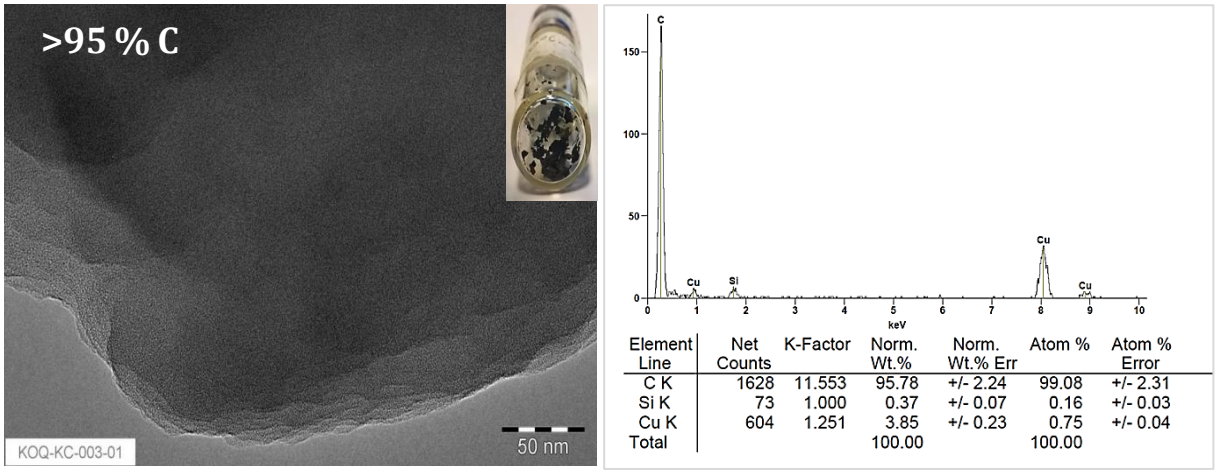

Element Line	Net Counts	K-Factor	Norm. Wt.%	Norm. Wt.% Err	Atom %	Atom % Error
C K	1628	11.553	95.78	+/- 2.24	99.08	+/- 2.31
Si K	73	1.000	0.37	+/- 0.07	0.16	+/- 0.03
Cu K	604	1.251	3.85	+/- 0.23	0.75	+/- 0.04
Total			100.00		100.00	

Figure 5-2: Micrograph of the solid material formed from the light fraction of crude oil (left) and its elemental analysis (right) after 3 days of thermal treatment at 450 °C.

One of the main parameters that significantly influences the fouling rates is the presence of oxygen. In a refinery unit, trace amounts of oxygen can enter oil streams through leaks into storage tanks due to poor storage conditions or in vacuum processes.[5] Several studies have shown that oxygen plays an important role in the formation of solid deposits in heat exchangers by triggering a number of highly complex reactions such as autoxidation and polymerization. Butler and co-workers have reported that naphthas and gas oils in the presence of oxygen are able to deposit insoluble gums on the surface of the heat exchangers at temperatures of 120 °C – 250 °C.[27] In addition, Eaton and co-workers have tested various hydrocarbon feedstocks under oxygen and inert (nitrogen) conditions with the results showing clearly that the oxygen was consumed in the formation of foulants, therefore its availability promoted the foulant generation.[28] On the other hand, in an inert environment the depletion of foulants and the decrease of the fouling rate was observed.[28, 29]

In this part, the effect of temperature on sulfur species as well as the influence oxygen has on them, was investigated. The graphical representation of the results in Figure 5-3 shows the changes of the sulfur species based on the number of assigned compositions obtained with the use of electrospray as ionization method before and after thermal treatment under oxygenated and inert conditions. The compounds were detected

as protonated molecules and are labelled S[H]. In case of the unreacted gas condensate, a low number of sulfur containing compounds has been detected. This is rather expected, since electrospray is not a suitable ionization method for nonpolar compounds. However, after reaction at 150 °C, an overall increase of the population abundance of these species can be observed under both conditions. While a total number of 114 compounds is detected in the unreacted sample, this amount has a 2-fold increase after heating. By further increasing the temperature to 250 °C, the sulfur species exhibit the highest number of abundance. Under both oxygenated and inert conditions the detected sulfur species reach a number of up to 623 and 500, respectively. This change is an indicator that a chemical transformation has taken place during heating, making the sulfur species detectable under electrospray. However, this trend changes rapidly at higher temperatures of 350 °C and 450 °C. In this case, the sulfur containing compounds were detected only under inert conditions. The absence of them under oxidative conditions could be an indicator of their high reactivity in the presence of oxygen.

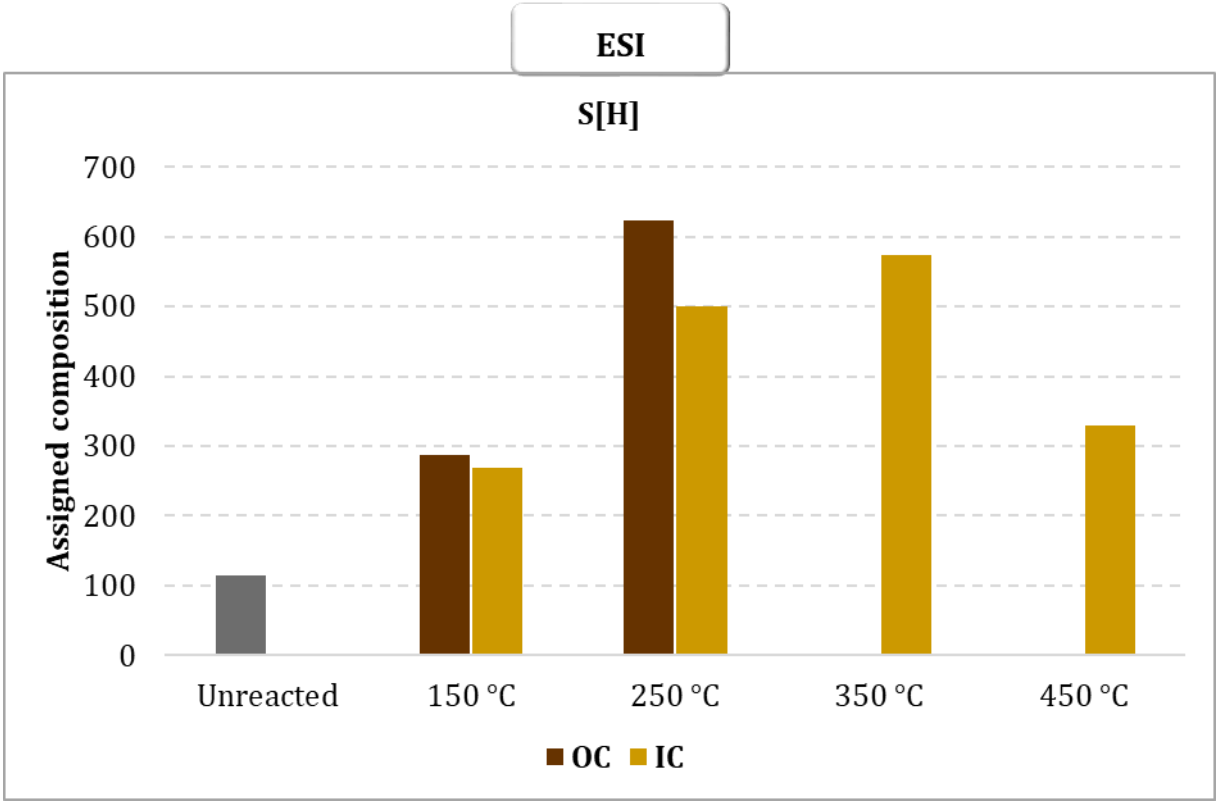

Figure 5-3: Comparison of the sulfur class based on distribution of the assigned compounds detected as protonated molecules (S[H]) for the gas condensate before (top) and after thermal treatment at different reaction temperatures under oxygenated (OC) or inert conditions (IC).

In order to obtain insight information regarding the sulfur species, a Kendrick plot is used in Figure 5-3.[30] This kind of representation provides a better visualization of the results by illustrating the aromaticity of the S-containing compounds in terms of DBE versus number of carbon atoms per molecule. Here, the S[H] class of compounds is shown, before and after thermal treatment under oxygenated and inert conditions. Sulfur species in the unreacted gas condensate contained 15-34 carbon atoms, with a DBE distribution in the range of 4-12. Sulfur containing compounds with a DBE higher than 4 are likely cyclic-ring or aromatic sulfides while a DBE distribution higher than 6 might be an indication that sulfur compounds are enriched with thiophenic compounds, while a DBE of 10 can be dibenzothiophene homologues with an additional napthenic ring. After reaction at 150 °C, an overall increase in the number of carbon atoms as well as in DBE was observed under both conditions. Here, under oxygenated conditions, the sulfur containing compounds had a carbon number of 24-37 with a DBE distribution of 4-21, whereas under inert conditions these values were in the range of 10-43 and 6-23 respectively. By increasing the temperature to 250 °C, the sulfur species exhibit even higher carbon and DBE values. Sulfur species detected (as protonated molecules) after reaction under oxidative conditions contained 15-54 carbon atoms, with a DBE distribution in the range of 4-31, while under inert conditions they were in the range of 13-46 carbon atoms and DBE 4-29, respectively.

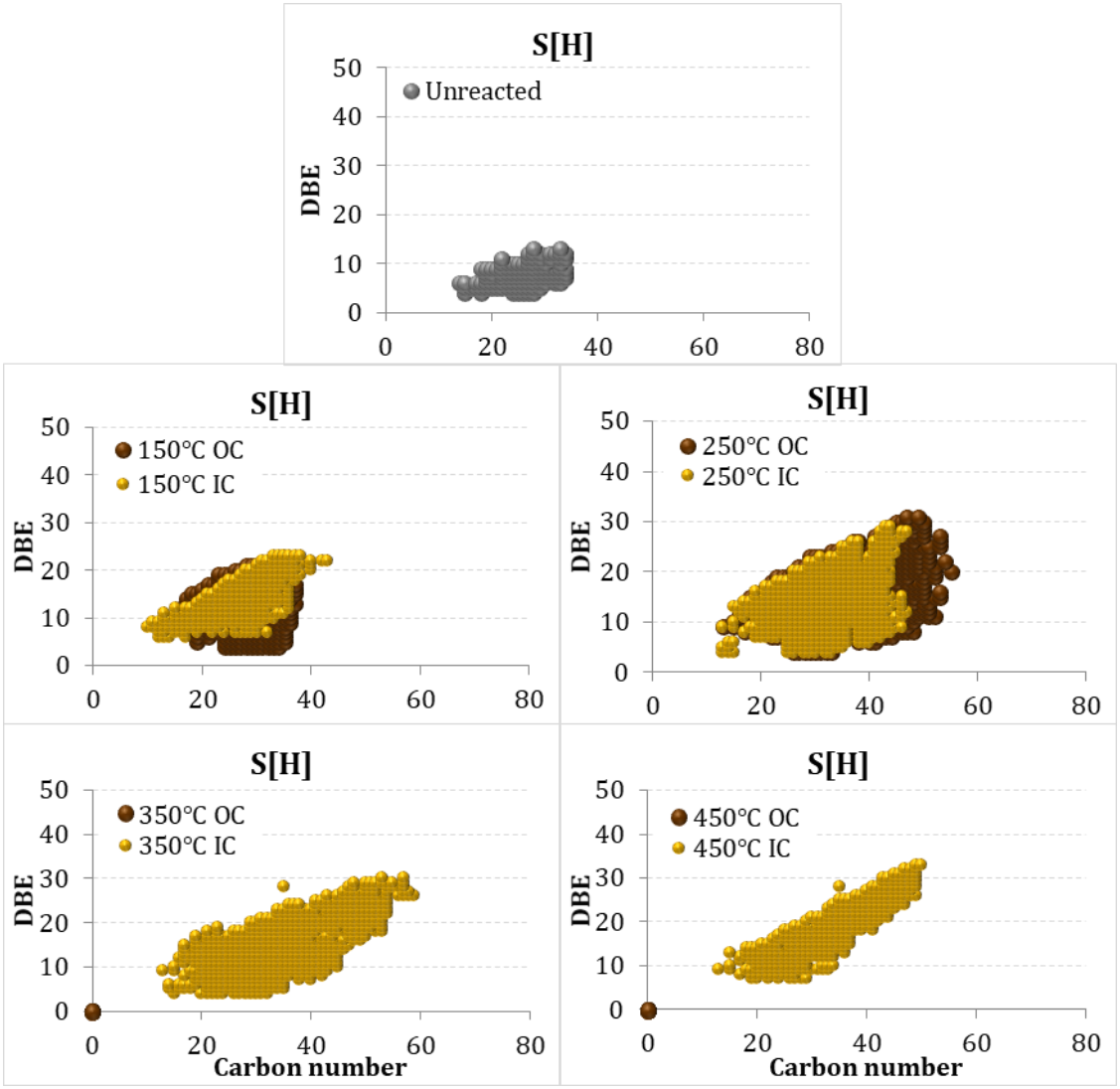

Figure 5-4: Double bond equivalent (DBE) vs. amount of carbon atoms per molecule for the sulfur containing compounds before and after thermal treatment under oxygenated (OC, darker dots) or inert conditions (IC, lighter dots).

At elevated temperatures, various chemical reactions take place, which not only change the stability of the system, but also the composition of it. Fouling is a very complex phenomenon in which new compounds can be formed, while others might be chemically transformed. This trend can be seen at the highest reaction temperatures of 350 °C and 450 °C. In this case, the sulfur species were detected only under inert conditions with a DBE distribution of 4-30 and 17-57 carbon atoms at 350 °C, while at 450 °C the DBE and carbon number was in the range of 7-33 and 13-50, respectively. The results show the

absence of sulfur species under oxygenated condition are in accordance with some results reported in the literature, indicating that sulfur compounds are very reactive in autoxidation reactions. Offenhauer and co-workers have shown that aromatic thiols could increase the rate of sediment formation in catalytically cracked middle distillates as well as decrease the fuel stability in the presence of oxygen.[31] In addition, some studies have demonstrated sulfides and thiols to increase the rate of formation of deposits even if trace amounts of oxygen exists within the system.[32]

5.4.1. Investigation of possible mechanism for the detection of sulfur species with ESI

The ionization and the reactivity of the sulfur containing compounds depends on their structure. In order to understand the increase of the sulfur species detected with electrospray, a possible reaction mechanism is suggested. The ionization of thiophenic species is not favored with electrospray and this can easily explain the low number of compounds observed in the unreacted sample. Supposedly, thiophenic compounds start to decompose first by breaking of the relatively weak C-S bond, forming a sulfur radical when subjected to elevated temperatures. Further reactions with the surrounding material result in the formation of a thiol compound, here e.g. biphenylthiol as can be seen in Figure 5-5. This group of compounds is possible to be detected with electrospray, thus explaining the increased amount of sulfur containing compounds found using this technique. According to the literature, aliphatic or aromatic thiols are intermediates in ring-opening reactions of cyclic sulfur containing compounds.[33, 34] They have high reactivity at high temperatures, thus the sulfur atom can be easily removed. When the temperature reaches up to 350 °C formation of H_2S occurs as a subsequent step. This can justify the absence of sulfur compounds at higher temperatures as well as the strong smell observed when opening the reactor.

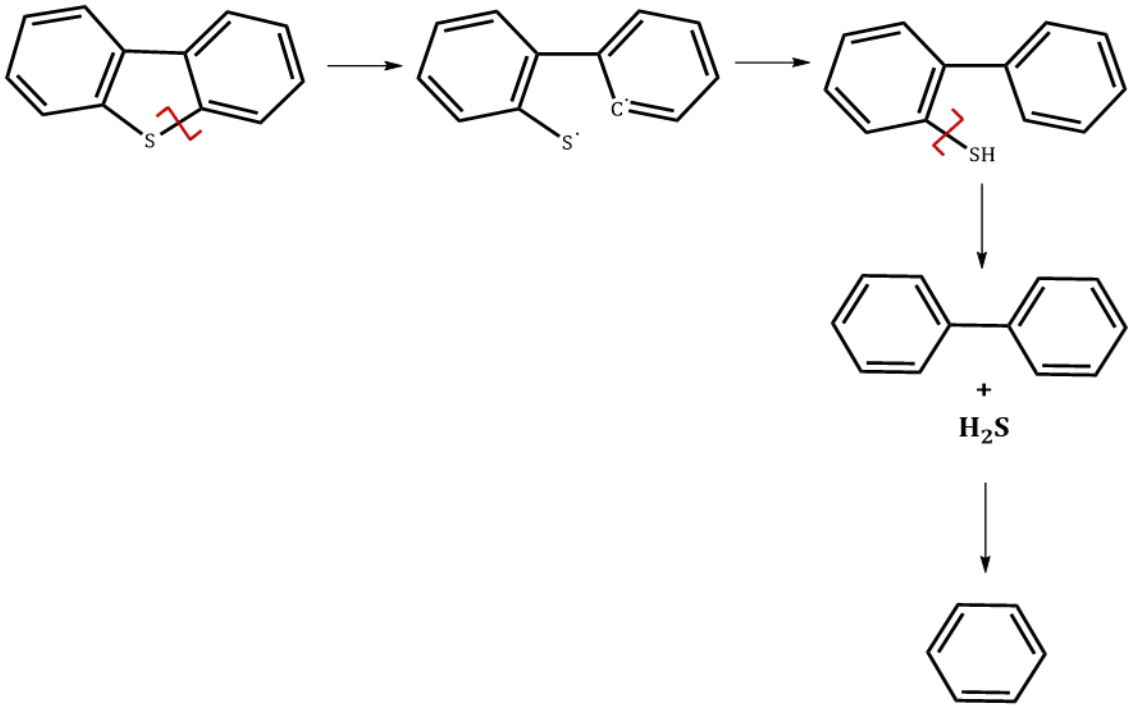

Figure 5-5: Proposed reaction mechanism of sulfur removing from dibenzothiophene

5.4.2. Investigation of the sulfur containing compounds with the use of APPI

APPI is the method of choice not only for the nonpolar hydrocarbons (HC) but also for the nonpolar sulfur containing compounds. Thus, this method was selected as an alternative in order to investigate the behavior of sulfur species before and after the fouling reactions. Figure 5-6 demonstrates the changes of these species under various reaction temperatures within an oxygenated or inert environment. As can be seen from the graph, a different trend was observed compared to the results obtained with ESI. In case of the unreacted sample, 171 sulfur species were detected, while by increasing the reaction temperature, minor changes were observed. At 150 °C the number of sulfur containing compounds detected under oxidative conditions was slightly decreased to 166, while at 350 °C the number of assigned compositions was reduced to 132. At the highest temperature of 450 °C, there was no detection of sulfur species. Regarding the inert conditions, the increase of the reaction temperature resulted in a slight increase of the sulfur containing compounds. The highest number of assigned protonated S_1-compounds was found at 350 °C, with the detection of 260 species. Similar results as previously were observed at 450 °C, with no sulfur species being detected.

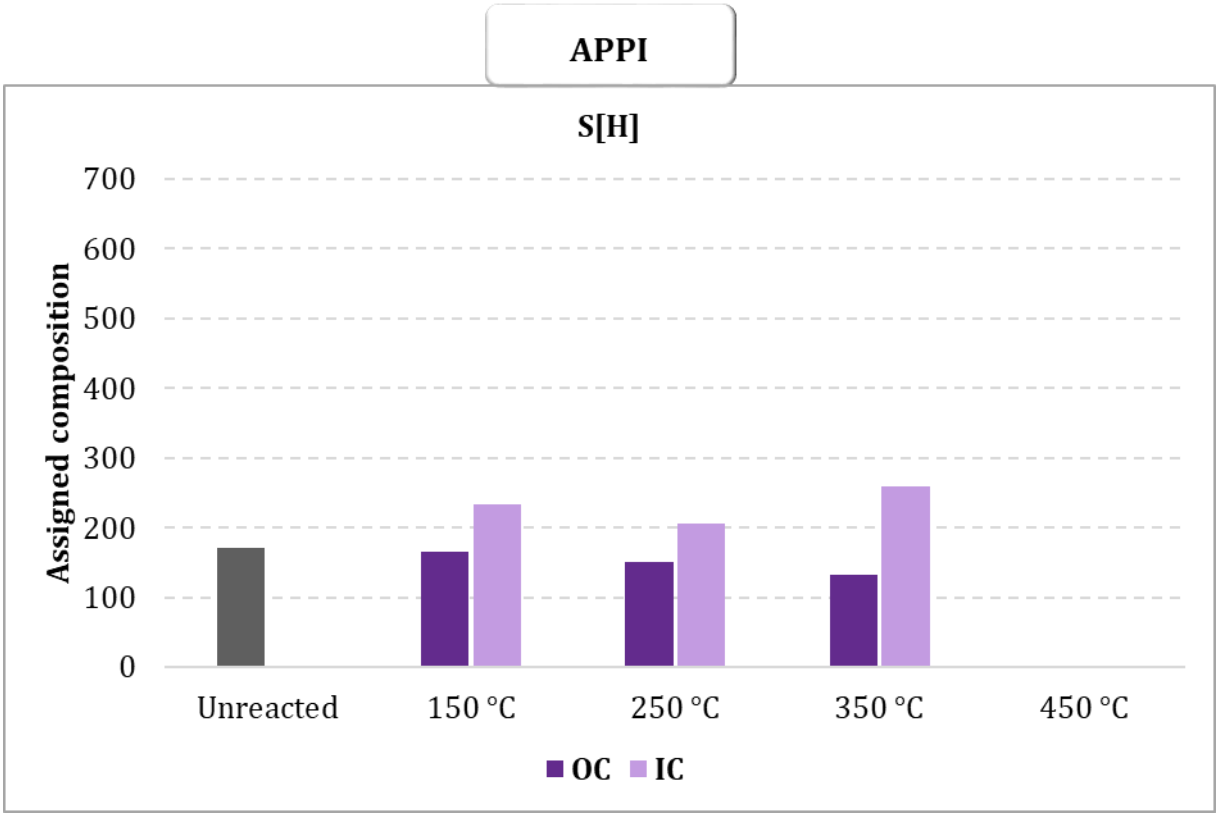

Figure 5-6: Comparison of the sulfur class based on distribution of the assigned compounds detected as protonated molecules (S[H]) for the gas condensate before (top) and after thermal treatment at different reaction temperatures under oxygenated (OC) or inert conditions (IC) with the use of APPI as ionization.

A better representation of these species regarding their aromaticity can be seen in Figure 5-7, with the assist of Kendrick plots. Here, sulfur species detected at the unreacted sample contained 9-29 carbon atoms, with a DBE distribution in the range of 2-12. The value of DBE = 2 indicates non-aromatic compounds and might correspond to cyclic sulfides or thiols with one naphthenic ring, while a DBE of 3 might correspond to thiophenes. Higher DBE number indicates that the sulfur containing compounds were enriched with thiophenic compounds, and in this case, a DBE of 6, 9 and 12 can be attributed to benzothiophenes (BTs), dibenzothiophenes (DBTs) or benzonaphthothiophenes (BNT), respectively.[35] With the increase of the reaction temperature to 150 °C, the sulfur containing compounds detected under oxygenated conditions contained a carbon number of 9-29 with DBE values of 2-14, while this number was slightly higher in case of inert conditions with 9-36 carbon atoms and a DBE value of 2-15. Although at 250 °C no big differences on the detected species were observed, this

trend changes once the temperature is increased even higher. At 350 °C, the species detected under inert conditions exhibit not only the highest DBE distribution but also carbon content. Here, the sulfur species contained 9-39 carbon atoms and DBE of 3-30, while under oxygenated conditions this number was in the range of 12-30 and 4-12, respectively. Finally, at the highest reaction temperature of 450 °C no sulfur species were detected. This indicates that under high temperature, several reactions took place leading to chemical transformations of these species.

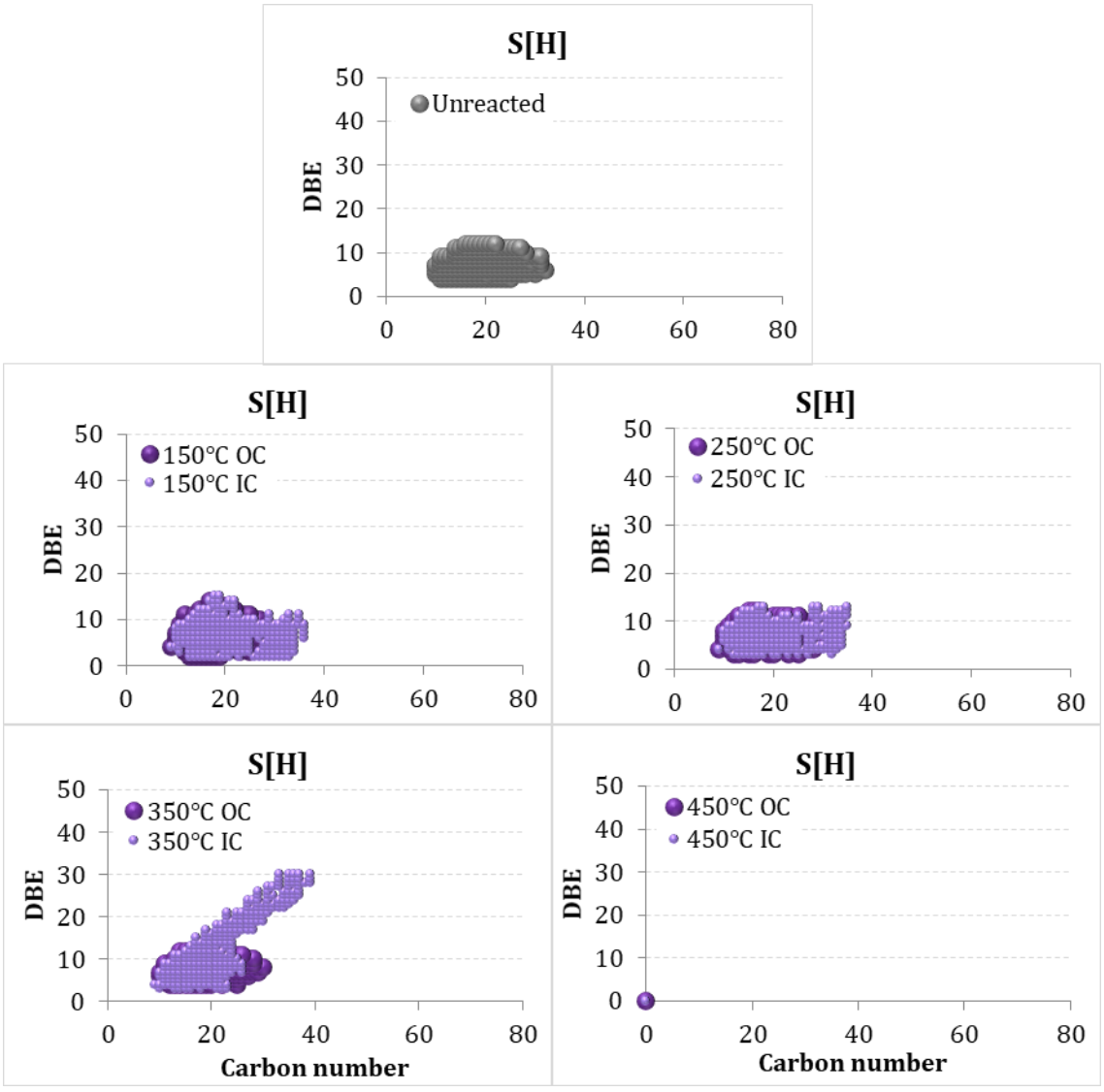

Figure 5-7: Double bond equivalent (DBE) vs. amount of carbon atoms per molecule for the sulfur containing compounds before and after thermal treatment under oxygenated (OC, darker dots) or inert conditions (IC, lighter dots).

5.5. Conclusion

Sulfur-containing compounds are among the most undesirable constituents of crude oil since they decrease the quality of the products and cause various problems during refinery processes. In order to solve problems related to the presence of sulfur species in petroleum industries, it is important not only to understand the reaction mechanisms involved, but also the various parameters that influence their behavior. The results obtained here show that different reactions were triggered under the influence of different temperature ranges as well as atmospheres. Although ESI is not employed for the analysis of sulfur species, here the detection of them was possible due to the chemical changes these species undergo. With the use of ESI, the detection of new sulfur-containing compounds of high molecular weight and aromaticity was observed after thermal treatment under oxygenated conditions. However, a further increase of the temperature, promoted a different trend. Sulfur species at 350 and 450 °C were detected only under inert conditions, since under the presence of oxygen appeared to have high reactivity. Sulfur species such as thiols, sulfides, disulfides and some thiophenic compounds can decompose at elevated temperatures resulting in the formation of free radicals. In addition, decomposition of thiols or sulfides can produce hydrogen sulfide at high temperatures, thus explaining the absence of sulfur species at oxygenated conditions as well as the strong smell during the opening of autoclaves. On the other hand, with the use of APPI no significant changes were observed up to 250 °C. A small increase of the sulfur species was observed only under inert conditions at the reaction temperature of 350 °C, while a complete absence of them occurred at the highest temperature.

5.6. References

1. Cronshaw, I., World Energy Outlook 2014 projections to 2040: natural gas and coal trade, and the role of China. *Aust. J. Agric. Resour. Econ.* **2015,** *59* (4), 571-585.

2. Chopra, S.; Lines, L., Introduction to this Special Section: Heavy Oil. *Geophysics* **2008,** *27*.

3. Mohr, S. H.; Evans, G. M., Long term prediction of unconventional oil production. *Energy Policy* **2010,** *38*, 265-276.

4. Prado, G. H. C.; Rao, Y.; de Klerk, A., Nitrogen Removal from Oil: A Review. *Energy Fuels* **2017,** *31* (1), 14-36.

5. Watkinson, P., Deposition from Crude Oils in Heat Exchangers. *Heat Transfer Eng.* **2007,** *28*, 177-184.

6. Watkinson, A. P.; Wilson, D. I., Chemical reaction fouling: A review. *Exp. Therm. Fluid Sci.* **1997,** *14* (4), 361-374.

7. Andersson, J., Schwefel in Erdöl: Ein problematisches Element? *Chem. unsere Zeit* **2005,** *39* (2), 116-120.

8. Javadli R.; Klerk, A. d., Desulfurization of heavy oil. *Appl Petrochem Res* **2012,** *1* (1), 3-19.

9. Dunleavy, J., Final Analysis: Sulfur as a Catalyst Poison. *Platin. Met. Rev.* **2006,** *50*, 110-110.

10. McCue, A. J.; Anderson, J. A., Sulfur as a catalyst promoter or selectivity modifier in heterogeneous catalysis. *Catal. Sci. Technol.* **2014,** *4* (2), 272-294.

11. Khaksar, L.; Shirokoff, J., Effect of Elemental Sulfur and Sulfide on the Corrosion Behavior of Cr-Mo Low Alloy Steel for Tubing and Tubular Components in Oil and Gas Industry. *Materials* **2017,** *10* (4), 430.

12. Young, J., Chapter 8 Corrosion by Sulfur. In *Corrosion Series*, Young, D. J., Ed. Elsevier Science: 2008; pp 361-396.

13. F. Taylor, W., Deposit Formation from Deoxygenated Hydrocarbons. II. Effect of Trace Sulfur Compounds. *Industrial & Engineering Chemistry Product Research and Development* **1976,** *15*.

14. Coletti, F.; Hewitt, G. F., *Crude Oil Fouling: Deposit Characterization, Measurements, and Modeling*. Gulf Prefessional Publishing: 2015.

15. Li, D.-p.; Zhang, L.; Yang, J.-w.; Lu, M.-x.; Ding, J.-h.; Liu, M.-l. J. I. J. o. M., Metallurgy,; Materials, Effect of H2S concentration on the corrosion behavior of pipeline steel under the coexistence of H2S and CO2. *Int. J. Min. Met. Mater.* **2014,** *21* (4), 388-394.

16. Tang, J.; Shao, Y.; Guo, J.; Zhang, T.; Meng, G.; Wang, F., The effect of H2S concentration on the corrosion behavior of carbon steel at 90°C. *Corros. Sci.* **2010,** *52* (6), 2050-2058.

17. Diaz-Bejarano, E.; Coletti, F.; Macchietto, S., Modeling and Prediction of Shell-Side Fouling in Shell-and-Tube Heat Exchangers. *Heat Transfer Eng.* **2019,** *40* (11), 845-861.

18. Lababidi, S.; Schrader, W., Online normal-phase high-performance liquid chromatography/Fourier transform ion cyclotron resonance mass spectrometry: effects of different ionization methods on the characterization of highly complex crude oil mixtures. *Rapid Commun. Mass Spectrom.* **2014,** *28* (12), 1345-52.

19. Panda, S. K.; Andersson, J. T.; Schrader, W., Characterization of Supercomplex Crude Oil Mixtures: What Is Really in There? *Angew. Chem.* **2009,** *48* (10), 1788-1791.

20. Zhao, H., Determination of Elemental Sulfur in Naphtha and Gasoline by Gas Chromatography/Mass Spectrometry. *Pet. Sci. Technol.* **2007,** *25* (5), 569-576.

21. Panda, S. K.; Alawani, N. A.; Lajami, A. R.; Al-Qunaysi, T. A.; Muller, H., Characterization of aromatic hydrocarbons and sulfur heterocycles in Saudi Arabian heavy crude oil by gel permeation chromatography and ultrahigh resolution mass spectrometry. *Fuel* **2019,** *235*, 1420-1426.

22. Vetere, A.; Profrock, D.; Schrader, W., Quantitative and Qualitative Analysis of Three Classes of Sulfur Compounds in Crude Oil. *Angew. Chem.* **2017,** *56* (36), 10933-10937.

23. Panda, S. K.; Andersson, J. T.; Schrader, W., Mass-spectrometric analysis of complex volatile and nonvolatile crude oil components: a challenge. *Anal Bioanal Chem* **2007,** *389* (5), 1329-39.

24. Vetere, A.; Schrader, W., Mass Spectrometric Coverage of Complex Mixtures: Exploring the Carbon Space of Crude Oil. *ChemistrySelect* **2017,** *2* (3), 849-853.

25. Panda, S. K.; Schrader, W.; Andersson, J. T., Fourier transform ion cyclotron resonance mass spectrometry in the speciation of high molecular weight sulfur heterocycles in vacuum gas oils of different boiling ranges. *Anal. Bioanal. Chem.* **2008,** *392* (5), 839-848.

26. Wang, X.; Schrader, W., Selective Analysis of Sulfur-Containing Species in a Heavy Crude Oil by Deuterium Labeling Reactions and Ultrahigh Resolution Mass Spectrometry. *Int J Mol Sci* **2015,** *16* (12), 30133-30143.

27. Butler, R.; McCurdy Jr, W. J. T. A., Fouling rates and cleaning methods in refinery heat exchangers. *Trans. ASME* **1949,** *71*, 843-849.

28. Eaton, P.; Lux, R., Laboratory fouling test apparatus for hydrocarbon feedstocks. In *Fouling in Heat Exchange Equipment*, Suitor, J. W.; Pritchard, A. M., Eds. HTD: New York, 1984; Vol. 35, pp 33-42.

29. Beaver, B., Petroleum Products: Instability and Incompatibility By George W. Mushrush (George Mason University) and James G. Speight (Western Research Institute). Taylor & Francis: Bristol, PA. 1995. x + 390 pp. $69.95. ISBN 1-56032-297-7. *Journal of the American Chemical Society* **1996,** *118* (12), 3071-3072.

30. Kendrick, E., A Mass Scale Based on CH2 = 14.0000 for High Resolution Mass Spectrometry of Organic Compounds. *Anal. Chem.* **1963,** *35* (13), 2146-2154.

31. Offenhauer, R. D.; Brennan, J. A.; Miller, R. C., Sediment Formation in Catalytically Cracked Distillate Fuel Oils. *Ind. Eng. Chem.* **1957,** *49* (8), 1265-1266.

32. Yap, S.; Dranoff, J.; Panchal, C. *Fouling formation of an olefin in the presence of oxygen and thiophenol*; Argonne National Lab., IL (United States): 1995.

33. Nelson, N.; Levy, R. B. J. J. C., Organic chemistry of hydrodenitrogenation. *J. Catal.* **1979,** *58* (3).

34. Girgis, M. J.; Gates, B. C., Reactivities, reaction networks, and kinetics in high-pressure catalytic hydroprocessing. *Ind. Eng. Chem. Res.* **1991,** *30* (9), 2021-2058.

35. Vetere, A.; Schrader, W., 1- and 2-photon ionization for online FAIMS-FTMS coupling allows new insights into the constitution of crude oils. *Anal. Chem.* **2015,** *87* (17), 8874-9.

CHAPTER 6. INVESTIGATION OF THE BEHAVIOR OF HYDROCARBONS DURING FOULING BY HIGH-RESOLUTION ELECTROSPRAY IONIZATION MASS SPECTROMETRY

Redrafted from:

Kondyli, W. Schrader. "Investigation of the behavior of hydrocarbons during fouling by high-resolution electrospray ionization mass spectrometry", will be submitted to *Applied Energy Materials.*

6.1. Abstract

Crude oil fouling can be defined as the undesirable deposition of solid material on a surface and it is considered a chronic problem in petroleum industry. However, the compounds involved in fouling, let alone the underlying reaction mechanisms are to date not understood. Here, in order to investigate chemical fouling, the process was simulated under laboratory conditions, focusing on hydrocarbons as the main constituents of crude oil. The results demonstrate large differences within the hydrocarbon class of compounds before and after thermal treatment with and without water, even for a very light crude oil fraction. After heating, new, higher molecular weight hydrocarbon compounds with high aromaticity were detected as a result of polymerization mechanisms which can take place at high temperatures. The findings were verified by the use of a model hydrocarbon compound.

6.2. Introduction

The term fouling describes the undesirable deposition of solid materials on a surface and remains one of the biggest and until now unresolved problems in petroleum industry.[1] This side reaction of petroleum processing leads to the deposition of unwanted material during upstream operation and results in loss of thermal efficiency on the heat transfer equipment, catalyst poisoning, plugged pipelines or thermal instability.[2-4] These in turn, can cause a series of operating difficulties which might finally end up with the units being shut down.[5] Fouling has a great economic impact in petroleum industry, where the removal of fouling deposits is a multi-billion dollar problem.[6] The need to control and reduce this phenomenon has become even more intense lately since the incorporation of heavier crude oils (e.g. extra heavy oil, oil shale) into the market is necessary in order to cover the world's energy needs.[7, 8] However, utilization of these types of oil is unfavorable since their high content of heteroatoms (N, O, S), metals (e.g. V, Fe, Ni) and asphaltenes causes additional problems during production, refining, storage and transportation.[9, 10] In order to overcome these problems, various attempts have been made not only to optimize the refining and related processes.[11] However, the main challenge regarding the formation of solid deposits is that the reaction mechanisms let alone the compounds which are responsible for fouling are poorly understood.[3, 12] The ability of gaining information is limited due to the complex nature of the feedstocks which contain more than a million different chemical compounds[13] and additionally, due to the various reaction pathways (e.g. autoxidation, polymerization and thermal decomposition) involved in fouling.[14, 15] In addition, parameters such as temperature, pressure or presence of water can have a significant impact on the fouling rate.[16-18] Understanding the chemical composition of crude oil on a molecular lever is the key to solve this problem.[19, 20]

Over the years, various analytical techniques have been used in fouling studies, but these are mainly focused on the characterization of the fouling deposits. Techniques such as X-Ray diffraction (XRD)[21, 22] or scanning electron microscopy (SEM),[23] have been successfully used to gain information regarding the morphology of the deposits (e.g. presence of salts such as FeS, NaCl). Information about the chemical structure, the aromaticity of the sample, the chemical bonds or the functional groups has been obtained with the use of ultraviolet-fluorescence (UV-F),[24] Fourier-transform infrared (FT-IR)[25] or nuclear magnetic resonance spectroscopy (NMR),[26] respectively. However, the use of

these techniques is limited since they provide only a small piece of information regarding fouling, while more frequently several studies emphasize on characterization of the heavier fractions of crude oil since these are responsible for the physical part of fouling.[27-29] As part of this physical process, asphaltenes, resins or high-molecular weight paraffins that are stable in solution within the unaltered oil, tend to accumulate and precipitate once a change at the system occurs, either by altering the operating conditions (e.g. temperature, pressure) or the composition of crude oil.[1] However, the chemical part of fouling, where compounds react with each other, forming new products that have not been present before, is still unexplored.

One of the biggest obstacles to be overcome is that it is impossible to directly simulate an industrial scale reaction in the laboratory because of all the different parameters and conditions that cannot be reproduced one-to-one. Nevertheless, in this study, attempts were made in order to simulate the fouling reactions under laboratory conditions, with the formation of fouling deposits being used as a guideline. Therefore, the reactions were simulated with the use of a lab-build reactor and a light fraction of crude oil, which is known for its fouling tendencies. In order to understand the chemical transformation in such complex mixtures, the use of special analytical tools is required. Thus, one way to study fouling on a molecular lever would be using ultra-high resolution mass spectrometry (UHRMS).[30, 31] Its high mass accuracy and high resolving power enables obtaining in-depth information regarding the elemental composition of each detected signal, the level of aromaticity and the class distribution based on the heteroatom content.[32, 33] Although electrospray (ESI) is the most commonly used method for the analysis of polar constituents in crude oil samples, its exact mechanism and capabilities have not been fully explored.[34] Lately, an increasing number of reports describe a rather unexpected behavior of ESI which involves the formation of radical ions from polycyclic aromatic hydrocarbons (PAHs).[35]

In this study the fouling behavior of the hydrocarbon class within different temperature ranges as well as with or without the addition of water with the use of ESI is investigated. In order to understand the reaction mechanisms in detail, a model hydrocarbon compound (pyrene) was selected for additional studies to the oil fraction.

6.3. Experimental

6.3.1. Simulation of fouling under laboratory conditions

A lab-build reactor was used for fouling simulation. Figure 6-1 shows the equipment used for this purpose. The experimental set-up was the following: A quartz crucible was filled with 0.3 mL of a light crude oil fraction and was placed inside a stainless steel autoclave. A quartz cover was set on the top of the crucible in order to avoid sample loses. The autoclave was then closed, using a stainless steel ring as sealing. The autoclave was positioned in a heating mould which was installed inside a safety box. A thermometer was connected to the heater in order to control and regulate the temperature. The sample was heated for 3 days at a temperature of 150 °C, 250 °C, 350 °C or 450 °C. In order to test the influence of water on fouling, in a second experimental set-up, 1.0 µl of distilled water was added to the oil fraction before closing the autoclave. Experimental conditions remained the same for the experiments with and without water. The model compound of pyrene was dissolved in 0.1 mL toluene and heated for 3 days at the lowest (150 °C) and the highest (450 °C) temperature.

Figure 6-1: Equipment used in crude oil fouling simulation

6.3.2. Solid deposit analysis

The solid material was analyzed microscopically by transmission electron microscopy (TEM) and energy-dispersive X-ray spectroscopy (EDX). High-resolution imaging and chemical analysis were performed using a 200 kV electron microscope with cold field emitter and CCD-camera (Hitachi HF-2000).

6.3.3. Mass spectrometric studies and data analysis

For mass spectrometric analysis a research-type Orbitrap Elite (Thermo Fisher, Bremen, Germany) was used. Mass spectra were acquired using the spectral stitching method[36] (30 Da window with 5 Da overlap) in a range of *m/z* 200-1000 and with a resolving power of *R* = 480,000 (FWHM at *m/z* 400). All samples were first dissolved in toluene (HPLC grade, Sigma-Aldrich, Germany) and then diluted with methanol (LC-MS grade, J. T. Baker, Germany) (1:4 v/v), to a final concentration of 250 ppm and then analyzed without further treatment. Electrospray (ESI) in positive ion mode was used as ionization method. The ionization was performed using a stainless steel needle at a capillary voltage of 4kV. Nebulization was assisted by a sheath gas flow of 4.0 a.u. (arbitrary units) while the auxiliary and the sweep gas flow were set to 1.0 a.u. The transfer capillary temperature was set to 275 °C. External mass calibration was performed prior to sample analysis in order to meet a mass accuracy better than 1 ppm. The recorded mass spectra were recombined by Xcalibur 4.0 software (Thermo Fisher, Bremen, Germany) and further processed using the Composer software (version 1.5.0, Sierra Analytics, Modesto, CA, USA). Calculations and assignments of molecular formulas were performed using the following restrictions regarding the number of possible elements and the number of double bond equivalent (DBE): H: 0-1000, C: 0-200, N: 0-3, O: 0-3, S: 0-2 and DBE: 0-100. The calculated molecular formulas were sorted into heteroatom classes based on their denoted Kendrick mass defects and their double bond equivalent distribution. The obtained mass lists were transferred to Excel (Microsoft Office Professional Plus 2010, Microsoft Corporation, Redmond, WA, USA) for further data evaluation. Double bond equivalent refers to the sum of the rings and double bonds present within a molecule and is calculated from the chemical composition $C_cH_hN_nO_oS_s$ of the analyte using the following equation: $\mathrm{DBE} = \mathrm{c} - \frac{\mathrm{h}}{2} + \frac{\mathrm{n}}{2} + 1$. A higher DBE value indicates higher aromaticity of a compound.

6.4. Results and discussion

In order to characterize crude oil components that are responsible for fouling, the development of analytical methods is required. One of the biggest challenges to investigate this phenomenon was to simulate fouling conditions in the laboratory. Here, for the first time, the successful simulation of a costly and very important industrial process was achieved under laboratory conditions. Formation of solid material was observed only at the highest temperature of 450 °C after 3 days of reaction in both cases, with and without water. The resulting solid material indicates that various chemical reactions have taken place in the system, which eventually led to the formation of a highly carbonaceous product, such as coke. As can be seen from Figure 6-2, the insoluble fouling deposit consists of more than 95 wt.-% amorphous carbon.

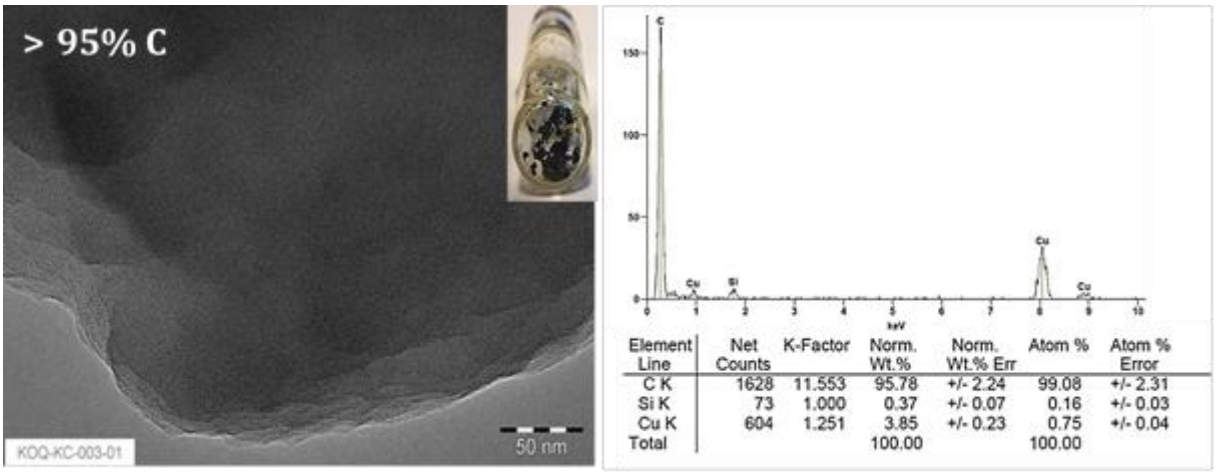

Element Line	Net Counts	K-Factor	Norm. Wt.%	Norm. Wt.% Err	Atom %	Atom % Error
C K	1628	11.553	95.78	+/- 2.24	99.08	+/- 2.31
Si K	73	1.000	0.37	+/- 0.07	0.16	+/- 0.03
Cu K	604	1.251	3.85	+/- 0.23	0.75	+/- 0.04
Total			100.00		100.00	

Figure 6-2: Micrograph of the solid material formed from the light fraction of crude oil (left) and its elemental analysis (right) after 3 days of thermal treatment at 450 °C.

The analysis of the fouling deposits can reveal a small piece of information regarding fouling, but unfortunately alone is not adequate to study the fundamental changes within a sample on a molecular level. In order to understand the chemical changes, an investigation on the remaining components still present in the liquid phase is necessary. Inextricable part for better understanding these reactions is the investigation of the reaction mechanisms involved as, well as the parameters that can influence the fouling rate. It has already been suspected that the conversion of organic compounds to insoluble products involves multiple reaction mechanisms such as autoxidation, thermal decomposition and/or polymerization.[37] In addition, according to Albright and co-

workers, parameters such as temperature, nature of the sample, construction material of the reactor and time can play a significant role in the formation of coke material.[38] Several studies have shown that an increase of the bulk temperature can increase the fouling rate, while the presence of water, which is usually added as steam for processing purposes, can cause damage in the distillation tower, corrosion of the crude oil distillation column as well as decrease the product quality.[39, 40] Therefore, these conditions have been investigated in detail. Since the majority of compounds present in a crude oil belongs to the class of hydrocarbons, this class is investigated in detail in this study. In Figure 6-3, the changes of purely hydrocarbon compounds based on the number of assigned compositions are illustrated. The results show the differences of these species before heating (unreacted) as well as after thermal treatment at different reaction temperatures with or without water. The compounds were detected either as protonated molecules and are labelled HC[H] or as radical ions and in this case, are shown without the bracket.

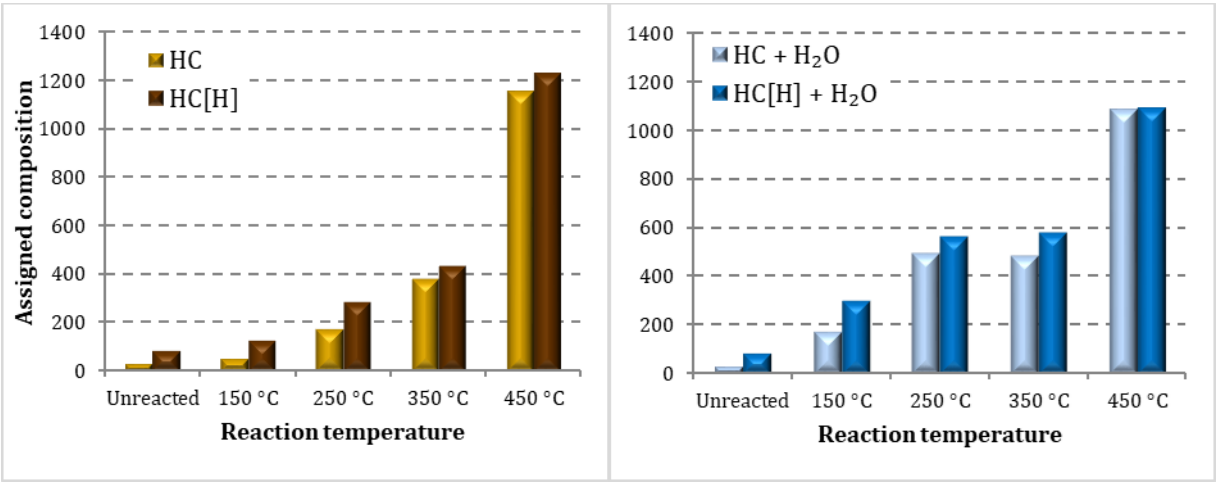

Figure 6-3: Comparison of the amount of compounds within the hydrocarbon class detected as radical ions (HC) or protonated molecules (HC[H]) for the gas condensate as unreacted or after thermal treatment at different reaction temperatures without (left) or with (right) water.

In case of the unreacted oil fraction only few hydrocarbon compounds have been detected. This is rather expected, since according to the literature, ESI is not the method of choice for non-polar hydrocarbons. Minor changes regarding the assigned compositions can be observed at 150 °C and 250 °C without water, while a further increase of the temperature to 350 °C resulted in a slight increase of the hydrocarbon species. However, by reaching the highest temperature of 450 °C, the degree of change is rather surprising. Here, the number of hydrocarbon species detected is ten times higher

(over thousand compounds) compared to the unreacted sample. This drastic change indicates that various chemical reactions were triggered due to the higher temperature, resulting in the formation of new compounds which are efficiently ionized by ESI. Regarding the results with the addition of water, a similar trend can be observed, but in this case, the increase in the number of the assigned compositions is already apparent after thermal treatment at 250 °C.

The population-based distribution graph indicates that many differences can be observed, but a deeper look on the aromaticity of the hydrocarbon compounds will provide further information on these species. Thus, the Kendrick plots (DBE versus number of carbon atoms per molecule) of the hydrocarbon compounds in the form of radical ions or protonated molecules for the unreacted gas condensate and the gas condensate after thermal heating at 250 °C and 450 °C with and without water can be seen in Figure 6-4.

Hydrocarbon radical species in the unreacted gas condensate contained 10-34 carbon atoms, with a DBE distribution in the range of 6-16. The compound with the lowest carbon number and DBE corresponds to a compound similar to dihydronaphthalene ($C_{10}H_{10}$ and a DBE of 6), while the hydrocarbon compound with the chemical formula of $C_{20}H_{10}$ and a DBE value of 16 showed the highest aromaticity. This compound might correspond to the polycyclic aromatic hydrocarbon corannulene, consisting of a central cyclopentane ring fused with five 6-membered rings. Hydrocarbon species detected in their protonated form exhibit slightly lower values with a carbon number of 10-21 and a DBE distribution of 4-17. However, after thermal treatment at 250 °C, a different trend was observed. In this case, an increase in both carbon and DBE number occurs in the sample with and without water. Hydrocarbon species contained 12-52 carbon atoms with a DBE distribution of 6-45 in case of radicals, while the protonated molecules exhibit values of 11-57 and 3-46, respectively. At this temperature, an interesting observation found in both cases was the presence of a narrow band of high intensity compositions which was not present in the unreacted sample. With the further increase of temperature to 450 °C, a drastic increase of the hydrocarbon compounds can be observed in the sample with and without water. Hydrocarbon compounds reach a size up to 72 carbon atoms with a DBE up to 49 for the radicals and up to 73 and 53 for the protonated molecules, respectively. Similar results were observed for the heated sample with water with radical hydrocarbon compounds having a carbon number up to 79 and DBEs up to 59, while

compounds with carbon number up to 78 and DBE values up to 55 were detected as protonated molecules.

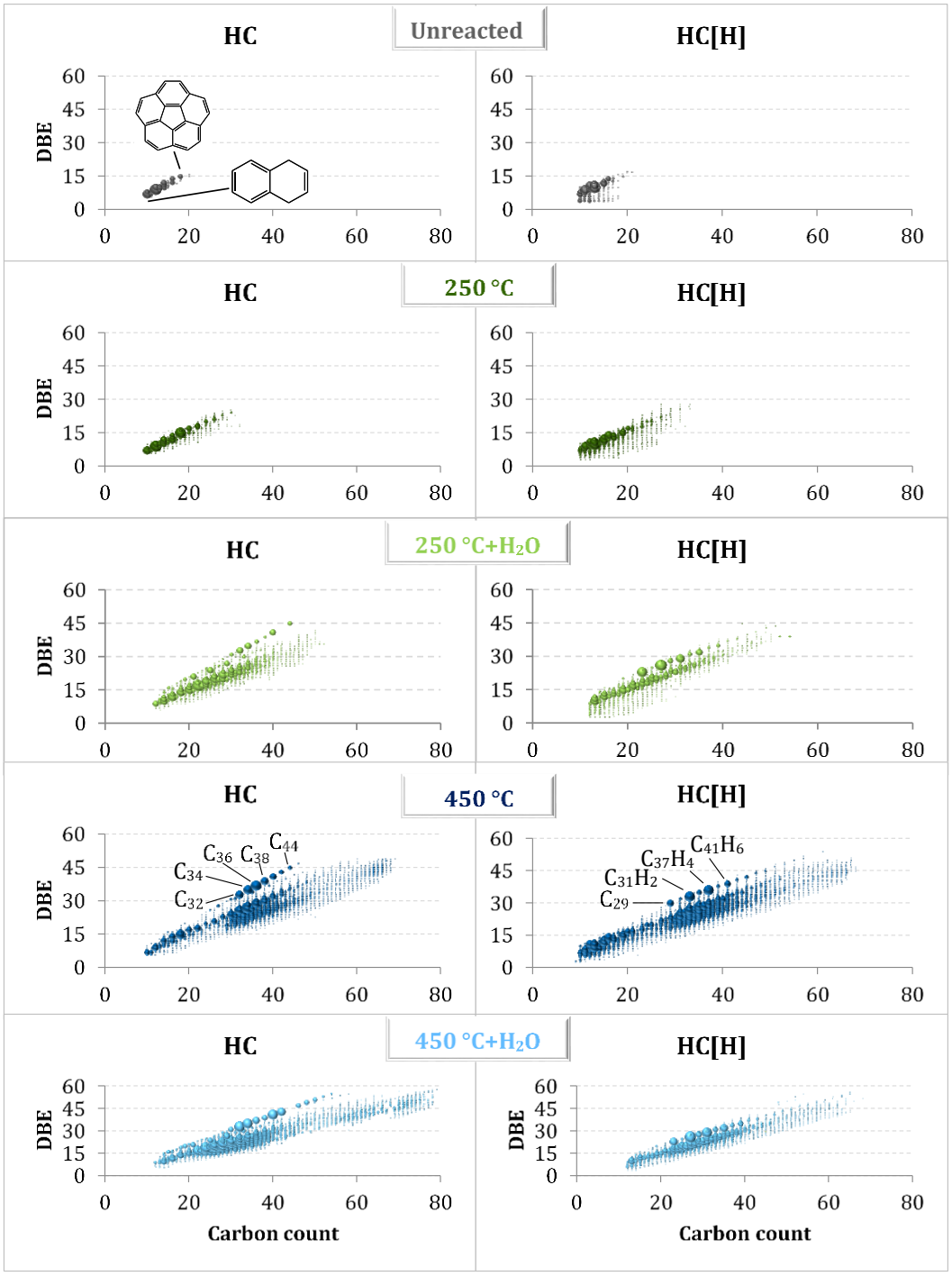

Figure 6-4: DBE versus number of carbon atoms per molecule of hydrocarbon compounds detected as radical ions (left) or protonated molecules (right) in case of the unreacted gas condensate (top), or after thermal treatment at 450 °C without (middle) or with (bottom) water.

The chemical changes occurring after thermal treatment are extremely difficult to understand, since the chemistry behind fouling involves different reaction pathways. It is known that, at high temperatures crude oil compounds undergo thermal decomposition (cracking), which can eventually lead to the formation of coke.[3] During this process, higher molecular mass hydrocarbons break down into smaller ones, usually alkanes and alkenes, with the latter ones to get further involved into autoxidation and polymerization reactions. The Kendrick plots demonstrate clearly the formation of new, higher molecular weight hydrocarbon compounds after thermal treatment. Their formation is necessarily attributed to carbon-carbon coupling reactions which have probably been initiated via radical mechanisms. Radical species are known to be highly reactive and can easily attack and connect to other hydrocarbon compounds forming larger molecules. The narrow band of high intensity compositions is indicative of the compounds being formed by dehydrogenation and fusion of aromatic systems, rather than alkyl chain polymerization. In fact, long alkyl chains are not observed here. Additionally, for radical ions, a new line of compounds can be observed on the top of the distribution that is free of hydrogen. These newly formed carbon-only species can only correspond to fullerenic-type compounds. In case of protonated molecules related species are observed that contain few (2-6) hydrogen atoms within their structure. After heating, small carbon molecules (e.g. C_{15}), fullerenes (e.g. C_{34}, C_{40}, C_{48}, C_{60}) as well as their hydrides (e.g. $C_{16}H_2$, $C_{18}H_2$, $C_{20}H_2$) are observed in high intensity. Previous experimental studies from Kharlomov and co-workers demonstrated that such compounds were possibly formed also as products of benzene pyrolysis.[41] Other studies suggested that the fullerene formation is a three step process involving dehydrogenation, followed by a folding process and finally cage closure by C_2 or C_3 elimination.[42, 43] Various attempts have been done to correlate the role of PAHs in fullerene formation with Taylor et. al. to demonstrate that it is possible to form C_{60} and C_{70} fullerene from pyrolysis of naphthalene at around 1000 °C. The results showed that by repeated addition of C_{10} fragments, and subsequent elimination of hydrogen, the formation of C_{60} can be achieved.

6.4.1. Studying the mechanism of fouling using a model compound

For a better understanding of the reaction mechanism that leads to the formation of fouling material, a standard hydrocarbon compound (pyrene) was reacted under similar conditions. While Figure 6-5, illustrates the ESI mass spectrum of the unreacted compound, measurements before and after thermal treatment at 450 °C are shown in Figure 6-6.

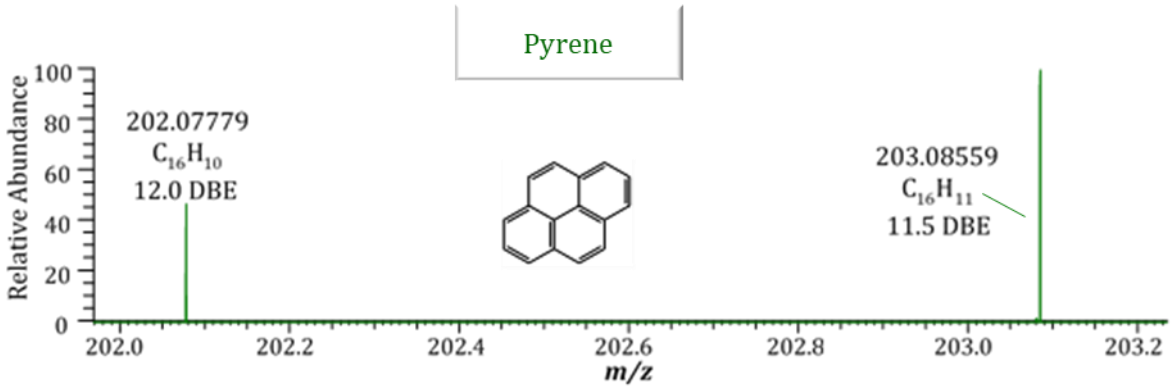

Figure 6-5: Positive electrospray mass spectrum of pyrene at m/z 202.0-203.2 detected as radical ions and protonated molecules.

As can be seen from the spectrum in Figure 6-5, the model compound was efficiently ionized by ESI and detected in both radical (e.g $C_{16}H_{10}$ with DBE of 12) and protonated form (e.g. $C_{16}H_{11}$ with DBE of 11.5). As mentioned before, a better visualization of the results can be obtained with the use of Kendrick plots. Figure 6-6 shows the differences on the DBE vs. carbon distribution of the HC class for the unreacted pyrene and after thermal treatment.

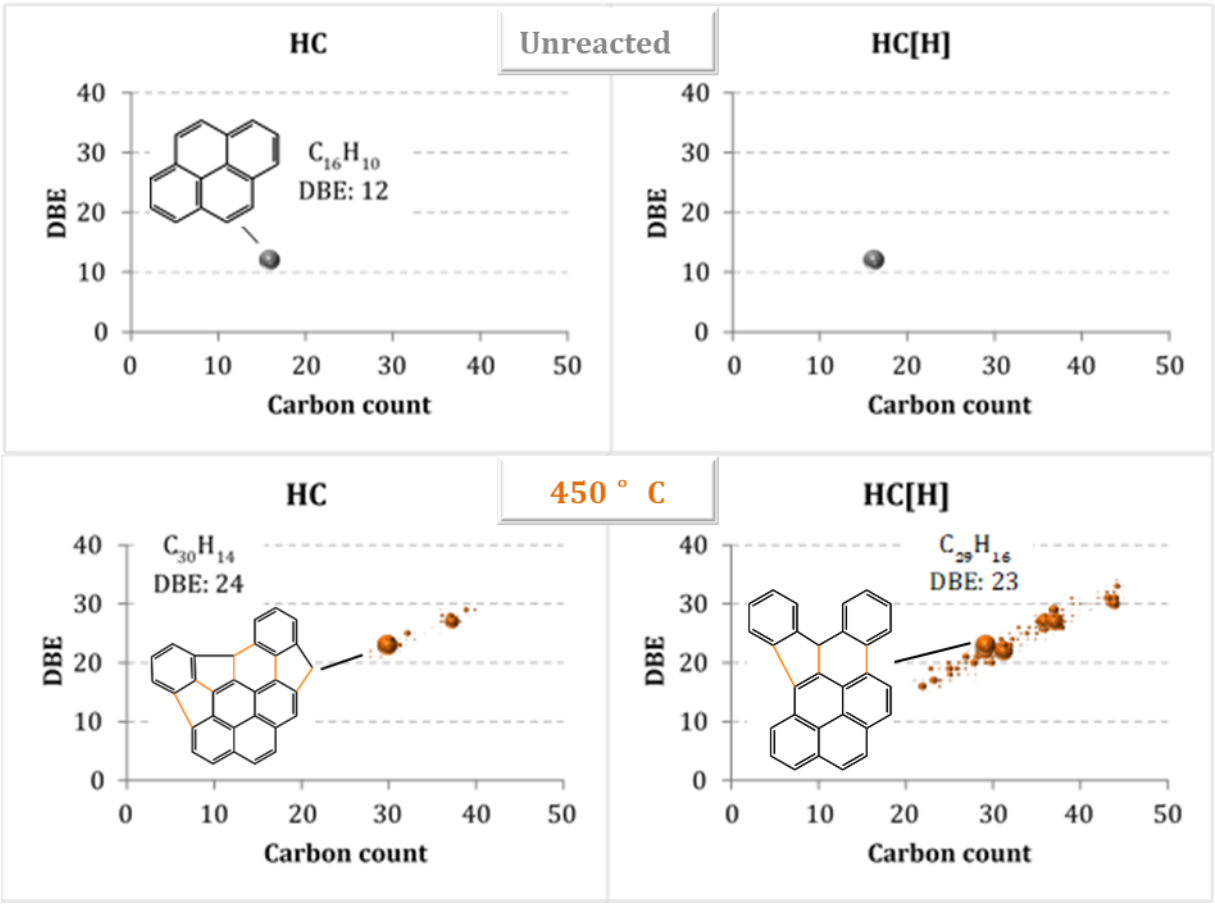

Figure 6-6: DBE vs. carbon distribution Kendrick plots of the HC class detected as radical ions (left column) and as protonated molecules (right column) for the unreacted pyrene (top) and after thermal treatment at 450 °C (bottom). Possible structures of some newly created compounds are shown as insets with newly formed carbon-carbon bonds shown in orange.

At the highest temperature of 450 °C not only the DBE value is increasing but also the carbon number per molecule, indicating that additional aromatic systems have been added to the initial model compound. It has to be noted that toluene was used as a solvent, because it is present in a light crude oil fraction and can not only serve as a solvent, but also as a reactant. The radical hydrocarbon compound with the highest intensity detected has a composition of $C_{30}H_{14}$ and might originate from a pyrene moiety joined with two molecules of toluene, while in case of the protonated hydrocarbon species, the compound with the chemical formula of $C_{29}H_{16}$ is potentially derived from pyrene joined with diphenylmethane, which might be first produced from toluene. In both cases, radical ions and protonated molecules, a pattern of high intensity signals can be observed that differ in a DBE of 4 and a carbon number of 7, i.e. one toluene moiety. However, at this point

some structural suggestions based on the chemical compositions calculated from the experimental data are demonstrated here.

A possible reaction pathway for the generation of the compound with composition $C_{30}H_{14}$, seen in Figure 6-6 is depicted in Figure 6-7. In this case the reaction is likely to be initiated by forming a radical from excess toluene. Subsequently C-C-coupling reactions can take place to join the different aromatic moieties, similar to radical polymerization reactions. Ring-closure and dehydrogenation reactions then lead to a reformation of the aromatic system. A similar process can happen multiple times, eventually leading to a compound of composition $C_{30}H_{14}$ after addition of two toluene units. At present, however, is cannot be concluded at which point dehydrogenations take place, i.e. if these are intermediate steps, as depicted in Figure 6-7, of if they occur only at a later stage.

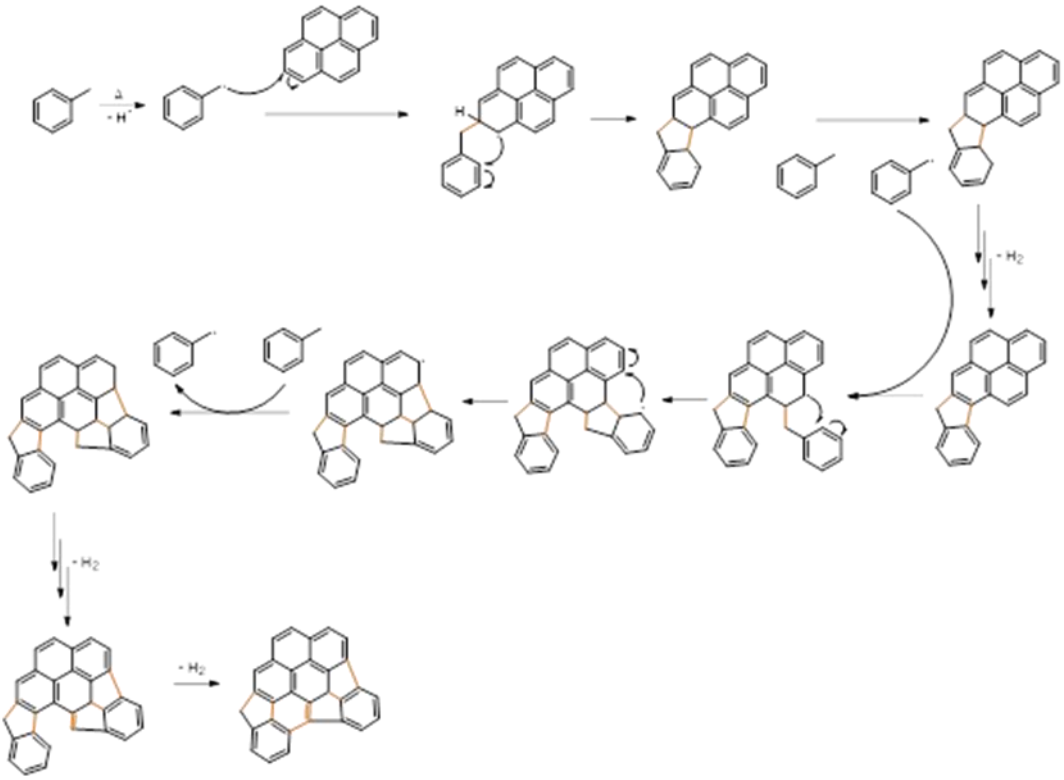

Figure 6-7: Possible reaction pathway leading to the product compound $C_{30}H_{14}$ after fouling reaction of the standard hydrocarbon compound of pyrene with toluene.

6.5. Conclusion

The first step to solve the fouling problem in petroleum industries is to understand the reaction mechanisms involved. During this work, simulation of fouling under laboratory conditions was successfully performed. The results obtained here were focused on the HC class detected with ESI as ionization method, and clearly show that high temperature plays a significant role on fouling. Formation of new hydrocarbon compounds of high molecular mass and aromaticity were observed after thermal treatment at 450 °C. These compounds were able to be ionized and detected with the use of ESI either as radical cations (HC) or as protonated molecules ([HC]). By means of model compounds some potential reaction pathways could be established. The results suggest that mainly radical driven conjugations of aromatic moieties are taking place, potentially preceded or followed by dehydrogenation reactions. This resembles the results obtained from the real world sample were also additions of relatively aromatic subunits were observed, while C-C couplings involving the radical addition of alkyl chains were not observed.

6.6. References

1. Deshannavar, U.; Rafeen, S.; Marappa Gounder, R.; D, S., Crude Oil Fouling: A Review. *J. Appl. Sci.* **2010,** *10*.

2. Fan, Z.; Rahimi, P.; McGee, R.; Wen, Q.; Alem, T., Investigation of Fouling Mechanisms of a Light Crude Oil Using an Alcor Hot Liquid Process Simulator. *Energy Fuels* **2010,** *24* (11), 6110-6118.

3. Macchietto, S.; Hewitt, G. F.; Coletti, F.; Crittenden, B. D.; Dugwell, D. R.; Galindo, A.; Jackson, G.; Kandiyoti, R.; Kazarian, S. G.; Luckham, P. F.; Matar, O. K.; Millan-Agorio, M.; Müller, E. A.; Paterson, W.; Pugh, S. J.; Richardson, S. M.; Wilson, D. I., Fouling in Crude Oil Preheat Trains: A Systematic Solution to an Old Problem. *Heat Transfer Eng.* **2011,** *32* (3-4), 197-215.

4. Müller-Steinhagen, H.; Malayeri, M. R.; Watkinson, A. P., Fouling of Heat Exchangers-New Approaches to Solve an Old Problem. *Heat Transfer Eng.* **2005,** *26* (1), 1-4.

5. Nategh, M.; Malayeri, M. R.; Mahdiyar, H., A Review on Crude Oil Fouling and Mitigation Methods in Pre-heat Trains of Iranian Oil Refineries *Journal of Oil, Gas and Petrochemical Technology* **2017,** *4* (Number 1), 1-17.

6. Wiehe, I. In *Petroleum fouling: Causes, tools and mitigation methods*, Proceedings of the 9th Topical Conference on Refinery Processing, 2006.

7. Jia, C., Breakthrough and significance of unconventional oil and gas to classical petroleum geology theory. *Petrol. Explor. Develop.* **2017,** *44* (1), 1-10.

8. Miller, R. G.; Sorrell, S. R., The future of oil supply. *Philos. Trans. R. Soc., A* **2014,** *372* (2006), 1-27.

9. Prado, G.; Rao, Y.; de Klerk, A., Nitrogen Removal from Oil: A Review. *Energy Fuels* **2017,** *31* (1), 14-36.

10. Watkinson, A. P., Deposition from Crude Oils in Heat Exchangers. *Heat Transfer Eng.* **2007,** *28* (3), 177-184.

11. Diaz-Bejarano, E.; Coletti, F.; Macchietto, S., Modeling and Prediction of Shell-Side Fouling in Shell-and-Tube Heat Exchangers. *Heat Transfer Eng.* **2018**, 1-17.

12. Saleh, Z. S.; Sheikholeslami, R.; Watkinson, A. P., Fouling Characteristics of a Light Australian Crude Oil. *Heat Transfer Eng.* **2005,** *26* (1), 15-22.

13. Beens, J.; Blomberg, J.; Schoenmakers, P. J., Proper Tuning of Comprehensive Two-Dimensional Gas Chromatography (GCxGC) to Optimize the separation of Complex Oil Fractions. *J. High Resolut. Chromatogr.* **2000,** *23*, 182-188.

14. Epstein, N., Thinking about Heat Transfer Fouling: A 5 × 5 Matrix. *Heat Transfer Eng.* **1983,** *4* (1), 43-56.

15. Watkinson, A. P.; Navaneetha-Sundaram, B.; Posarac, D., Fouling of a Sweet Crude Oil under Inert and Oxygenated Conditions. *Energy Fuels* **2000,** *14* (1), 64-69.

16. Harris, J. S.; Lane, M. R.; Smith, A. D., Investigating the Impact of Boiling Conditions on the Fouling of a Crude Oil. *Heat Transfer Eng.* **2017,** *38* (7-8), 703-711.

17. Ishiyama, E. M.; Paterson, W. R.; Wilson, D. I., The Effect of Fouling on Heat Transfer, Pressure Drop, and Throughput in Refinery Preheat Trains: Optimization of Cleaning Schedules. *Heat Transfer Eng.* **2009,** *30* (10-11), 805-814.

18. Ramasamy, M.; Deshannavar, U. B., Effect of Bulk Temperature and Heating Regime on Crude Oil Fouling: An Analysis. *Adv. Mater. Res.* **2014,** *917*, 189-198.

19. Lababidi, S.; Schrader, W., Online normal-phase high-performance liquid chromatography/Fourier transform ion cyclotron resonance mass spectrometry: effects of different ionization methods on the characterization of highly complex crude oil mixtures. *Rapid Commun. Mass Spectrom.* **2014,** *28* (12), 1345-52.

20. Panda, S. K.; Andersson, J. T.; Schrader, W., Characterization of supercomplex crude oil mixtures: what is really in there? *Angew. Chem.* **2009,** *48* (10), 1788-91.

21. Pinto, D. A. M.; Camargo, S. M. C.; Parra, M. O.; Laverde, D.; Vergara, S. G.; Pinzon, C. B., Formation of fouling deposits on a carbon steel surface from Colombian heavy crude oil under preheating conditions. *J. Phys.: Conf. Ser.* **2016,** *687* (1), 01-04.

22. Venditti, S.; Berrueco, C.; Alvarez, P.; Morgan, T.; Millan-Agorio, M.; Herod, A. A.; Kandiyoti, R., Developing characterisation methods for foulants deposited in refinery heat exchangers. In *Conference: Heat Exchanger Fouling and Cleaning Eurotherm Conference* 2009.

23. Young, A.; Venditti, S.; Berrueco, C.; Yang, M.; Waters, A.; Davies, H.; Hill, S.; Millan, M.; Crittenden, B., Characterization of Crude Oils and Their Fouling Deposits Using a Batch Stirred Cell System. *Heat Transfer Eng.* **2011,** *32* (3-4), 216-227.

24. Ryder, A. G., Analysis of Crude Petroleum Oils Using Fluorescence Spectroscopy. In *Reviews in Fluorescence 2005*, Geddes, C. D.; Lakowicz, J. R., Eds. Springer US: Boston, MA, 2005; pp 169-198.

25. Aske, N.; Kallevik, H.; Sjöblom, J., Determination of Saturate, Aromatic, Resin, and Asphaltenic (SARA) Components in Crude Oils by Means of Infrared and Near-Infrared Spectroscopy. *Energy Fuels* **2001,** *15* (5), 1304-1312.

26. Bennett, C. A.; Appleyard, S.; Gough, M.; Hohmann, R. P.; Joshi, H. M.; King, D. C.; Lam, T. Y.; Rudy, T. M.; Stomierowski, S. E., Industry-Recommended Procedures for Experimental Crude Oil Preheat Fouling Research. *Heat Transfer Eng.* **2006,** *27* (9), 28-35.

27. Wiehe, I. A.; Kennedy, R. J., The Oil Compatibility Model and Crude Oil Incompatibility. *Energy Fuels* **2000,** *14* (1), 56-59.

28. García, M. d. C., Crude Oil Wax Crystallization. The Effect of Heavy n-Paraffins and Flocculated Asphaltenes. *Energy Fuels* **2000,** *14* (5), 1043-1048.

29. Molina V, D.; Ariza León, E.; Chaves-Guerrero, A., Understanding the Effect of Chemical Structure of Asphaltenes on Wax Crystallization of Crude Oils from Colorado Oil Field. *Energy Fuels* **2017,** *31* (9), 8997-9005.

30. Olsen, J. V.; de Godoy, L. M.; Li, G.; Macek, B.; Mortensen, P.; Pesch, R.; Makarov, A.; Lange, O.; Horning, S.; Mann, M., Parts per million mass accuracy on an Orbitrap mass spectrometer via lock mass injection into a C-trap. *Mol. Cell. Proteomics* **2005,** *4* (12), 2010-21.

31. Panda, S. K.; Andersson, J. T.; Schrader, W., Mass-spectrometric analysis of complex volatile and nonvolatile crude oil components: a challenge. *Anal. Bioanal. Chem.* **2007,** *389* (5), 1329-1339.

32. Liu, P.; Shi, Q.; Chung, K.; Zhang, Y.; Pan, N.; Zhao, S.; Xu, C., Molecular Characterization of Sulfur Compounds in Venezuela Crude Oil and Its SARA Fractions by Electrospray Ionization Fourier Transform Ion Cyclotron Resonance Mass Spectrometry. *Energy Fuels* **2010,** *24* (9), 5089-5096.

33. Wu, Z.; Rodgers, R. P.; Marshall, A. G.; Strohm, J. J.; Song, C., Comparative Compositional Analysis of Untreated and Hydrotreated Oil by Electrospray Ionization Fourier Transform Ion Cyclotron Resonance Mass Spectrometry. *Energy Fuels* **2005,** *19* (3), 1072-1077.

34. Konermann, L.; Ahadi, E.; Rodriguez, A. D.; Vahidi, S., Unraveling the Mechanism of Electrospray Ionization. *Anal. Chem.* **2013,** *85* (1), 2-9.

35. Schäfer, M.; Drayß, M.; Springer, A.; Zacharias, P.; Meerholz, K., Radical Cations in Electrospray Mass Spectrometry: Formation of Open-Shell Species, Examination of the Fragmentation Behaviour in ESI-MSn and Reaction Mechanism Studies by Detection of Transient Radical Cations. *Eur. J. Org. Chem.* **2007,** (31), 5162-5174.

36. Vetere, A.; Schrader, W., Mass Spectrometric Coverage of Complex Mixtures: Exploring the Carbon Space of Crude Oil. *ChemistrySelect* **2017,** *2* (3), 849-853.

37. Watkinson, A. P., Chemical reaction fouling of organic fluids. *Chem. Eng. Technol.* **1992,** *15* (2), 82-90.

38. Albright, L. F.; McConnell, C. F.; Welther, K., Types of Coke Formed During the Pyrolysis of Light Hydrocarbons. In *Thermal Hydrocarbon Chemistry*, AMERICAN CHEMICAL SOCIETY: 1979; Vol. 183, pp 175-191.

39. Schorr Wiener, M.; Valdez Salas, B., Corrosion Problems and Solutions in Oil Refining and Petrochemical Industry. *Corros. Eng., Sci. Technol.* **2018,** *53* (1), 80-80.

40. Bhowmik, P.; Emam Hossain, M. D.; Ahmed Shamim, J. In *CORROSION AND ITS CONTROL IN CRUDE OIL REFINING PROCESS*, 6th International Mechanical Engineering Conference & 14th Annual Paper Meet, Bangladesh, Bangladesh, 2012.

41. Kharlamov, A.; Kharlamova, G.; Bondarenko, M.; Fomenko, V., Joint Synthesis of Small Carbon Molecules (C3-C11), Quasi-Fullerenes (C40, C48, C52) and their Hydrides. *Chemical Engineering and Science* **2013,** *1*, 32-40.

42. Goroff, N. S., Mechanism of Fullerene Formation. *Acc. Chem. Res.* **1996,** *29* (2), 77-83.

43. Berné, O.; Montillaud, J.; Joblin, C., Top-down formation of fullerenes in the interstellar medium. *Astron. Astrophys.* **2015,** *577*, A133.

CHAPTER 7. UNDERSTANDING "FOULING" IN EXTREMELY COMPLEX PETROLEUM MIXTURES

Redrafted from:

A. Kondyli, W. Schrader. "Understanding "fouling" in extremely complex petroleum mixtures", submitted to *Angew. Chemie.*

7.1. Abstract

"Fouling", the unwanted deposition of solids causes significant operational difficulties in petroleum producing and processing industries and is considered a billion dollar problem. There are two problematic ways of petroleum fouling: physical fouling, where material of low solubility accumulates and precipitates, and chemical fouling, where a chemical reaction occurs that produces insoluble material, often on the surface of a heat exchanger or any type of high temperature reactor. Here, we show by implementing laboratory-scale experimental simulations of the industrial process using a petroleum derived light crude oil fraction, that fouling proceeds via multi-step pathways involving dehydrogenation and radical formation reactions on polyaromatic hydrocarbons and polyaromatic heterocycles, resulting in the formation of carbonaceous deposits. These studies simulating an industrial side reaction under laboratory conditions lead to a better understanding of the mechanism of petroleum fouling on a molecular level.

7.2. Introduction

Industrial processes in oil refineries and petrochemical industries involve chemical reactions in an ultra-large scale range, where often thousands of barrels of crude oil or petroleum feedstocks are produced, processed and stored within an hour. As in almost every chemical reaction under industrial conditions also side reactions can occur which have an enormous economic and environmental impact.[1] One of the most important chemical reactions which causes the deposition of materials often on the surface of hot metallic components is called fouling.[2-5] These deposits need to be removed regularly, which makes fouling a billion dollar problem.[6] In addition to the high operational, maintenance and remediation costs the material is considered to be environmentally toxic due to the large content of polyaromatic compounds (PAH) within. In order to gain insight information of the reactions that occur during fouling, we constructed a laboratory-scale reactor to simulate the conditions of an oil processing unit. This setup cannot be considered a comprehensive simulation of the industrial scale process, since all the different parameters such as mass flow, temperature, and pressure as well as all the other conditions cannot be reproduced one-to-one in the laboratory. However, the goal was to reproduce the formation of fouling material and to understand the processes that lead to such materials.

The two most important reactions of fouling in crude oil processing are physical and chemical fouling.[3] Physical fouling can occur from petroleum materials that contain some heavy and low- soluble compounds, such as asphaltenes.[7-11] They can be deposited when lighter compounds present in the oil, acting as a solvent, are evaporated or removed. Chemical fouling describe chemical reactions leading to the formation of a solid material, often on heated surfaces.[12] Here, the reaction pathways are not yet understood. For these studies we used a gas condensate for the simulation reaction which was known for its tendency to form deposits but does not contain any low volatile components to exclude any formation of deposits by physical fouling and the formation of fouling material can solely be attributed to chemical reactions.[13]

Studying the chemical transformation of such complex mixtures with often more than one million different chemical compounds present[14] needs special analytical tools. Here, ultrahigh resolution mass spectrometry allows analyzing the molecular changes of complex petroleum mixtures and as a very accurate analytical technique allows the calculation of elemental compositions from each detected signal.[15-21]

The direct simulation of an industrial operation under laboratory conditions is not possible. Therefore, the target for these studies was to run a reaction that produces the fouling deposits from a chemical reaction in a laboratory in a small scale experiment. To achieve this goal, a reactor was constructed and optimized that includes a stainless steel autoclave that was heated in a heating box and allows the use of inserts made of different materials.

7.3. Experimental

7.3.1. Simulation of fouling under laboratory conditions

A lab build reactor was used for fouling simulation. The experimental set up was the following: A quartz crucible was filled with 0.3 mL of a gas condensate and was placed inside a stainless steel autoclave. Afterwards, a quartz cover was placed on the top of the crucible in order to avoid sample loses. The autoclave was then positioned in a heating plate which was operated using a temperature controller. The sample was heated for 3 days at a temperature of 150 °C, 250 °C, 350 °C or 450 °C under oxygenated conditions (OC). In order to verify the mechanism, the model nitrogen compound of quinoline in the presence of oct-3-ene as initiator was dissolved in 0.1 mL of toluene and heated for 3 days at 150 °C and 450 °C.

7.3.2. Sample preparation for MS analysis

All samples were first dissolved in toluene (HPLC grade, Sigma-Aldrich, Germany) and then diluted with methanol (LC-MS grade, J. T. Baker, Germany) (1:4 v/v) to a final concentration of 250 ppm and then analyzed without further treatment.

7.3.3. Instruments and methods

For mass spectrometric analysis a research-type Orbitrap Elite (Thermo Fisher, Bremen, Germany) was used. Mass spectra were recorded in a range of m/z 150-1000 using spectral stitching method (scanning the whole mass range in windows of 30 a with 5 a overlap) at a resolving power of R=480,000 and 960,000 (FWHM at m/z 400). Ionization was performed using an Electrospray (ESI) source in positive mode with a stainless steel needle at a capillary voltage of 4 kV. Nebulization was assisted by a sheath gas flow of 3.0 a.u. (arbitrary units) while the auxiliary and the sweep gas flow were set

at 0.0 a.u. The transfer capillary temperature was set at 275 °C. For the fragmentation experiments MS/MS measurements were performed by collision-induced dissociation (CID). The precursor mass was selected with an isolation window of 1.0 a and the isolated ions were kinetically excited with high (around 45 %) energy using helium as collision gas.

7.3.4. Data analysis

External mass calibration was performed prior to sample analysis in order to meet a mass accuracy of < 1 ppm. The recorded mass spectra were recombined by Xcalibur 4.0 software (Thermo Fisher, Bremen, Germany) and further processed using the Composer software (version 1.5.0, Sierra Analytics, Modesto, CA, USA). Calculations and peak assignments were carried out using the following restrictions regarding the number of possible elements and the number of double bond equivalent: H 0-1000, C: 0-200, N: 0-3, O: 0-6, S: 0-2 and DBE: 0-100. The calculated molecular formulae were sorted into heteroatom classes based on their denoted Kendrick mass defects and their double bond equivalent distribution. The obtained mass lists were transferred to Excel (Microsoft Office Professional Plus 2010, Microsoft Corporation, Redmond, WA, USA) for further data evaluation. Double bond equivalent refers to the sum of the rings and double bonds present within a molecule and is calculated from the general CcHhNnOoSs of the analyte using the following equation: $\mathrm{DBE} = \mathrm{c} - \frac{\mathrm{h}}{2} + \frac{\mathrm{n}}{2} + 1$. A higher DBE value indicates higher aromaticity of a compound.

7.4. Results and discussion

The fouling reactions were simulated by heating a light crude oil fraction within this airtight stainless steel autoclave, equipped with a quartz crucible, to temperatures of 150, 250, 350 and 450 °C for up to three days. The major product of the reaction is an insoluble fouling deposit that was analyzed by electron microscopy (Figure 7-1, bottom left). The deposit has been found to be amorphous carbon material with a carbon content of >98 %. The mass spectrometric results of the original sample (unreacted) and the soluble portion obtained after heating at 450 °C reveal drastic changes during the reaction (see Figure 7-1, top). Generally, a shift towards higher *m/z* can be observed. While for the unreacted sample the observed distribution is mainly centered around *m/z* 300, for the reacted

sample the highest abundance of intensities is observed around *m/z* 400. Additionally, many individual elemental compositions have been removed from the spectrum after reaction at 450 °C, while new compounds have been formed. Details on the changes on the assigned chemical compositions can be seen from the zoomed-in spectra in Figure 7-1(top right).

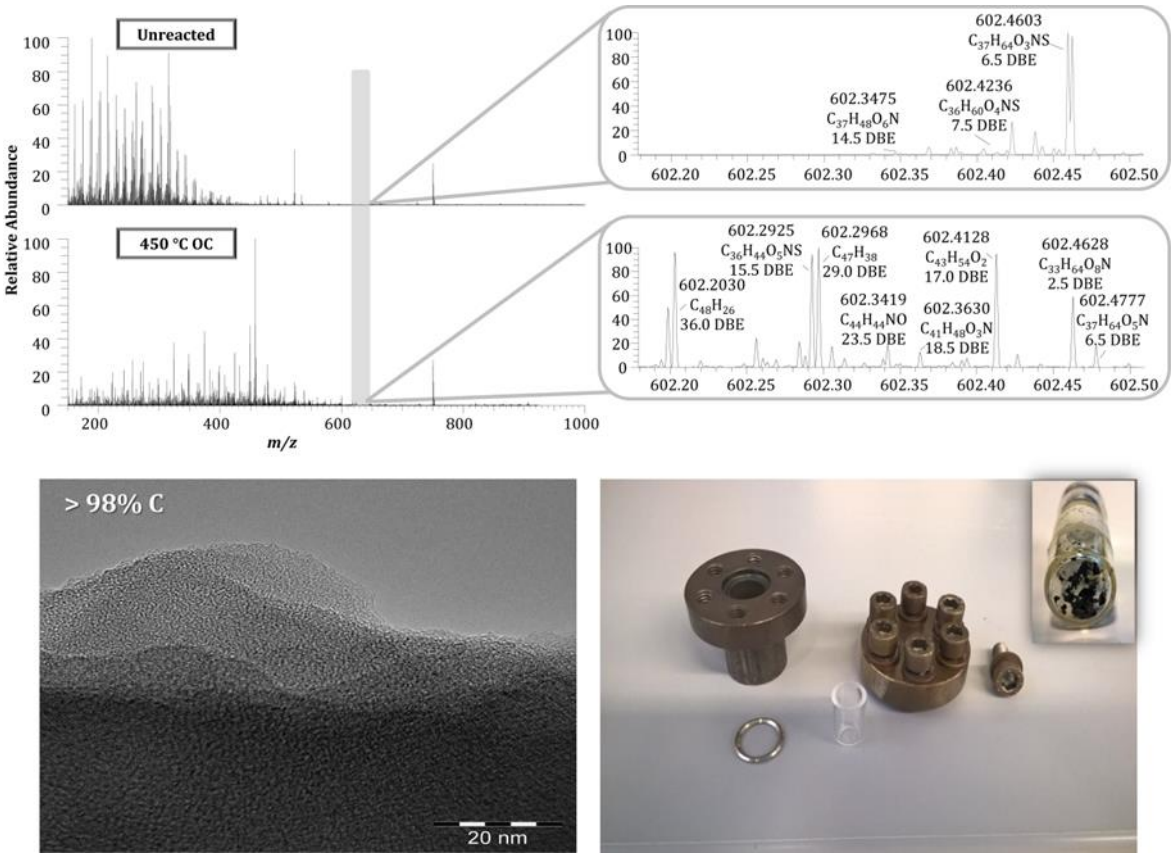

Figure 7-1: Simulation of a fouling reaction was carried out using a stainless steel autoclave with a quartz inlet and a stainless steel ring for sealing (bottom right). The fouling material (inset on the bottom right) consists of more than 98 % amorphous carbon, determined from micrographs by SEM/TEM (bottom left). The changes in composition can be seen from the mass spectra shown on top. The left side displays the overall spectrum of the light crude oil fraction before heating (unreacted) and after heating at 450 °C, while the top right spectra show the zoomed-in views at *m/z* 602. The data reveal that not only solid material is being formed after the reaction but also a number of different reaction products remain in solution, drastically changing the composition of the light crude oil fraction.

To explore a chemical reaction of the individual molecule in many thousands of different chemical compounds is difficult to follow. Instead, we can follow the reaction according to changes within a class. A class in this context is defined by the heteroatom content. Without any heteroatom, a compound belongs to the hydrocarbon class (HC), while compounds having one nitrogen atom belong to the N_1 class. Here it needs to be mentioned that all of the N_1 compounds are detected as protonated molecules (N[H]). This class is shown here as an example to study the fouling mechanism. The N_1-class in the unreacted sample is represented by different chemical compounds with a carbon number (i.e. carbon atoms per molecule) range from 8 to almost 40 and a double bond equivalent (DBE) between 4 and 16. The DBE refers to the sum of ring closures and the number of π-bonds within a molecule and its value is an indicator for the aromaticity of a chemical compound. The distribution of the N_1-class, summarized in Kendrick plots[22] (see Figure 7-2), shows the increase of nitrogen species both in aromaticity and mass, i.e. new compounds are created during the fouling reaction that contain one nitrogen atom. While at temperatures of 150 and 250 °C only minor reaction activities occur, at higher temperatures the reaction is more effective. At the highest temperature of 450°C the resulting compounds reach a size of up to 70 carbon atoms with a DBE of up to 45. Compared to the unreacted sample, size and aromaticity are doubled or tripled. The data show that the reaction starts with the dehydrogenation of single compounds, leading to an increase in aromaticity. Then, aromaticity and molecular size are increased together, which is indicative of the addition of aromatic moieties to existing compounds by C-C coupling reactions.

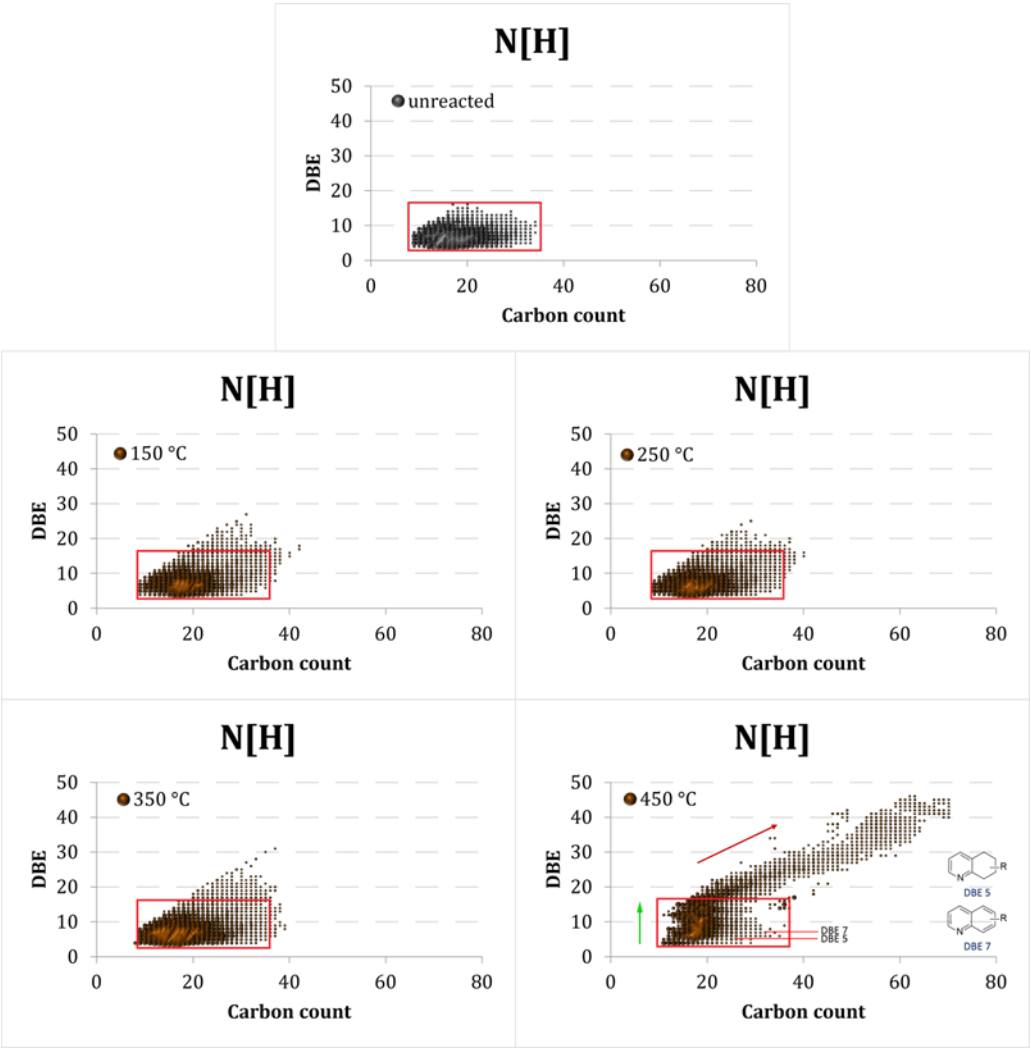

Figure 7-2: Kendrick plots of the N-containing species after reaction for 3 days at different temperatures showing double-bond equivalents (DBE) vs. carbon number. The top graphic shows the N1–class of the light crude oil fraction before reaction (unreacted). The other plots show the results obtained after reaction at 250, and 450 °C. The red rectangles in the plots indicate the area spanned by the compounds found in the unreacted sample and show the overall differences observed after the reaction. The data reveal that initially the DBE value increases, suggesting a dehydrogenation reaction. At higher temperatures not only the DBE is increasing but also the carbon number, suggesting that additional aromatic systems are added to the initial compounds fraction.

Although a tendency of the mechanism can be deduced from the data shown in Figure 7-2, it is extremely difficult to explain individual molecular changes within such a complex mixture. Therefore, a reaction set-up was developed that allows the formation of a fouling deposit with only a limited number of reactants. The Kendrick plots in Figure 7-2 reveal that major nitrogen compounds within effective reactivity belong to the DBE 7 series. This corresponds to quinoline ($C_9H_7N_1$). For this reason quinoline was chosen as a reactant for further studies in a simpler set-up. Qunoline was dissolved in toluene for the reaction. This solution alone did not show any reactivity and the addition of an initiator was necessary – in this case 3-octene was used, since alkenes are known to promote radical oligomerization reactions.[23] The reaction was performed under the same conditions as the reaction of the gas condensate sample. Here, also a fouling deposit was found as the major reaction product with an additional number of compounds still present in solution. Using high resolution MS/MS measurements and *collision-induced dissociation* (CID), structural elucidation of the resulting compounds is possible.[24] Figure 7-3 shows the results of such an example using one of the reaction products with elemental composition $C_{25}H_{18}N_2$ (N_2-class, detected as protonated molecule). CID studies reveal that the compound consists of a quinoline dimer joined together with one toluene moiety. The different fragments reveal the toluene molecule to be attached in different ways. The loss of 15 a, (m/z 332) representing a methyl-group is only possible, when a terminal methyl group is present, such that the toluene and the quinoline moieties must be directly connected by ring-to-ring reaction. Alternatively, the loss of a 78 a fragment (phenyl-group, m/z 269) can only occur when a toluene moiety is connected to the quinoline through the methyl group, which is forming a methylene bridge between the two ring systems. A loss of 91 a, yielding an ion at m/z 256 is possible from both variants. Fragment ions at m/z 128, 130 and 218 result from the cleavage of the bond between the two quinoline moieties, involving an additional proton shift. Details of the fragmentation behavior are depicted in Figure 7-3.

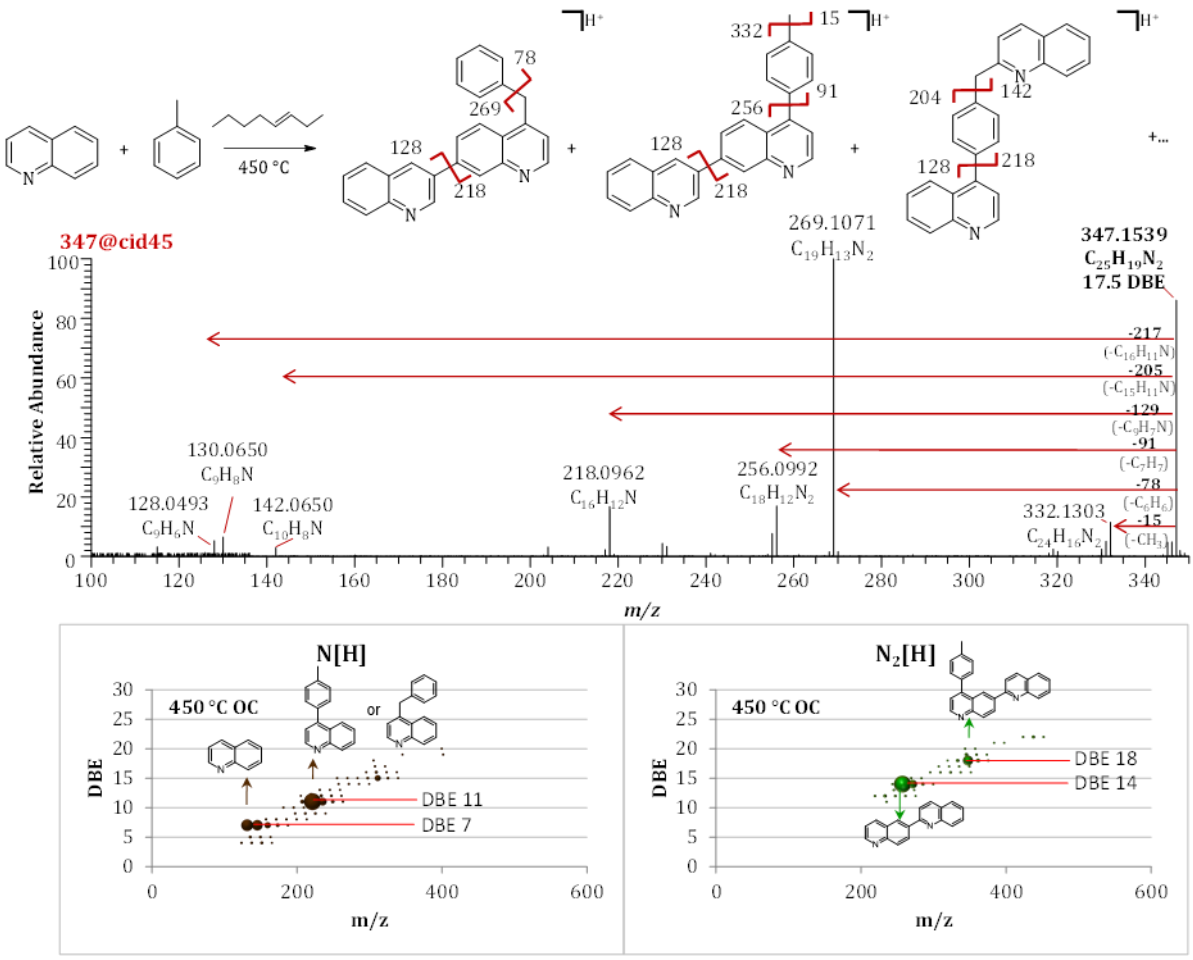

Figure 7-3: Results of a fouling reaction using the standard compound quinoline in the presence of toluene. The mixture alone is not reacting and the addition of 3-octene as an initiator was necessary. The high resolution MS/MS spectrum shows the fragmentation of the reaction products at *m/z* 347, which correspond to a quinolone dimer with the addition of a toluene moiety. The different fragment signals allow a detailed characterization of the structure, revealing that toluene is added to the quinoline moiety either directly through a bond between both aromatic core structures as well as through the methyl-group of toluene. The two Kendrick plots at the bottom show the different product compounds in the reaction mixture for the N_1- and N_2-class. In addition, solid material was formed after the reaction at 450 °C. It has to be noted that the structures shown here are suggestions retrieved from the data. At this point, no information is available regarding the exact position of the individual coupling sites.

The results shown here indicate that the formation of larger compounds consists of two different reaction pathways as summarized in Figure 7-4. One reaction step involves the thermal dehydrogenation of the initial compounds present. This can lead to the

formation of radical intermediates which in turn can react with each other to form different types of oligomers and polymers in a random reaction where both aromatic cores can be directly fused or connected through an aliphatic bridge. For the initiation of the radical reaction, elevated temperatures are necessary as well as a radical initiator. Both are often present in industrial processes, as the production temperature can easily exceed 800 °C and within the complexity of the petroleum, alone enough starter compounds can be found for every radical reaction.

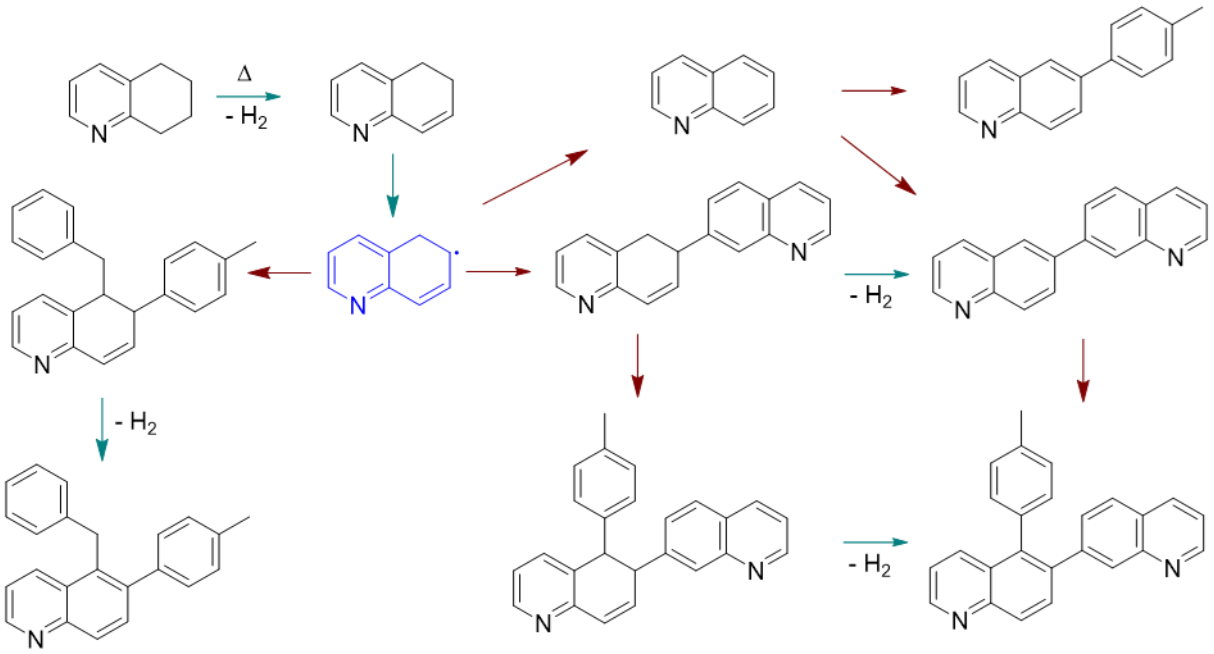

Figure 7-4: Suggested reaction mechanisms of tetrahydro-quinoline. The mechanism is based on the data obtained during these reactions. A compound such as tetrahydro-quinoline would lose hydrogen atoms in multiple steps thus increasing the aromaticity and the DBE value. The thermal removal of hydrogen allows the formation of radical intermediates which then can easily react with other aromatic or aliphatic sites in the mixture. Shown here is the addition of toluene and/or additional quinoline moieties as an example. The green arrows depict the increase of DBE while the red arrows show the increase of both DBE and carbon number by addition of another aromatic moiety.

7.5. Conclusion

These results show that it is possible to simulate a very important and cost intensive industrial side reaction under laboratory conditions and to understand the mechanism in an experimental environment. The formation of organic solid deposits during petroleum processing is a highly complex phenomenon involving not only different processes but also different chemical reaction pathways. As our results demonstrate for the first time, understanding the reaction mechanisms of fouling is the first step to solve this problem. Until now it was not clear why some petroleum feedstocks have fouling tendencies and some have not. The reason could be that in one the radical oligomerization reaction is initiated while in the other it is suppressed.

Most of the current work on fouling focuses on improving the operational conditions as well as the design of heat exchangers and other parts of the equipment. But the understanding of the corresponding mechanisms, using here the example of nitrogen containing compounds, is the foundation for reducing the formation of fouling deposits. One way could be by designing the process in a manner that the radical polymerization reaction that leads to higher molecular weight materials is inhibited. This will ultimately lead to a decrease in maintenance costs and reduces the environmental contamination of an industrial process. Additionally, this mechanism can be an indication on how asphaltene aggregation works, as these are similar systems.

7.3 References

1. Bott, T. R., The fouling of heat transfer surfaces. In *2nd International Conference on Process Intensification in Practice: Applications and Opportunities*, Semel, J., Ed. 1997; pp 3-16.

2. Bott, T. R., *Fouling: Needs and opportunities*. 2001; p 3-7.

3. Deshannavar, U. B.; Rafeen, M. S.; Ramasamy, M.; Subbarao, D., Crude Oil Fouling: A Review. *J. Appl. Sci.* **2010,** *10* (24), 3167-3174.

4. Diaz-Bejarano, E.; Behranvand, E.; Coletti, F.; Mozdianfard, M. R.; Macchietto, S., Organic and inorganic fouling in heat exchangers – Industrial case study: Analysis of fouling state. *Applied Energy* **2017,** *206*, 1250-1266.

5. Watkinson, A. P.; Wilson, D. I., Chemical reaction fouling: A review. *Exp. Therm. Fluid Sci.* **1997,** *14* (4), 361-374.

6. Coletti, F.; Crittenden, B. D.; Macchietto, S., *Basic Science of the Fouling Process*. 2015; p 23-50.

7. Gaspar, A.; Zellermann, E.; Lababidi, S.; Reece, J.; Schrader, W., Characterization of Saturates, Aromatics, Resins, and Asphaltenes Heavy Crude Oil Fractions by Atmospheric Pressure Laser Ionization Fourier Transform Ion Cyclotron Resonance Mass Spectrometry. *Energy Fuels* **2012,** *26* (6), 3481-3487.

8. Indo, K.; Ratulowski, J.; Dindoruk, B.; Gao, J.; Zuo, J.; Mullins, O. C., Asphaltene Nanoaggregates Measured in a Live Crude Oil by Centrifugation. *Energy Fuels* **2009,** *23*, 4460-4469.

9. Loegel, T. N.; Danielson, N. D.; Borton, D. J.; Hurt, M. R.; Kenttamaa, H. I., Separation of Asphaltenes by Reversed-Phase Liquid Chromatography with Fraction Characterization. *Energy Fuels* **2012,** *26* (5), 2850-2857.

10. Asomaning, S.; Watkinson, A. P., Petroleum stability and heteroatom species effects in fouling of heat exchangers by asphaltenes. *Heat Transfer Eng.* **2000,** *21* (3), 10-16.

11. Mullins, O. C., The Asphaltenes. In *Annual Review of Analytical Chemistry, Vol 4*, Cooks, R. G.; Yeung, E. S., Eds. Annual Reviews: Palo Alto, 2011; Vol. 4, pp 393-418.

12. Epstein, N., Thinking about Heat Transfer Fouling: A 5 × 5 Matrix. *Heat Transfer Eng.* **1983,** *4* (1), 43-56.

13. Crittenden, B. D.; Kolaczkowski, S. T.; Phillips, D. Z., *Chemical reaction fouling*. 1999; p 91-103.

14. Beens, J.; Blomberg, J.; Schoenmakers, P. J., Proper tuning of comprehensive two-dimensional gas chromatography (GC x GC) to optimize the separation of complex oil fractions. *J. High Resol. Chromatogr.* **2000,** *23* (3), 182-188.

15. Panda, S. K.; Andersson, J. T.; Schrader, W., Characterization of Supercomplex Crude Oil Mixtures: What Is Really in There? *Angewandte Chemie-International Edition* **2009,** *48* (10), 1788-1791.

16. Vetere, A.; Schrader, W., Mass Spectrometric Coverage of Complex Mixtures: Exploring the Carbon Space of Crude Oil. *ChemistrySelect* **2017,** *2* (3), 849-853.

17. Barrow, M. P.; Witt, M.; Headley, J. V.; Peru, K. M., Athabasca Oil Sands Process Water: Characterization by Atmospheric Pressure Photoionization and Electrospray Ionization Fourier Transform Ion Cyclotron Resonance Mass Spectrometry. *Anal. Chem.* **2010,** *82* (9), 3727-3735.

18. Headley, J. V.; Peru, K. M.; Barrow, M. P., Advances in mass spectrometric characterization of naphthenic acids fraction compounds in oil sands environmental samples and crude oil-A review. *Mass Spectrom. Rev.* **2016,** *35* (2), 311-328.

19. Miettinen, I.; Mäkinen, M.; Vilppo, T.; Jänis, J., Compositional Characterization of Phase-Separated Pine Wood Slow Pyrolysis Oil by Negative-Ion Electrospray Ionization Fourier Transform Ion Cyclotron Resonance Mass Spectrometry. *Energy Fuels* **2015,** *29* (3), 1758-1765.

20. Rüger, C. P.; Miersch, T.; Schwemer, T.; Sklorz, M.; Zimmermann, R., Hyphenation of Thermal Analysis to Ultrahigh-Resolution Mass Spectrometry (Fourier Transform Ion Cyclotron Resonance Mass Spectrometry) Using Atmospheric Pressure Chemical Ionization For Studying Composition and Thermal Degradation of Complex Materials. *Anal. Chem.* **2015,** *87* (13), 6493-6499.

21. Ruger, C. P.; Grimmer, C.; Sklorz, M.; Neumann, A.; Streibel, T.; Zimmermann, R., Combination of Different Thermal Analysis Methods Coupled to Mass Spectrometry for the Analysis of Asphaltenes and Their Parent Crude Oils: Comprehensive Characterization of the Molecular Pyrolysis Pattern. *Energy Fuels* **2018,** *32* (3), 2699-2711.

22. Kendrick, E., A mass scale based on CH_2=14.0000 for high resolution mass spectrometry of organic compounds. *Anal. Chem.* **1963,** *35* (13), 2146.

23. Odian, G., *Principles of Polymerization*. 4th. Ed. ed.; John Wiley & Sons, Inc.: 2004.

24. Vetere, A.; Alachraf, W.; Panda, S. K.; Andersson, J. T.; Schrader, W., Studying the fragmentation mechanism of selected components present in crude oil by CID mass spectrometry. *Rapid Commun. Mass Spectrom.* **2018,** *32* (24), 2141-2151.

CHAPTER 8. GENERAL CONCLUSION

Crude oil fouling is a chronic and till now unresolved problem in the producing and processing petroleum industries. The investigation of this phenomenon is of paramount importance since the deposition of solid material on surfaces has various operating, environmental and financial effects. Although the physical part of fouling is attributed to the accumulation and precipitation of asphaltenes, paraffins and/or insoluble inorganic particles, the chemical part of fouling remains unexplored. Until now, the limitation of gaining information regarding the oil compounds which are responsible for fouling, the parameters which influence the fouling rate as well as their complex chemical transformations involved in the formation of solid deposits, relies on the inability to simulate one-to-one fouling under laboratory conditions. Here, for the first time, the successful simulation of fouling was achieved on a laboratory scale with the use of a light crude oil fraction, which does not contain any low soluble components but is known for its fouling tendencies, usinglab-built reactors.

First of all, the gas condensate which was selected to study crude oil fouling, was tested with the newly introduced Orbitrap-based mass spectrometer. The high resolving power needed for oil characterization and the efficient chromatographic separation for the distinction of structural isomers was combined for first time, enabling a deeper understanding of the components of the sample on a molecular level. Information regarding the volatile components of the sample was obtained not only with the commonly used high or low electron ionization, but also with the atmospheric pressure photoionization as an alternative interface. The ability to switch from high to low energy ionization provided complementary information for a broad range of compounds from nonpolar to medium polar.

In order to study chemical changes within a complex mixture, the need of high-resolution mass spectrometry and high ionization efficiency is necessary. Therefore, different atmospheric pressure ionization methods (ESI, APPI and APCI) alone, as well as in combination with each other were tested for a crude oil sample. In some cases, the combination of these methods can be used as an alternative in order to gain complementary information regarding the crude oil constituents.

One of the biggest challenges during this study was to simulate fouling under laboratory conditions. For this purpose, lab-built reactors of stainless steel, quartz vials, quartz covers, sealing rings and heating plates were used. The gas condensate was heated at different temperature ranges as well as at different reaction conditions. The first parameter that was tested was the influence of oxygen on fouling rates. The class of sulfur compounds was selected in order to investigate the chemical changes, since it is considered as one of the most undesirable constituents of crude oil. Various chemical reactions were triggered due to different temperatures and atmospheres. Formation of new sulfur species was observed at moderated temperatures while absence of sulfur containing compounds was observed at 450 °C under oxygenated conditions, indicating the high reactivity of sulfur species.

Another parameter that was tested was the influence the water has on fouling. Therefore, the gas condensate was heated at different temperatures with and without water. The simulation of fouling was successful with the formation of an insoluble solid material after thermal treatment at 450 °C. The microscopic analysis by SEM/TEM revealed that the solid material consists of more than 95 % of amorphous carbon. The results focused only on purely hydrocarbon compounds demonstrated the formation of new high molecular weight compounds with high aromaticity. With the assist of the standard hydrocarbon compound of pyrene, a possible reaction pathway was suggested.

For a better understanding of the fouling reaction, the determination of a reaction mechanism is necessary. This was possible using the reactions of nitrogen containing compounds. The results suggested that fouling is a multi-step process involving different mechanisms. The increase of only of the aromaticity of the nitrogen containing compounds occurs due to dehydrogenation reaction, while a further increase in both molecular size and aromaticity involves radical polymerization reaction. In order to follow chemical reactions and verify the potential reaction pathways, a limited number of reactants (quinoline and toluene) was chosen for the reaction. Structural elucidation of a nitrogen containing compound, detected as a product after the reaction, was performed. The different fragment signals suggest that more than one reaction pathway is possible in the formation high aromatic compounds.

CHAPTER 9. APPENDIX

9.1. List of abbreviations

Δm	mass deviation
°C	degree Celsius
µA	microampere
AGC	automatic gain control
APCI	atmospheric pressure chemical ionization
API	atmospheric pressure ionization
	American Petroleum Institute
APLI	atmospheric pressure laser ionization
APPI	atmospheric pressure photoionization
ATR-FTIR	attenuated total reflection-Fourier transform infrared
bbl	barrel
CCE	controlled-current electrolytic
CDU	crude distillation unit
CEC	contaminants of emerging concern
CI	chemical ionization
CID	collision-induced dissociation
Da	Dalton
DBE	double bond equivalent
e.g	exampli gratia (lat.)
EA	elemental analysis
EI	electron ionization
ESI	electrospray ionization
eV	electron volts
FT	Fourier transform
FT-ICR	Fourier transform ion cyclotron resonance
FT-IR	Fourier transform-infrared
FWHM	full width at half maximum height

GC	gas chromatography
GC×GC	2-dimensional GC
GPC	gel permeation chromatography
HDS	hydrodesulfurization
HOMO	highest occupied molecular orbital
IC	inert conditions
ICP-OES	inductively coupled plasma optical emission spectrometry
KMD	Kendrick mass defect
kV	kilovolts
LC	liquid chromatography
LTQ	linear trapping quadrupole
LVEI	low-voltage electron ionization
m	mass
m/z	mass-to-charge ratio
mDa	millidalton
mL	milliliter
MS	mass spectrometry
NMR	nuclear magnetic resonance
OC	oxygenated conditions
OM	optical microscopy
PAH	polycyclic aromatic hydrocarbons
PASH	polycyclic aromatic sulfur heterocycles
ppm	parts per million
R	resolving power
RF	radio frequency
s	second
SEC	size-exclusion chromatography
SEM	scanning electron microscopy
SIM	selected ion monitoring
TEM	transmission electron microscopy
TGA	thermo-gravimetric analysis
UHRMS	ultra-high resolution mass spectrometry
UV-F	ultraviolet-fluorescence

vs	versus
VUV	vacuum ultraviolet
wt-%	percentage of weight
XRD	X-Ray diffraction
XRF	X-Ray fluorescence

9.2. List of Figures

addition of a toluene moiety. The different fragment signals allow a detailed characterization of the structure, revealing that toluene is added to the quinoline moiety either directly through a bond between both aromatic core structures as well as through the methyl-group of toluene. The two Kendrick plots at the bottom show the different product compounds in the reaction mixture for the N_1- and N_2-class. In addition, solid material was formed after the reaction at 450 °C. It has to be noted that the structures shown here are suggestions retrieved from the data. At this point, no information is available regarding the exact position of the individual coupling sites. 115

Figure 7-4: Suggested reaction mechanisms of tetrahydro-quinoline. The mechanism is based on the data obtained during these reactions. A compound such as tetrahydro-quinoline would lose hydrogen atoms in multiple steps thus increasing the aromaticity and the DBE value. The thermal removal of hydrogen allows the formation of radical intermediates which then can easily react with other aromatic or aliphatic sites in the mixture. Shown here is the addition of toluene and/or additional quinoline moieties as an example. The green arrows depict the increase of DBE while the red arrows show the increase of both DBE and carbon number by addition of another aromatic moiety. 116

9.3. List of publications

Publications in Peer-reviewed Journals

- A. Kondyli, W. Schrader. "High-resolution GC/MS studies of a light crude oil fraction." *J. Mass Spectrom.* **2019**, *54*, 47-54.
- Kondyli, W. Schrader. "Investigation on the analysis of extremely complex mixtures by combining different atmospheric pressure ionization sources", accepted for publishing in *Rapid Commun. Mass Spectrom.*
- A. Kondyli, W. Schrader. "Studying crude oil fouling with focus on sulfur containing compounds using high-resolution mass spectrometry", will be submitted to *Fuel*.
- Kondyli, W. Schrader. "Investigation of the behavior of hydrocarbons during fouling by high-resolution electrospray ionization mass spectrometry", will be submitted to *Applied Energy Materials.*
- A. Kondyli, W. Schrader. "Understanding "fouling" in extremely complex petroleum mixtures", submitted to *Angewandte Chemie.*

Oral Presentations

- Kondyli A., Schrader W., "Investigation of chemical alteration on crude oil fouling by high resolution mass spectrometry ", Treffen der 'Fachgruppe FT-MS und Hochauflösende Massenspektrometrie" der DGMS.
  21-22 September 2017, Kaiserslautern, Germany

Poster Presentations

- Kondyli A., Schrader W., "Combination of different ionization sources expands the analysis of complex mixtures", International Mass Spectrometry Conference (IMSC).
  26-31 August 2018, Florence, Italy.

- Kondyli A., Schrader W., "Investigation on the chemical changes of the acidic compounds in crude oil by fouling using high resolution mass spectrometry", European Mass Spectrometry Conference (EMSC), 51. Jahrestagung der DGMS.
  11-15 March 2018, Saarbrücken, Germany.

- Kondyli A., Schrader W., "Effect of temperature on crude oil fouling under inert and oxygenated conditions and subsequent analysis by HRMS", 50. Jahrestagung der DGMS.
  05-08 March 2017, Kiel, Germany.

- Kondyli A., Schrader W., "Analysis of volatile organic compounds in crude oil using high resolution Orbitrap GC/MS", 64th ASMS Conference on Mass Spectrometry and Allied Topics.
  05-09 June 2016, San Antonio, TX, USA.

- Kondyli A., Schrader W., "GC-Orbitrap: A new hyphenation for the analysis of complex mixtures ", 49. Jahrestagung der DGMS.
  28 February-02 March 2016, Hamburg, Germany.

9.4. Curriculum Vitae

For reasons of data privacy the CV is not part of this version.

9.5. Acknowledgment

The ancient Chinese sage Confucius once said ‘’choose a job you love, and you will never have to work a day in your life” and I could not agree more to this statement. In this joyful and fascinating journey during my PhD I wasn’t alone, and I wouldn’t have made it without the support and the help of the people of the MS department.

First of all, I would like to express my deepest and sincere gratitude to my supervisor Professor Wolfgang Schrader, for his trust, constant guidance, encouragement and continuous support throughout my thesis. You were not just a supervisor, but a constant source of motivation, inspiration and creativity. Apart from the scientific knowledge, you taught me to think outside of the box and not be afraid to exploit new opportunities. I will miss your sarcastic humor which was cheering me up in times with (and without) stress. I really hope our pathways to cross again in the future. Thank you for everything boss!!

My special words of thanks go also to my second supervisor, PD Dr. Ursula Telgheder for always being so kind, helpful and motivating. I am grateful for all her support and for taking the time to evaluate my thesis.

Furthermore, I am deeply grateful to my colleague and friend Alessandro Vetere who provided me from the beginning all his help not only in scientific level but also in personal. You were always there for me not only to assist my research with your insight comments, but also to teach me new things. Next to you I have learned not to be afraid to open the instruments, disassemble parts of them and understand their function. I was feeling always safe working next to you, since there was nothing that couldn’t be fixed with your assist. Echt jetzt, thank you kunavi!

I would like to thank all the members of the Mass Spectrometry department for the enjoyable time I spend at the institute, for their embracement from the first moment, and for the fact that they made me feel comfort and part of the group immediately. Many thanks to Frau Marion Blumenthal for been always so helpful and for encouraging me to practice with her the German language. I thank all the technicians and especially Daniel Margold and Dirk Kampen for their contribution to my experiments and for their tolerance to answer all my questions.

During this journey I had the opportunity to meet a lot of people from all over the world that apart from colleagues we became also very good friends. Special thanks to Lilla Guricza for showing me always the positive site of the things, Ruoji Luo for his friendship and the unique experience to try the moon-cake, my dear friend Zahra Farmani for her love

and support all these years; you were like a sister to me; furthermore Ilker Satilmis, Yun Xu and Oleksandra Kuzmich for the amazing time we spend together at the institute and outside. I will really miss you all!!

Also, I would like to express my heart-felt gratitude to my family and especially to my beloved mother Alexandra. She has been a constant source of love, support, concern and strength all these years. Without her I could not have made it here. Last but not least, a special thank to my ''ratman'' Daniel for all his love and constant support. You were always by my side and encourage me. You believed in me and gave me hope when I was losing mine. Σ΄ αγαπώ!